UNIVERSITÀ DEGLI STUDI
DI NAPOLI FEDERICO II

Bolaji Toheeb Sanusi

Assessing the benefits of FRP strengthening on the seismic performance of RC buildings through a framework for regional scale simulations

FRP++
Advanced structural analysis and design using composite materials

Master Dissertation
European Master Advanced Structural Analysis and Design using Composite Materials

Work developed under the supervision of
Professor Marco Di Ludovico
Professor Ciro Del Vecchio
PhD Carmine Molitierno

Funded by the European Union

September 2025

DECLARATION

Name: Bolaji Toheeb Sanusi

Email: bolajisanusi15@gmail.com **Phone number:** +351935502099

Citizen Card Number: B01667851

Title of the Thesis: Assessing the benefits of FRP strengthening on the seismic performance of RC buildings through a framework for regional scale simulations

Supervisors:

Professor Marco Di Ludovico

Professor Ciro Del Vecchio

PhD Carmine Molitierno

Year of Conclusion: 2025

Master Course in Advanced Structural Analysis and Design using Composite Materials

University of Naples Federico II, 01/09/2025

Signature: 

ACKNOWLEDGEMENTS

First and foremost, I would like to thank my supervisors, Professor Ciro Del
Vecchio, Professor Marco Di Ludovico, and Dr. Carmine Molitierno for their exceptional expertise, constant support, and invaluable insights during all the phases of my research. Their mentorship has been instrumental in shaping the direction and quality of my work, and I truly appreciate their patience, encouragement, and dedication.

I am profoundly thankful to my parents, siblings, and my wife for their unconditional love, encouragement, and unwavering support throughout this journey. My parents have been my guiding pillars, instilling strong values and perseverance in me; my siblings have always stood by me, offering motivation and positivity; and my wife has been my constant source of strength, understanding, and inspiration. This achievement would not have been possible without their collective support and belief in me.

I am deeply grateful for the generous support and funding provided by the Erasmus+ Program funded by the European Union, which has played a crucial role in enabling me to pursue my master's studies. I would also like to extend my sincere appreciation to the consortium behind the European Master's in Advanced Structural Analysis and Design using Composite Materials [FRP++] program. Being part of this innovative and forward-thinking initiative has not only expanded my academic perspective but also equipped me with advanced knowledge and expertise in the field of structural composites.

Lastly, I express my deepest gratitude to Almighty Allah for His countless blessings, guidance, and strength throughout this journey. It is by His mercy and grace that I have been able to overcome challenges and achieve this milestone. All praise and thanks are due to Him for granting me the opportunity, patience, and perseverance to reach this stage.

Valutazione dei benefici del rinforzo FRP sulle prestazioni sismiche degli edifici in cemento armato attraverso un framework per le simulazioni a scala regionale

RIASSUNTO

L'ingegneria strutturale e sismica moderna dovrebbe avere l'analisi costi-benefici multicriterio come guida per valutare l'impatto dei rischi naturali sulle città e progettare strategie efficaci di mitigazione del rischio. Nei paesi ad elevato rischio sismico, migliorare le prestazioni sismiche del patrimonio edilizio esistente è fondamentale per ridurre i danni e le perdite dirette ed indirette associate. In questo contesto, i materiali compositi a matrice polimerica come gli FRP sono ampiamente utilizzati per rinforzare gli elementi strutturali e non strutturali degli edifici esistenti in cemento armato. Ciò è dovuto alla facilità e rapidità di applicazione, alle elevate prestazioni, la reperibilità sul mercato dei prodotti da costruzione e alla disponibilità di linee guida di progettazione affidabili.

Questo lavoro di tesi si prefigge di valutare l'efficacia di interventi locali di rinforzo sismico attraverso FRP attraverso un framework semplificato per la stima della risposta simica e delle perdite economiche associate. Il framework precedentemente sviluppato presso l'Università degli Studi di Napoli Federico II è stato sviluppato in MATLAB ed è stato adattato ed utilizzato per eseguire l'analisi di 3 casi di studio (edifici di 2, 3 e 4 piani progettati con moderate azioni sismiche) estratti dal database dell'Aquila nella configurazione "as built", riprogettatati per sostenere solo i carichi gravitazionali e rinforzati con FRP.

Il lavoro è consistito nell'analisi non lineare (NLTH), eseguita su 7 set di accelerogrammi opportunamente scalati a 9 diversi periodi di ritorno dell'azione sismica di riferimento del sito sia in direzione X che Y. Tali analisi sono state utili per ricavare iparametri di domanda ingegneristica, ovvero EDP (spostamenti di interpiano, accelerazione e tagli di piano). Questi EDP sono stati poi utilizzati per l'analisi delle perdite utilizzando le funzioni di fragilità e le conseguenze e la probabilità di collasso associata. La stima delle perdite economiche diretteè stata eseguita utilizzando l'approccio FEMA P-58 (a livello di componente).

La risposta non lineare degli edifici progettati per sisma e gravità viene valutata e confrontata con diverse soluzioni di rinforzo in FRP per dimostrarne l'efficacia. Viene inoltre presentato un confronto in termini di costi di collasso e di rinforzo a diversi periodi di ritorno.

PAROLE CHIAVE: FRP, analisi dinamica non lineare, FEMA P-58, perdite economiche.

Assessing the benefits of FRP strengthening on the seismic performance of RC buildings through a framework for regional scale simulations

ABSTRACT

Modern structural and seismic engineering should use multi-criteria cost-benefit analysis as a guide to assess the impact of natural hazards on cities and design effective risk mitigation strategies. In countries with high seismic risk, improving the seismic performance of existing buildings is crucial to reducing damage and associated direct and indirect losses. In this context, polymer matrix composite materials such as FRP are widely used to strengthen the structural and non-structural elements of existing reinforced concrete buildings. This is due to their ease and speed of application, high performance, market availability of construction products, and the availability of reliable design guidelines.

This thesis aims to evaluate the effectiveness of local seismic strengthening interventions using FRP using a simplified framework for estimating seismic response and associated economic losses. The framework previously developed at the University of Naples Federico II was developed in MATLAB and adapted and used to perform analysis of three case studies (2-, 3-, and 4-story buildings designed with moderate seismic actions) extracted from the L'Aquila database in the as-built configuration, redesigned to support only gravity loads, and strengthened with FRP.

The framework consisted of a nonlinear (NLTH) analysis, performed on 7 sets of accelerograms appropriately scaled to nine different return periods of the site's reference seismic action in both the X and Y directions. These analyses were useful for deriving the engineering demand parameters, i.e., EDPs (interstory displacements, acceleration, and storey shears). These EDPs were then used for loss analysis using fragility functions and the associated consequences and probability of collapse. The estimation of direct economic losses was performed using the FEMA P-58 approach (at the component level).

The nonlinear response of buildings designed for earthquake and gravity is evaluated and compared with different FRP strengthening solutions to demonstrate their effectiveness. A comparison of collapse and strengthening costs at different return periods is also presented.

KEYWORDS: FRP, non-linear history analysis, FEMA P-58, EALs.

TABLE OF CONTENTS

CONTENTS

LIST OF FIGURES

LIST OF TABLES

LIST OF ABBREVIATIONS AND SYMBOLS

Abbreviations

AeDES	Agibilità e Danno nell'Emergenza Sismica
ACI	American Concrete Institute
ARC	Actual Repair Costs
ASCE	American Society of Civil Engineers
ATC	Applied Technology Council
BCJ	Beam Column Joint
BRC	Building Repair Cost
CA	Common Areas
CAM	Active Confinement of Manufactured Materials
CEN	European Committee for Standardization
CFRP	Carbon Fibre Reinforced Polymer
CNR	Consiglio Nazionale delle Ricerche
CU	Condominium Units
DBELA	Displacement-Based Earthquake Loss Assessment
DL_FRP	Double Layer Carbon Fiber Reinforced Polymer
DPC	Civil Protection Department
DRC	Direct Repair Costs
DS	Damage State
EALs	Expected Annual Losses
EDP	Engineering Demand Parameters
FEMA	Federal Emergency Management Agency
FRCM	Fiber Reinforced Cementitious Matrix
FRP	Fibre Reinforced Polymer
GEM	Global Earthquake Model Foundation
ID	Independent Dwelling
IDR	Interstory Drift Ratio
IPs	Infills And Partitions

LSLS	Life Safety Limit State
MDOF	Multi-Degree Of Freedom
NBS	New Building Standard
NLTH	Non-Linear Time History
OPCM	Ordinanze del Presidente del Consiglio dei Ministri
PACT	Performance Assessment Calculation Tool
PBT	Pay Back Time
PFA	Peak Floor Acceleration
PGA	Peak Ground Acceleration
RC	Reinforced Concrete
REDI	Resilience Based Earthquake Design Initiative
ReLUIS	Laboratories University Network of Seismic Engineering
SFRP	Steel Fibre Reinforced Polymer
SL_FRP	Single Layer Carbon Fiber Reinforced Polymer
TR	Return Period
TRC	Total Repair Costs

Symbols

V_R	Shear capacity of the column
A_c	Area of the cross-section
A_{sw}	Area of stirrups
L_v	Cutting gap
V_c	Shear resistance contributed by concrete
V_w	Shear provided by transverse reinforcement
f_c	Compressive resistance of concrete
f_d	Resistance of FRP
f_{ffd}	Design resistance of FRP
t_f	Thickness of FRP
$w_{f,max}$	FRP maximum usable length
$\mu_{\Delta,pl}$	Ratio between the plastic part of the chord rotation and the yielding rotation

ρ_{tot}	Geometrical percentage of longitudinal steel
h	Total height of the cross-section
N	Axial compressive force
s	Distance between two stirrups
x	Depth of the neutral axis
θ	Angle of FRP application

1. INTRODUCTION

Most of the existing reinforced concrete (RC) buildings in the Mediterranean area, such as those in Italy and Turkey, are prone to high seismic actions. They were built using old code provisions that do not comply with modern standards. This makes them highly vulnerable to seismic events. This is mainly related to lack of reinforcement details and poor material properties that often resulted in undesired shear failures during earthquakes. Additionally, the presence of stiff infills made of hollow clay bricks leads to high shear forces at the top of the columns often resulting in local or global collapses. This led to high direct and indirect losses after recent seismic events that cannot be sustained by modern societies.

Several retrofitting techniques have been used as an intervention to increase the seismic-response of existing buildings. They aim at increasing their ductility, thereby increasing their stiffness and/or strength. This includes the use of Fiber Reinforced Polymer (FRP), Fiber Reinforced Cementitious Matrix (FRCM), steel or concrete jacketing, base isolation, RC walls, bay infill, and steel bracing. The selection of the retrofit solution depends on several factors, like the geometry of the building, the damaged part, seismic demand, the costs, the benefits etc. Among these techniques, FRP solutions prove to be promising when designed and used properly to increase the seismic performance of existing RC structures due to their light weight, ease of application, and overall cost effectiveness [1]. This solution can be used as local strengthening when it is used to prevent local shear failures in the beam-column joint (BCJ) or short columns and overturning of the exterior infill walls, [1]. When used as a global strengthening solution, it involves the overall analysis of the structure to identify the weak structural and non-structural elements [1]. FRP layout can either be in the form of X shape, L shape, U shape, T shape, FRP strips or bars, multiaxial sheets with uni or quadriaxial fiber orientations, and full wrap, which directly depends on the design [2]. A novel solution which involves the use of quadriaxial carbon fiber–reinforced polymer (CFRP) fabric to increase the shear capacity of the BCJ, with the use of novel pultruded FRP mechanical anchors with one end splayed dry fibers, which helps to prevent debonding failure of this joint is proposed [3]. This minimally invasive local strengthening solution needs to be accounted in a large-scale portfolio as it is very easy to install, minimizes the level of disruption for the building's occupants (since it is applied at the exterior part of the building), and has an overall low intervention cost.

The lower strengthening cost of FRP, which is about 94.4€/m^2 and 281 €/m^2, makes it viable when compared to other strengthening solutions to increase the seismic demand of existing buildings to a safety index prescribed by the codes [1]. In addition, it makes FRP promising and can be extended for use in a large-scale intervention strategy. The direct cost accrued with FRP takes about 37% of the total strengthening cost when used as local strengthening and about 78% when used as a global strengthening solution. In this context, accurate regional-scale prediction of repair and reconstruction costs after earthquakes is crucial to quantify the cost and the benefits of strengthening interventions to planning effective, resilient strategies to mitigate economic losses. To this end an effective and computationally efficient tool that quantifies the direct cost associated with the retrofit intervention used calls for the development of a tool that accounts for the expected annual loss (EALs) to the direct cost is required. This is highly important at the regional scale intervention as it also estimates the payback time, which gives an idea of the number of years that is required to recover the initial economic investment Several loss-assessment frameworks, such as FEMA P-58, DBELA [4], Simcenter [5], GEM [7], and Resilience-based Earthquake Design Initiative (REDI), have been developed/implemented to predict earthquake losses at both regional or component level in different regions. DBELA, which is widely used in Turkey, accounts for repair loss at the regional level [4]. SimCenter workflows, which also account for repair loss at the regional level, use the city-scale nonlinear time history analysis method. [5]. FEMA P-58, on the other hand, accounts for the repair loss at a component level, which helps designers identify the most critical components and further propose befitting strengthening techniques [6].

In this thesis a novel framework was implemented and further developed to have a simplified tool for predicting cost that can be used by practitioners and engineers. This tool aims to assess the benefit of FRP strengthening on the seismic performance of reinforced concrete (RC) buildings through regional-scale simulations.

1.1. Motivation

Modern structural and seismic engineering should consider multi-criteria cost-benefit analysis as the driving criterion to assess the impact of natural hazards on cities and design effective risk mitigation strategies. In earthquake-prone countries, improving the seismic performance of the existing building stock is crucial to reducing the associated damage and losses. In this context, FRP materials are widely used to strengthen structural and non-structural members of existing

reinforced concrete buildings. This is due to the ease and fast application, high performance, reliable design guidelines, and availability on the market. However, quantifying the benefits derived from FRP strengthening existing buildings through prediction analysis is fundamental for developing a large-scale seismic risk mitigation strategy. This is crucial for government decision-making to quantify the amount of funding that needs to be provided to enable the owners to improve the seismic performance of buildings. In this context, a novel MATLAB framework to conduct seismic loss assessment of existing RC buildings and quantify the benefits of strengthening strategies has been developed at the University of Napoli Federico II [7]. To date, the framework has been used to assess the expected damage and losses of an existing RC building severely damaged by the L'Aquila earthquake. The predicted economic losses at increasing earthquake intensity have been validated with the results of more refined analyses and with the actual repair costs monitored during the L'Aquila reconstruction process. At this stage, predictive analyses on existing reinforced concrete buildings with different characteristics are needed to assess the sensitivity of the framework to building variables and extend the results at a large scale from a seismic risk mitigation perspective. Development of a simplified approach to determine the costs and the benefits of FRP strengthening at large-scale will be an added value for the scientific community and practitioners involved in seismic risk assessment and retrofitting.

It is crucial to understand that before the government can invest in these retrofit solutions, it is necessary to convince them that these solutions ensure the safety of the occupants and reduce economic losses.

In addition, using FRP, it is possible to strengthen structural and non-structural components with minimally invasive interventions applied from exterior of buildings in order to limit the level of disruption and the invasiveness of interventions [3].

1.2. Aim and Objectives

This thesis focuses on the assessment of the benefits of FRP strengthening on the seismic performance of reinforced concrete (RC) buildings through a framework for regional-scale simulations. The other objectives include:

- study of the architecture of the framework developed in MATLAB (literature review and analysis of available code and data).

- the analysis of an available database of existing reinforced concrete (RC) buildings in L'Aquila and identification of the characteristics of a selected number of buildings used for the seismic assessment.
- Nonlinear numerical modelling of existing buildings belongs to the provided database in the framework to perform the analysis.
- assessment of the structural performance of the selected buildings using the proposed framework through nonlinear time history analysis (NLTHs) assessment of probability of collapse and costs.
- analysis of the results obtained in terms of engineering demand parameters.
- assessment of costs and benefits of FRP strengthening at a large scale.
- Develop a simplified approach to define costs and benefits of FRP strengthening at a large scale.

1.3. Structure of the Dissertation

Chapter 1: Introduction: This chapter provides an overview of the need for the tool for assessment for strengthening, the motivation and objectives of this thesis

Chapter 2: Literature Review: This chapter provides the reconstruction procedure for the L'Aquila earthquake in terms of the structural type, construction age, number of storey e.t.c. It also highlights the overview of the database including the methodology and the cost effectiveness of the FRP

Chapter 3: Simplified Loss Assessment Framework: This part gives the overview of the each of the architecture of the framework and the characteristics of case building the assessment is performed on.

Chapter 4: Seismic Analysis: This chapter shows the results of the loss assessment performed in terms of the engineering demand parameters, loss analysis, probability of collapse, cost comparison for the as-built and FRP strengthened configurations.

Chapter 5: Gravity Analysis: This chapter also shows the results of the loss assessment performed in terms of the engineering demand parameters, loss analysis, probability of collapse, cost comparison for the as-built and FRP strengthened configurations.

Chapter 6: Conclusions and further development: This chapter summarizes the key findings of the research, providing recommendations for practice and suggesting areas for future research.

THIS PAGE WAS INTENTIONALLY LEFT BLANK

2. LITERATURE REVIEW

The benefits of fiber reinforced polymer (FRP) strengthening on the seismic performance of reinforced concrete (RC) buildings are a critical concern, particularly at regional scale where seismic events are common. Different strengthening techniques have been employed during seismic events to restore the affected buildings. FRP techniques have been known for their fast application for structural elements such as beams, columns and beam-column joints, and non-structural elements as infills and partitions. Therefore, employing FRP strengthening techniques at regional scale level is fundamental to understanding how impactful it would be in terms of the reduction inhuman threats and economic losses.

2.1. Reconstruction Procedure for the L'Aquila earthquake

The L'Aquila earthquake is one of the more than 60 devastating earthquakes that have occurred in Italy's history, resulting in over 149,000 deaths. The L'Aquila earthquake, which happened in 2009, left nearly 70,000 homeless and impacted strongly on the productivity of primary importance for the local and national economy of the country [8]. Following the L'Aquila earthquake (2009), the reconstruction process was followed to account for the information about the extent of building damage and the actual repair/retrofit costs of 5775 residential units of buildings, which are outside the historical centres of the city [6].

The 5775 buildings are seen as structural units with independent dwelling (ID) or common areas (CA) and relevant CU (that is, a condominium building which has common areas and residential units with other buildings) of ordinary construction, which also includes some residential buildings and commercial private units [8].

The level of damage of buildings was assessed according to the AeDES form, in which the conditions of the building were assessed [9]. The data collected in this form helps to understand if the building can be used after the earthquake damage, while making sure it satisfies the seismic safety requirements. [8]. According to the AeDES form, buildings are classified into A-F categories as shown below:

- A - Usable building (slightly damaged, but still capable of performing its allocated functions).

- B - Usable building, but only after short-term countermeasures (a building with limited or no structural damage but with severe non-structural damage).
- C - Partially usable building (a building with limited or no structural damage but with severe non-structural damage located in part of the building).
- D - Building to be re-inspected (due to typical damage, a specific, but still visual, investigation is required).
- E - Unusable building (high structural or non-structural risk, high external or geotechnical risk).
- F - Unusable building from external risk alone.

The 5775 buildings observed during the L'Aquila earthquakes, which contain the L'Aquila and other municipalities and were divided into B or C (3546 buildings – 62%) and E (2211 buildings – 38%) usability ratings without considering the D-and F-rated buildings [6]. Furthermore, the E-rated buildings were further classified into E-B (buildings with high non-structural risk and slight structural damage) where a local strengthening strategy can solve most of the structural weakness; and E_{dem} (buildings that needs to be demolished) because of the structural weaknesses, significant residual drift, local or global collapse, or insufficient economic value of requirements seismic retrofit strategy compared to the reconstruction costs [10].

Each of these buildings is further categorised based on the following data, as highlighted below:

i. Usability ratings (B or C, E)
ii. Structural type (Reinforced concrete (RC), masonry, steel, etc.)
iii. Construction age and number of storeys
iv. Gross plan area
v. Time-to-approval of funding application.
vi. Repair costs of residential units.
vii. Structural repair and local strengthening costs interventions (B or C, or E-B funding class) or seismic capacity enhancement interventions (E funding class)
viii. Strengthening solutions used to increase seismic capacity.
ix. Demolition and reconstruction costs (E_{dem} funding class).

2.1.1. Structural type

The 5775 buildings contain 49% RC, 46% masonry, with the remaining 5% being a mixture of RC and masonry, steel, or other building types, as shown in **Table 2.1**. It can be observed that B or C usability rating are commonly RC buildings, while E ratings are mainly masonry buildings.

Table 2.1: Number of buildings in each usability rating class and structural type **[8]**.

Building Stock	Usability rating	No. of buildings	Structural type	No. of buildings
5775	B or C	3564	**RC**	1738
			Masonry	1580
			Others	246
	E	2211	**RC**	1059
			Masonry	1093
			Others	59

2.1.2. Construction age and number of storeys

Buildings damaged by the earthquake were also classified based on the number of storeys and construction age for each usability rating. Seven periods (< 1919, 1919-1945, 1946-1961, 1962-1971, 1972-1981, 1982-1991, and >1991) were used in classifying the construction age, which are commonly used in census data collection and the AeDES form. Construction age and number of storeys of 4381 buildings are determined from this data, with 2498 being RC buildings and 1883 being masonry buildings. As shown in **Figure 2.1**, construction age and number of storeys are related to the structural types (RC and masonry buildings). The numbers of RC buildings are mostly used in periods after 1961, and high in 1972–1981 and 1982–1991 periods of about 795 and 705 buildings, respectively, as shown on **Figure 2.1a**. The number of storeys associated with the RC buildings is mostly 3 and 4 storeys, as shown on **Figure 2.1b**. Consequently, the number of masonry buildings is almost equal for the period before 1961 and decreases after. Additionally, the masonry buildings are mostly 2 and 3-storey buildings, i.e., 795 and 705, respectively [8].

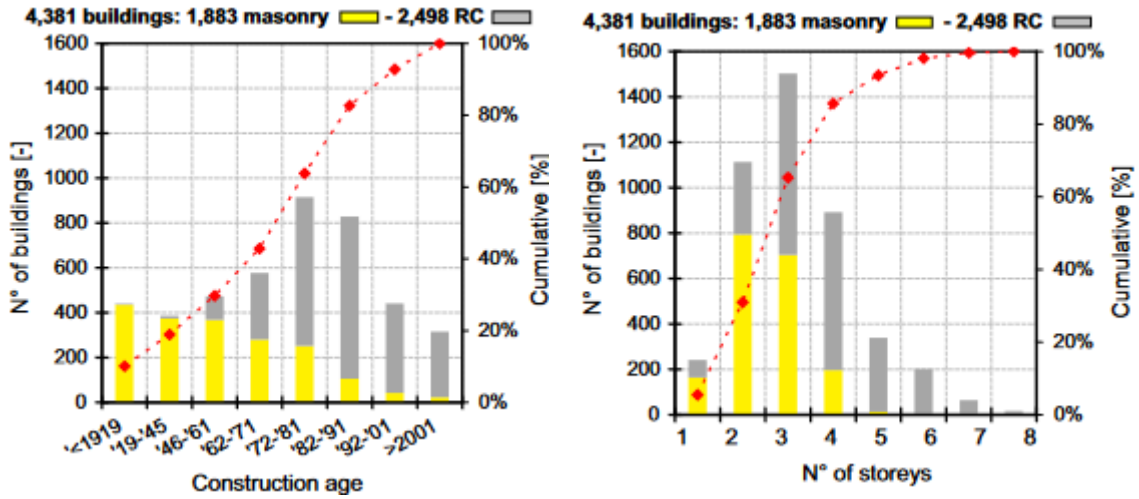

Figure 2.1: Construction age and number of storeys of buildings (RC and masonry buildings) [8].

2.1.3. Usability ratings

The buildings are also classified based on the usability ratings (B or C, and E) and correlated with the construction ages, and number of storeys. The RC buildings constructed before the period of 1946 or with several storeys more than six storeys are not considered because they are small, as shown in **Figure 2.1a-b,** therefore, are not reported in **Figure 2.2a-b.** The usability ratings associated with the RC buildings have the E buildings decrease as the construction age increases. Meanwhile, the B or C usability ratings buildings occupy more than 50% of the buildings from the construction age of 1972-1981. Consequently, the number of storeys increases with an increase in the number of buildings associated with the E buildings, as shown in **Figure 2.2b.** Additionally, the B or C buildings are higher than the E buildings if the 6-storey buildings associated with the E buildings (which take 55 % of the E buildings) are not considered.

However, the masonry buildings constructed after 1991 or with more than four storeys are not considered in **Figure 2.2c-d.** The usability ratings of the masonry buildings are less affected by the construction ages when compared to the RC buildings, with the B or C ratings being approximately twice that of E buildings and almost equal for all the construction periods. Consequently, the masonry buildings with B or C ratings increase as the number of storeys decreases, with 1 or 2 storeys having approximately 70 % and 3 or 4 storeys having 50 % proportion of the building.

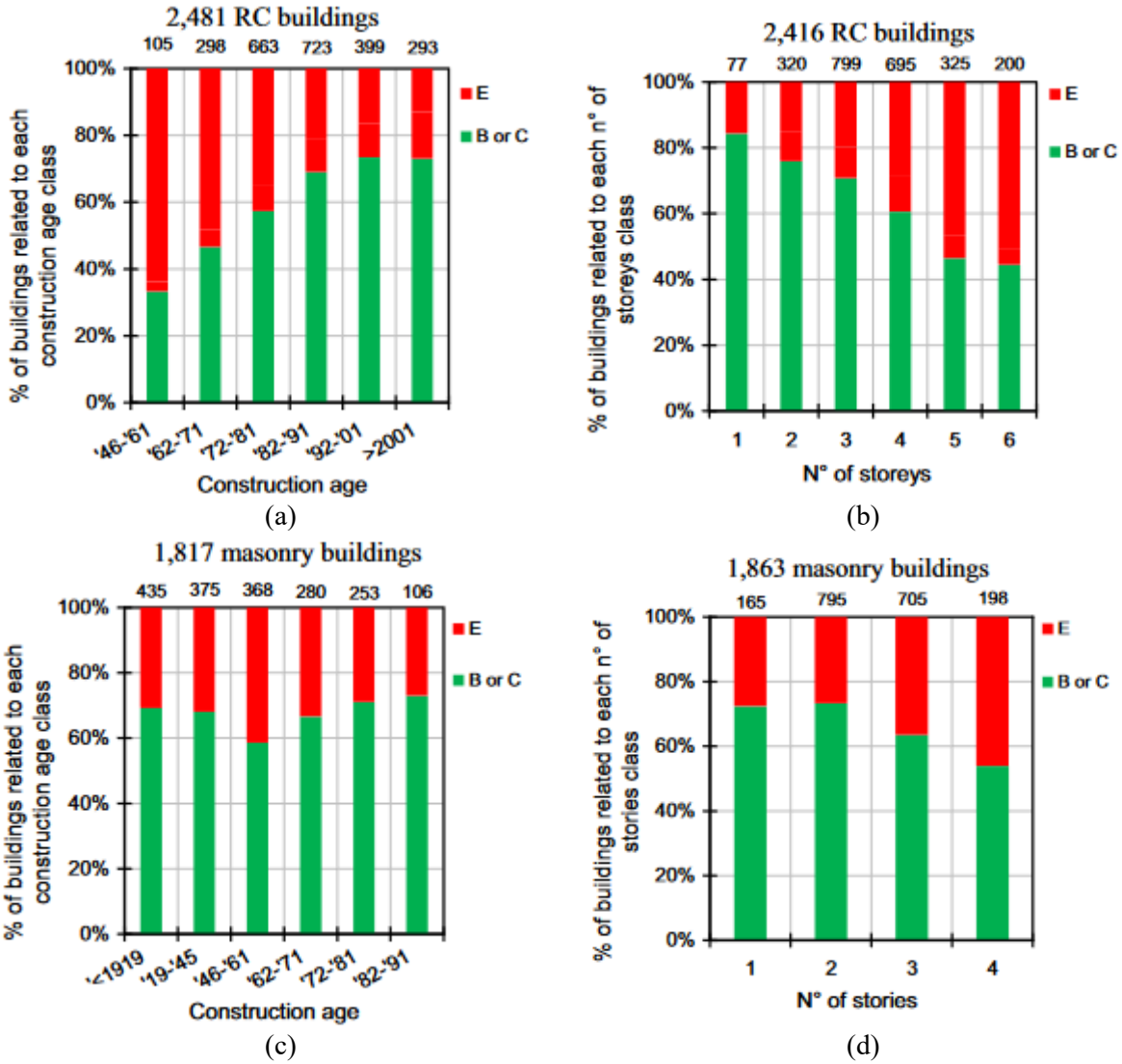

Figure 2.2: Usability rating of RC and masonry buildings measured against construction age (a and c) and number of storeys (b and d) [8].

2.1.4. Time-to-approval of funding application

Before the approval of funding for the reconstruction process, practitioners were required to submit technical documentation, which included a report of pictures depicting the extent of damage.

In order to speed up the reconstruction process of the damaged building after the earthquake event, repair designs and drawings, the type of strengthening interventions, and detailed calculation of funding application [8]. The Civil Protection Department (DPC) and ReLUIS in August 2009 published a document ‘‘Guidelines for Repair and Local Strengthening of

Structural and Non-Structural Members'' to support the engineers involved in the reconstruction process of the aftermath of the L'Aquila earthquake. This document outlines the type of damage that can be observed on both the structural and non-structural elements of the RC and masonry buildings. It further highlights the local strengthening interventions that can be used for both, with the description of the installation and design procedures. This local strengthening intervention includes the use of fibre reinforced polymer (FRP) for retrofitting of beam-column joints, strengthening of the columns, beams, and slabs; steel jacketing or prestressed steel on the RC elements; traditional and innovative techniques for strengthening of the masonry structures.

Full details on the application for funding (submissions and approvals) can be Di Ludovico et al. [8] and [10].

2.1.5. Repair and strengthening interventions

- **B-C buildings**

A local strengthening and repair intervention is proposed by OPCM no. 3779 [35] and the relevant Annex [35] which includes removing dangerous conditions and recovering the original seismic safety; repairing structural and non-structural damaged elements; and reducing building vulnerability by local strengthening interventions.

The repair interventions include the repair of non-structural parts and finishing works damaged; local repair of structural elements damaged; demolition and reconstruction of fully damaged or unsafe non-structural or secondary structural elements (such as interior or exterior infills, heavy plasters, fireplaces, eaves, etc).

Additionally, the local strengthening intervention was used to increase the seismic capacity of one or more under-designed components without inhibiting the structural performance of the structure. This intervention signifies an immediate cost-effective upgrading in seismic performance, with the local components being assessed according to the Italian seismic code. The local strengthening adopted targeted at increasing the shear capacity of exterior beam column joints (unconfined joints) and increasing the ductility of elements in case of RC structures and for masonry structures, focused on increasing the effectiveness of the connections between the masonry walls and slabs/roof and between orthogonal walls (through spikes or ties).

The local strengthening methods and their occurrence documented in the design drawings for applications concerning B or C buildings are individually detailed for reinforced concrete (RC)

and masonry structures in **Figure 2.3a and b**, respectively. The data analysis draws from a total of 1218 RC buildings and 1116 masonry buildings. Specifically, the interventions designed for restoring usability in RC buildings included repair and local strengthening efforts in 903 projects (74% of the RC dataset), whereas only repairs were implemented in 315 projects (26%).

For masonry buildings, 969 projects (87% of the masonry dataset) incorporated both repair and local strengthening interventions, with 147 projects (13%) involving solely repairs. The frequency of primary intervention types is presented in **Figure 2.3a-b**; since multiple intervention types were employed for each building, the total percentages exceed 100%. As displayed in **Figure 2.3a,** crack repair was the most frequently applied repair method (52% of projects) for RC structures.

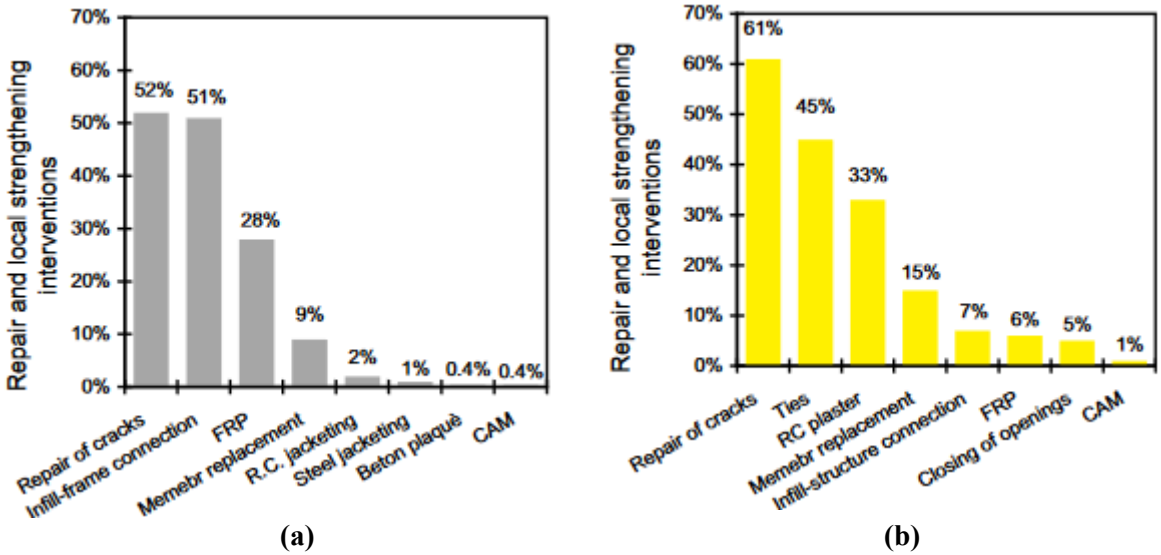

Figure 2.3: B or C buildings repair and local strengthening interventions of RC and masonry buildings (**a** and **b**) [8].

Within the local strengthening category, various techniques were utilized in the design, such as infill-frame connections, the implementation of FRP grids affixed with cement-based mortar, or steel profiles to prevent out-of-plane failures, as depicted in **Figure 2.4**, (DPC (Civil Protection Department) and ReLUIS (Laboratories University Network of Seismic Engineering) 2011). Interventions based on FRP, as seen on **Figure 2.5** were used to enhance the shear capacity of unconfined joints (external beam-column connections), the shear capacity of beams at their ends, and the deformation capacity in critical areas (mainly confinement at column ends) [11], [12], [13], [14].

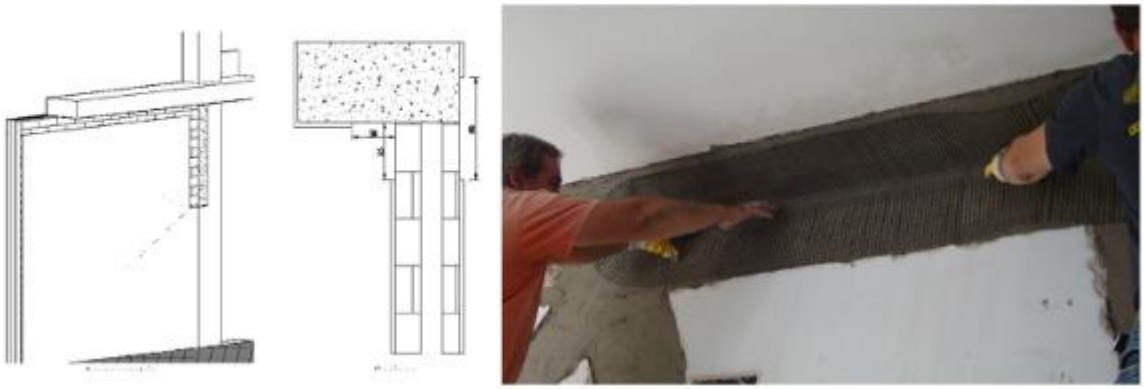

Figure 2.4: Infill-frame connections utilizing FRP grids bonded with a cement-based mortar [8].

(a) (b)

Figure 2.5: FRP-based interventions to increase the joint shear capacity of unconfined joints and the deformation capacity in the critical zones of columns (a and b) [8].

Additional methods comprised the substitution of structural elements; reinforcing members with RC or steel encasements to enhance their shear or flexural capacity and improve deformation potential in critical areas; applying steel plates to boost the flexural strength of beams (i.e., *beton plaqué*); and utilizing prestressed steel ribbons (CAM) as an alternative to FRP laminates. Notably, in 621 projects (representing 51% of the reinforced concrete building dataset), practitioners included various interventions to prevent out-of-plane collapses of both interior and exterior infill sections.

As illustrated in **Figure 2.3b**, for masonry structures, repairing cracks emerged as the most frequently implemented repair measure (61% of projects). The predominant methods used for this purpose involved injections (with either mortar or epoxy-based resins) alongside, or

without, the subsequent application of an FRP grid adhered with cement-based mortar; and the localized dismantling and rebuilding technique (known as *scuci-cuci*) to restore wall continuity along cracks (replacing damaged components with new ones and re-establishing structural integrity) and to fix heavily damaged sections of masonry walls. While also utilized for masonry buildings, interventions concerning infill-structure connections were less common than for reinforced concrete structures, being addressed in only 7% of projects to mitigate out-of-plane collapse of internal partitions.

In the case of local strengthening measures, the most commonly employed tactics included inserting ties (i.e., steel, reinforced concrete, or tie rods) to prevent out-of-plane wall failures (45% of projects) and applying in-plane reinforcement to masonry walls through RC plaster (33% of projects). In such cases, intervention strategies covering various building sections were regarded as comprehensive strengthening approaches, necessitating a global structural analysis and safety index evaluation both before and after the intervention. Demolishing and reconstructing structural components, along with FRP and CAM strengthening techniques, and closing openings, were also implemented as local strengthening solutions in a limited number of projects.

- **E-B buildings**

Instead of implementing a global retrofit strategy, OPCM no. 3790 [36] stated that, for certain buildings with usability rating E, local strengthening interventions could be implemented to increase the seismic capacity of under-designed elements. This would allow buildings with high non-structural damage but only minor structural damage to be quickly re-occupied by owners [8].

OPCM no. 3790 [36] and the relevant Annex [36] identify the following situations: (1) structures that have minimal to negligible damage to their structural members (with less than 60% of the structural members sustaining minor damage), and whose initial seismic safety rating (determined through a global analysis of the structure in its pre-earthquake state) was no less than 60% NBS; (2) structures with considerable damage but confined to a few structural elements and an original seismic safety rating of at least 60% NBS; (3) structures with minimal or no damage to structural elements. Provided that the global mass and structural stiffness are not affected by the local strengthening interventions, there is no need to run a global analysis after strengthening [11].

The E-B buildings also used the same standards adopted by B or C buildings, but the upper bound of public funding increased to €250/m^2 as opposed to €150/m^2 used for the B or C

buildings. It can be noted from the **Figure 2.6** that the type of local strengthening is implemented for 198 RC buildings and 73 masonry buildings, with one or more types that can be used in a building.

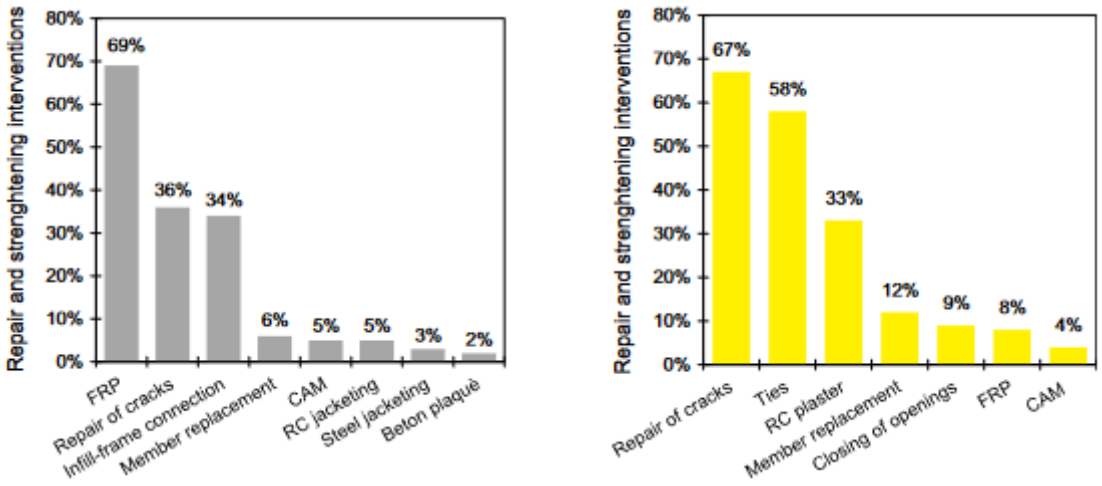

Figure 2.6: E-B buildings repair and local strengthening interventions of RC and masonry buildings (**a** and **b**) [10].

FRP systems are the most commonly used local strengthening techniques for RC buildings, as seen in **Figure 2.6a,** such as FRP grids with steel profiles or cement mortar in infill-frame connections to avoid out-of-plane collapse [11]. Also, RC or steel jacketing of the elements was used to increase their shear and flexural capacity; use of prestressed steel ribbon (Active Confinement of Manufactured materials, CAM); and addition of a steel plate to increase the beams' flexural capacity. Most of the crack repairs were done using the repair intervention.
In terms of the masonry building, it can be seen from **Figure 2.6b,** the local strengthening is done by insertion of ties (such as steel, RC, or tie rods) to avoid out-of-plane failure; use of RC plaster across the masonry walls for in-plane strengthening. The use of FRP strengthening techniques is therefore less used compared to the RC buildings, which is the case with the B or C buildings.

- **E buildings**

As stated by OPCM no. 3790 [36] and the relevant Annex [36], E buildings combined repair and seismic strengthening interventions to achieve nothing less than 60% NBS. The strengthening intervention implemented was used to increase the seismic capacity of the structure with techniques that reduce the seismic demand or increase the strength and deformation capacity of the structure. The use of FRP systems, RC jacketing, foundation

strengthening with micro piles, CAM, steel bracing/jacketing, RC shear walls were used to increase the strength and deformation capacity of the structure which is the same case for the B or C buildings except for the use of the steel bracing, strengthening of foundations, and RC shear walls.

Repairing the structural and non-structural damaged members, demolition and rebuilding of the destroyed or prone non-structural members (such as interior/exterior infills, heavy plaster, chimneypots, eaves) were implemented for the repair interventions.

For the E usability rating buildings, a global analysis check is required to evaluate the effectiveness of the strengthening solution implemented in order to check the attainment of the required seismic performance level. Base isolation systems or dissipation systems were mainly used for reducing the seismic demand by increasing either the damping or the period of the structures.

The different global strengthening methods and their prevalence, as identified in the design drawings for E and E_{dem} funding class structures, are detailed separately for 654 reinforced concrete (RC) buildings and 490 masonry buildings in **Figure 2.7a-b**. The total percentage shown in **Figure 2.7a-b** is higher than 100% since multiple intervention types may be applied to each structure.

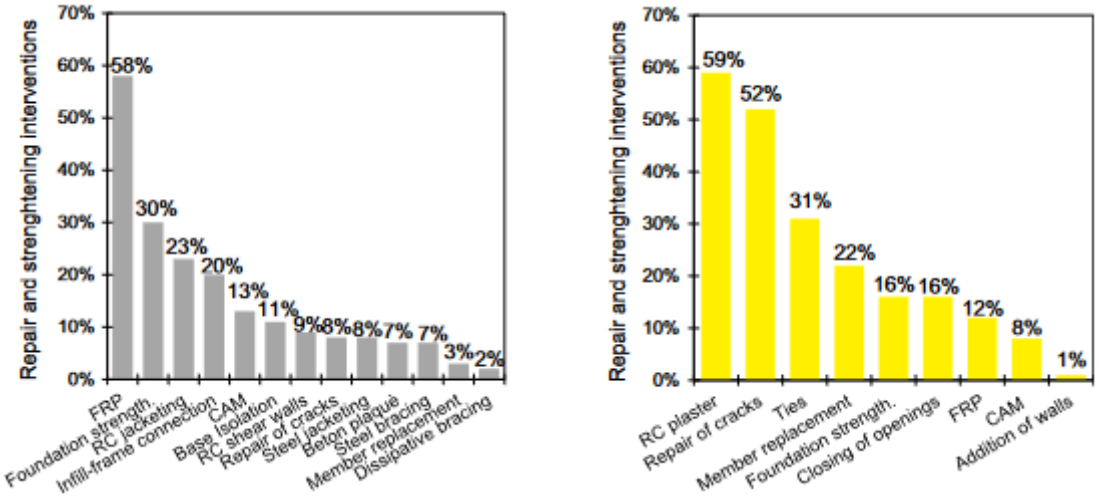

(a) (b)

Figure 2.7: E buildings repair and local strengthening interventions of RC and masonry buildings (a and b) [10].

In many structures, several strengthening methods were implemented to enhance the seismic performance; in numerous instances, the approach involved a mix of traditional and modern strengthening systems. [15]Fiber-reinforced polymer (FRP) was the most frequently employed method used with steel bracing to increase the overall stiffness and strength capacity of a pre-

existing structure by strengthening the beam-column joints to accommodate the localized stresses generated by the added bracing systems, as seen in **Figure 2.8**.

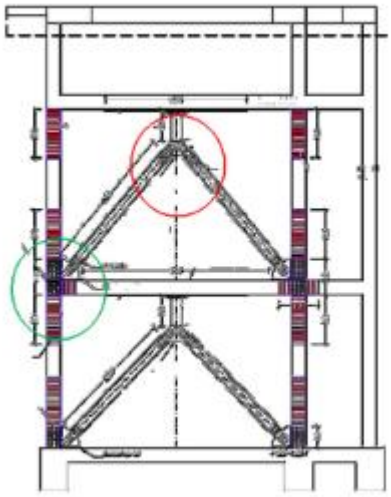

Figure 2.8: Seismic strengthening of RC buildings: steel bracing combined with FRP systems [10].

Figure 2.7a indicates that the predominant strengthening measures for RC buildings were based on FRP systems, foundation reinforcement, and RC jacketing. It is important to clarify that the category of foundation reinforcement applies exclusively to buildings that had initial capacity deficiencies in their foundation components and does not include interventions resulting from other strengthening techniques (such as adding shear walls, steel bracing, or base isolation systems).

Figure 2.7b illustrates that for masonry structures, the predominant methods utilized to enhance the seismic safety index and restore usability included: strengthening masonry walls in-plane with reinforced concrete plaster incorporating internal steel grids and ties or, in certain instances, FRP grids and spikes depicted in **Figure 2.9**. Interventions involving FRP and CAM techniques were observed less frequently in masonry buildings compared to RC structures. This likely stems from a lack of reference materials, particularly guidelines and codes, that provide straightforward and dependable design formulas specifically crafted for innovative strengthening methods tailored to masonry frameworks. Additionally, commercially available software for performing global analysis modeling on masonry buildings tends to be less effective at simulating innovative systems than it is for reinforced concrete structures. The most frequently implemented repair intervention in masonry buildings was crack repairs (52% of projects) through methods such as injections or local dismantling and rebuilding, known as *cuci-scuci*, aimed at restoring and recovering severely damaged components with new

materials. These repair costs cover their entirety, with the threshold set at 400 €/m^2 for the strengthening required to achieve a safety index between 0.6 and 0.8, except if private funding was also available [10].

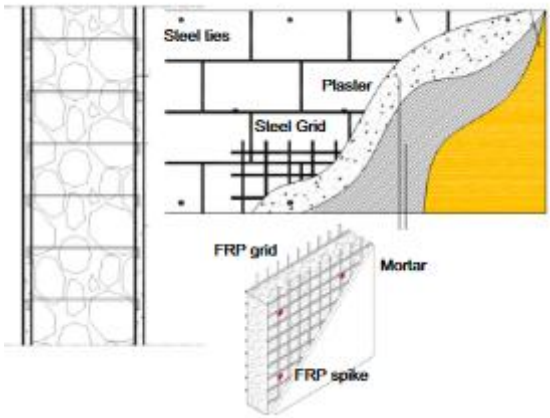

Figure 2.9: Seismic strengthening of masonry buildings: in-plane strengthening with RC plaster or FRP grid and mortar [10].

2.2. Repair costs related to the L'Aquila earthquake

2.2.1. Loss assessment methodology

Accurate regional-scale prediction of repair and reconstruction costs after earthquakes is crucial for planning effective, resilient strategies to mitigate economic losses. Several loss-assessment methodologies, such as FEMA P-58, DBELA, Simcenter, GEM, and Resilience-based Earthquake Design Initiative (REDI), have been developed/implemented to predict earthquake losses. DBELA, which is widely used in Turkey, accounts for repair loss at the regional level [4]. SimCenter workflows, which also account for repair loss at the regional level, use the city-scale nonlinear time history analysis method [5]. FEMA P-58, on the other hand, accounts for the repair loss at a component level, which helps designers identify the most critical components and further propose befitting strengthening techniques [6].
These methodologies commonly employ repair costs and fragility functions of components that are typical of the US standard making their use difficult for European building stock [15].

Significant research efforts have made in developing an empirical fragility and consequence functions for structural and non-structural components that are typical of the Mediterranean area with focuse on the costliest component to restore i.e. hollow clay brick infill walls [15],

[16], [17], [18]. The proposed consequence functions are significantly different showing the great variability of repair costs with respect to such components which is mainly due to uncertainties in estimating the additional work required to restore a component to its pre-earthquake condition and the relevant costs. In order to evaluate the accuracy of theoretical consequence functions, loss prediction cannot be benchmarked due to the lack of knowledge regarding actual repair costs (ARCs) at the building and component levels [6].

2.2.2. Definition of the database

Del Vecchio [6] extracted a subset of 120 RC existing buildings (representing about 5.3% of the full database) from the full database of 2245 RC buildings belonging to the B or C, E-B, and E classes for which repair costs are available to calculate the ARCs at the component level. Frequency distribution of the full database matching of ARCs, construction age, and the number of stories was done, and the selected buildings were randomly picked.

The frequency distributions of the ARCs can be seen in **Figure 2.10** for the full database of 2245 buildings and the subset of 120 RC buildings which satisfactorily match in terms of the mean repair costs, with some differences observed, especially for the E-B buildings, concerning the standard deviation.

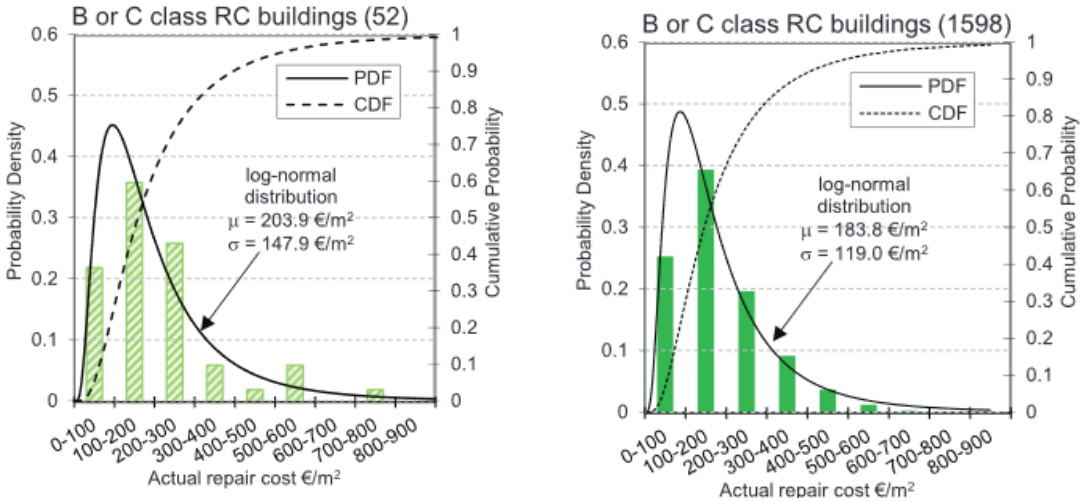

(a) (b)

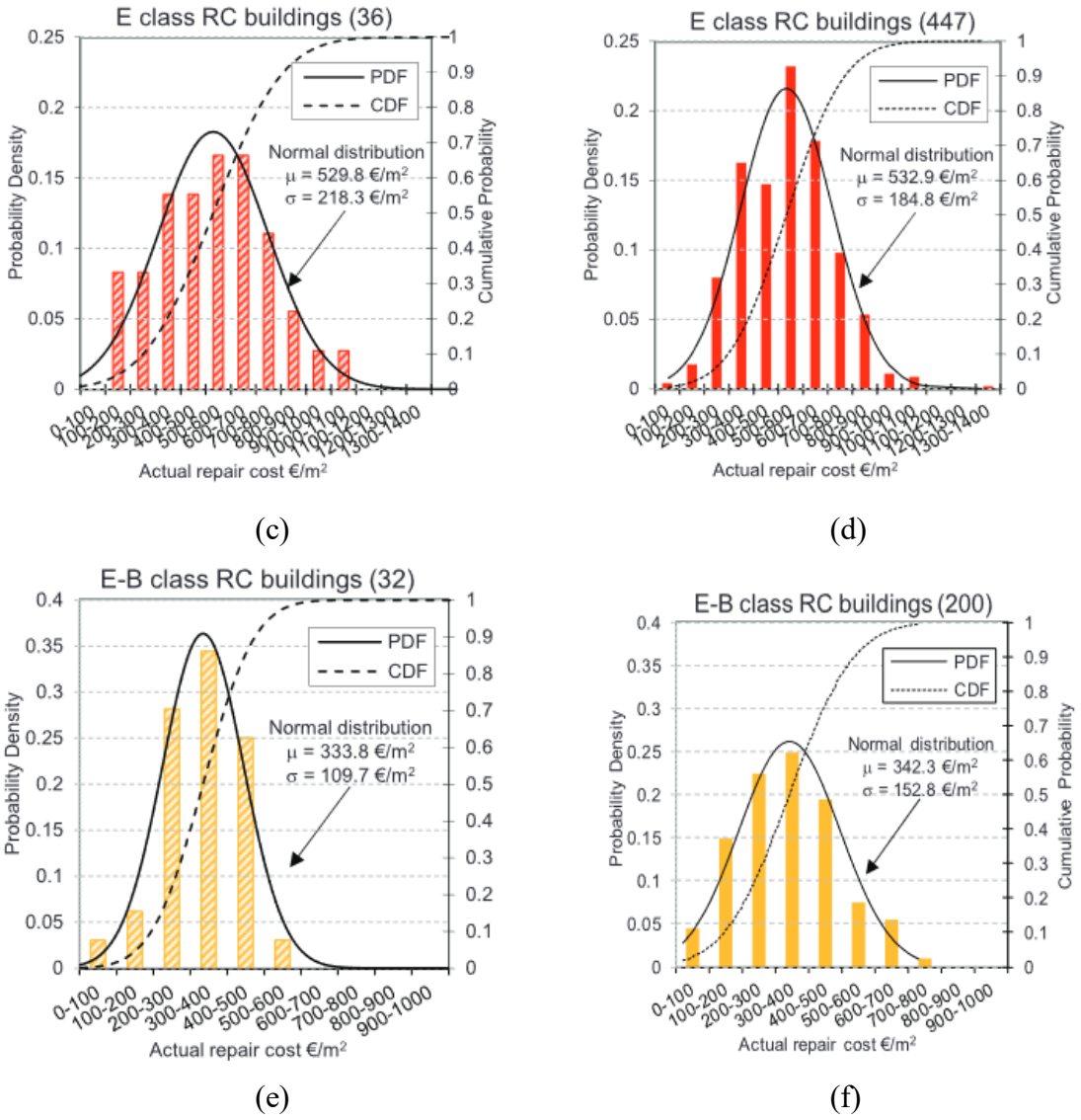

Figure 2.10: Frequency distribution of actual repair costs related to B or C, E-B, or E class RC buildings in the L'Aquila reconstruction process: (**a, c** and **e**) dataset of 120 RC buildings and (**b, d** and **f**) full L'Aquila database of 2245 RC buildings used in this study [6].

Figure 2.11 shows the frequency distributions of the construction age, number of stories, and number of buildings belonging to each usability class for the full database of 2245 RC buildings and the subset of 120 RC buildings **Figure 2.11a-c and d-f**, respectively which satisfactorily match the distributions of the full database in terms of the construction age and number of stories i.e. **Figure 2.11a-e**.

Since most of the buildings were built in the period 1962–1991, as shown on **Figure 2.11d,** they were, however, designed with an obsolete seismic design code [19]. **Figure 2.11e** also shows that most of the buildings are 3 to 5 stories in the subset extracted.

The percentage of the E-B and E class buildings selected is higher than the percentage computed on the full database, i.e. **Figure 2.11c and f,** which is because those buildings sustained more damage than the B or C buildings, which are important to obtain a detailed correlation between earthquake repair costs and rising damage levels. Since the buildings are analysed for different usability classes or damage states (DSs), this does not affect the reliability of the results.

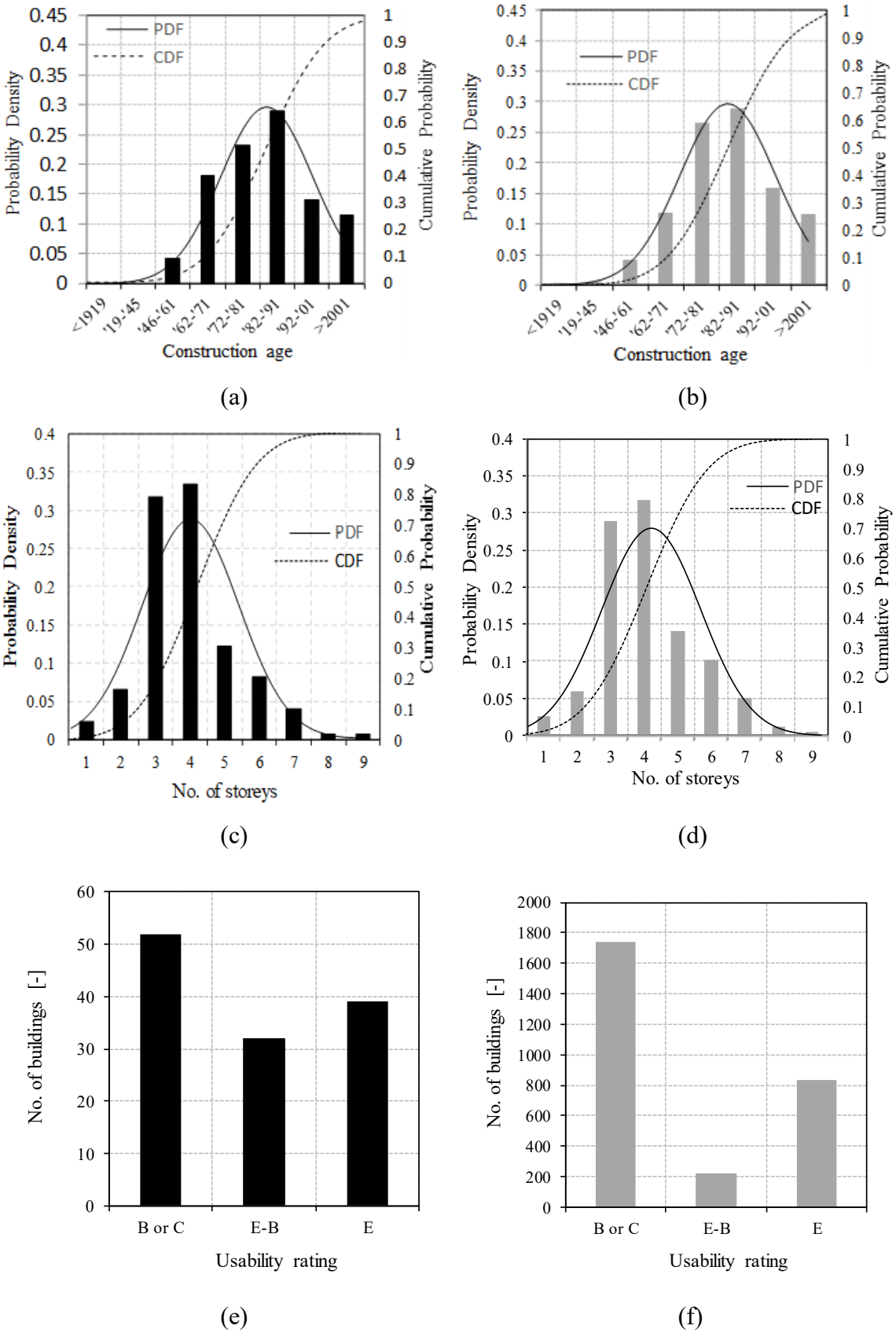

Figure 2.11: Frequency distribution of the building characteristics: (**a, c** and **e**) dataset of 120 RC buildings and (**b, d** and **f**) full L'Aquila database of 2245 RC buildings used in this study [6].

2.2.3. Methodology for the analysis at the component level/regional scale,

The first method employed is the study of the technical documents submitted during the funding application in order to classify 120 RC buildings in terms of the building damage and ARCs at the building and component levels. Information regarding various parameters such as dimension of the buildings (x and y direction), inter-storey height of the buildings, length and height of the infills (in both directions), column dimensions, beam depth, length of the beams, and concrete and steel grade. This information is crucial for modelling these buildings and for further seismic loss analysis. The methodology is as shown in **Figure 2.12** which Del Vecchio [6] has performed the damage analysis of 120 RC buildings of the database at the building level and classified the damage based on the usability rating of B, C, and E.

Consequently, the DSs of the building were classified according to section 4 of the AeDES form, which classifies the seismic damage effect as structural (i.e., vertical structures, floors, stairs, roofs) and non-structural components (i.e., infills and partitions). A further classification of the damage severity of the building was done with D0: null; D1: slight damage; D2-D3: medium or heavy damage; D4-D5: very heavy damage or collapse, and its extent as <1/3, 1/3-2/3, and >2/3. This information is necessary for the calculation of DSs as proposed in the literatures of De Martino *et al.* [20] and Del Gaudio *et al.* [21].

Visual observation of the building includes crack patterns and pictures of the damage contained in the technical documents, which were collected during the reconstruction process for each building, giving further details on the damage classifications at the component level [6].

The analyses of the actual reconstruction costs were carried out using the cost data available in the quotes developed by practitioners according to the price list of the Abruzzo region**,** taking into consideration the repair costs of condominium units (CU), common areas (CA), and independent dwelling (ID) [6].

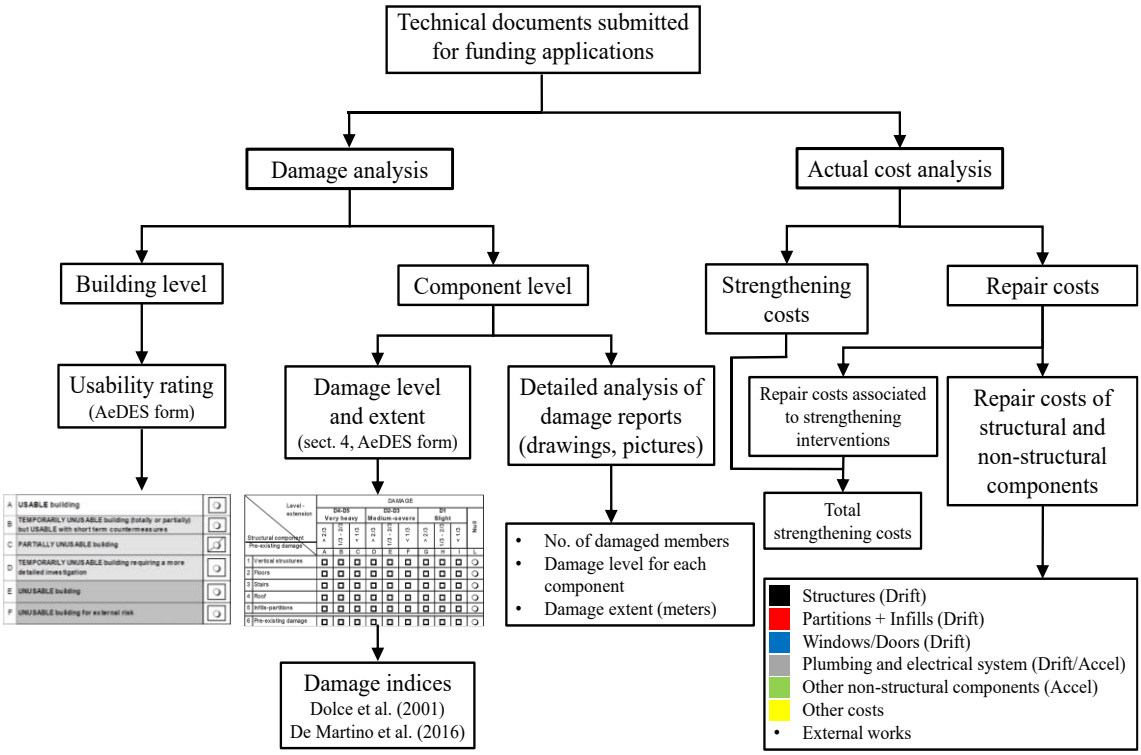

Figure 2.12: Proposed methodology for the analysis of damage and actual costs [6].

The total repair costs (TRCs) were divided into direct repair costs (DRC) and costs related to strengthening interventions, which were incorporated in the estimates with respect to the repair costs for the E-B and E class buildings during the L'Aquila reconstruction process. The functionality of damaged building components is shown in **Figure 2.13 (1–7)** were restored using the DRCs. The FEMA-P-58 classification was to name the structural and non-structural components [15].

The costs associated with repairs that pertain specifically to building components are classified under the macro-category referred to as building repair cost (BRC). **Figure 2.13** shows the subdivision of the BRC which is as follows: (1) structural components (foundations, beams, columns, beam-column joints, slabs, stairs, roofs); (2) infills and partitions; (3) windows and/or doors; (4) plumbing and electrical systems; and (5) other non-structural components, including the repair costs of floor finishes, roofs and tiles, chimneys, sanitary and other equipment, and communication and security. The BRCs also includes: (6) other costs (including the cost of safety measures, professional fees and construction field installations related to repair actions); (7) external works (including the repair costs related to external boxes, retaining walls, or other components external to the building); and (8) strengthening interventions related repair costs. Meanwhile, the other costs (6) were separated from the BRCs, since they are commonly

calculated as a percentage of DRCs, while it is difficult to predict the external works (7) using available probabilistic frameworks based on building performances [6].

Figure 2.13: Sample of earthquake-damaged building components and categories of repair costs [6].

2.2.4. Repair costs for component categories

The ARCs of the 120 buildings were done by evaluating the costs reported in the costings submitted for funding applications. The Abruzzo regional price list includes many repair actions leading to different repair options for the same component type. Each category of the ARCs was normalized by the overall building gross surface area (i.e., €/m^2). The subset of 120 buildings categorized based on the three usability classes (i.e., B or C, E-B, and E) of the reconstruction process and corresponding actual costs with their standard deviation (i.e., figures in brackets) is as shown in **Figure 2.14** [6].

	Mean repair cost (standard deviation)								
Usability class	B or C			E-B			E		
No. of buildings	52			32			36		
Component category	€/m²	%BRC	%TRC	€/m²	%BRC	%TRC	€/m²	%BRC	%TRC
(1) Structural components	3.24 (5.40)	2.13	1.59	3.96 (6.49)	1.68	1.19	19.53 (29.64)	5.63	3.69
(2) Infills and Partitions	87.99 (65.09)	57.69	43.15	124.01 (44.82)	52.48	37.15	148.02 (83.75)	42.63	27.94
(3) Plumbing and electrical system	23.35 (23.48)	15.31	11.45	38.43 (22.02)	16.26	11.52	56.48 (39.38)	16.27	10.66
(4) Windows/Doors	13.80 (20.93)	9.05	6.67	29.55 (18.14)	12.51	8.85	46.41 (31.37)	13.37	8.76
(5) Other non-structural components[a]	24.14 (23.92)	15.83	11.85	40.34 (26.33)	17.07	12.09	76.75 (44.05)	22.11	14.49
Building Repair Cost (BRC = (1) + (2) + (3) + (4) + (5))[b]	152.54 (115.85)	100.00	74.81	236.30 (82.97)	100.00	70.80	347.19 (161.72)	100.00	65.53
(6) Other costs[c]	46.39 (30.83)	–	22.75	57.15 (29.74)	–	17.12	86.37 (65.10)	–	16.30
(7) External works	4.99 (14.69)	–	2.45	12.65 (46.13)	–	3.79	15.01 (23.85)	–	2.83
(8) Repair costs for strengthening interventions	–	–	–	27.66 (28.08)	–	8.29	81.26 (66.26)	–	15.34
Total Repair Cost (TRC = BRC + (6) + (7) + (8))	203.91 (147.86)	–	100.00	333.76 (109.74)	–	100.00	529.82 (218.32)	–	100.00

Note that these costs can be normalised by the reconstruction costs of RC buildings divided by 1213.4 €/m².
BRC: building repair cost; TRC: total repair cost.
[a]This includes stairs, floor finishes, roofs and chimneys, sanitary equipment, and communication and security.
[b]This is the sum of the repair costs of all the building components: (1)–(5).
[c]This includes general costs for construction field installation, safety measures, and professional fees related to repair actions.

Figure 2.14: Repair costs for the subset of 120 RC buildings at the category level [6].

Each cost category is calculated as the mean ARC is expressed in €/m^2, and shown in **Figure 2.15a** and **Figure 2.15b** representing the mean costs expressed in % of BRC. The increase in TRCs and DRCs associated with the building components (known as BRCs) commensurate

with an increase in the damage severity (B or C to E rating) from 203.91 €/m² to 529.82 €/m² and 152.54 to 347.19 €/m², respectively [6].

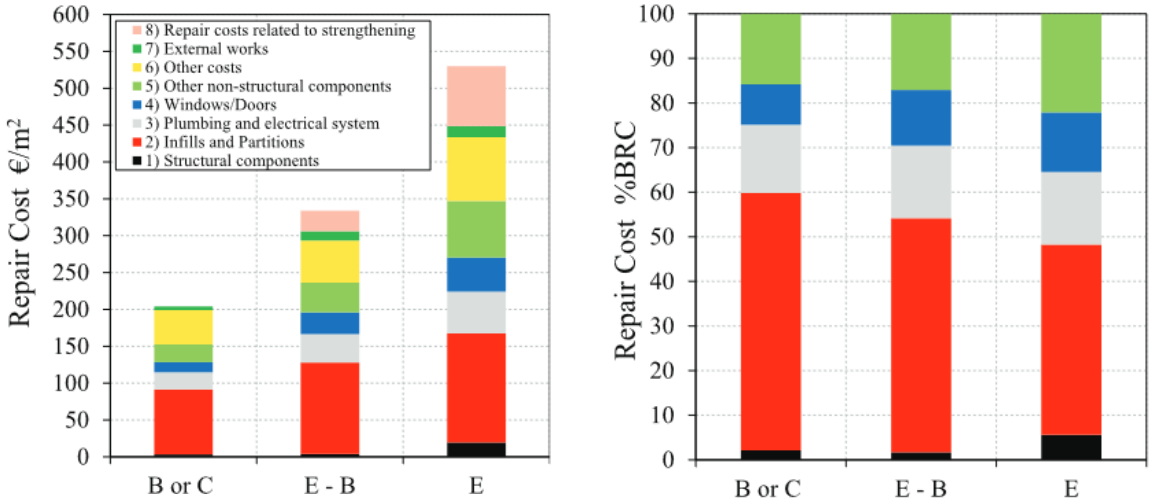

Figure 2.15: Repair costs of RC building component categories expressed: (a) in €/m² and (b) as a percentage of the building repair costs (%BRC) [6].

Most of the repair costs of 57.69% BRC, 52.48% BRC, and 42.63% BRC (B or C, E-B and E usability ratings) are associated with the IPs (brittle component) which are due to the damage experienced during the earthquake since IPs are made of hollow clay bricks and cannot sustain the high lateral force encountered. There is a percentage decrease in repair costs of IPs for E ratings buildings compared to the E-B and B or C, where increases for plumbing and electrical systems, windows/doors, and other non-structural components as the severity of the building increases [6].

2.2.5. Drift and acceleration-sensitive component categories

According to the FEMA P-58, ARCs are grouped in the categories of drift (D) or acceleration (A) sensitive components [22]. Drift-sensitive components are associated with the structural components, infills and partitions (Ips), and windows/doors, while acceleration-sensitive components are associated with plumbing and electrical systems, floor finishing, roofs, tiles, chimneys, sanitary and other equipment, and communication and security (grouped in other non-structural components). Meanwhile, the plumbing and electrical systems (which include electrical cables, pipes, lighting, and rain-drainage systems) are grouped into acceleration and drift-sensitive (A/D) components since it is not easier to determine if they are embedded in the

infill walls or placed externally to the walls or roofs. **Figure 2.16** depicts the mean cost and standard deviations associated with the 120 subsets of buildings, and can also be seen in **Figure 2.17** with 63% to 70% of the BRC associated with drift-sensitive and 15% to 21% that are acceleration-sensitive components [6].

To design and develop an efficient retrofit, it is important to increase the lateral stiffness of the RC structure to reduce the damage caused to drift-sensitive components, which in turn increases the floor acceleration demand on the acceleration-sensitive components, therefore increasing the costs [6].

	Mean repair cost (standard deviation)					
Usability class	B or C		E-B		E	
No. of buildings	52		32		36	
Component category	(€/m^2)	%BRC	(€/m^2)	%BRC	(€/m^2)	%BRC
Drift-sensitive (D)	107.39 (80.70)	70.13	158.86 (56.06)	67.83	214.35 (109.00)	62.68
Acceleration-sensitive (A)	21.80 (23.73)	15.50	39.01 (25.84)	16.47	71.27 (43.65)	21.01
Acceleration- and Drift-sensitive (A/D)	23.35 (23.48)	14.37	38.43 (22.02)	15.70	55.98 (39.24)	16.28

Note that these costs can be normalised by the reconstruction costs of the RC buildings divided by 1213.4 €/m^2.
BRC: building repair cost.

Figure 2.16: Repair costs of drift and acceleration components of the 120 subset buildings [6].

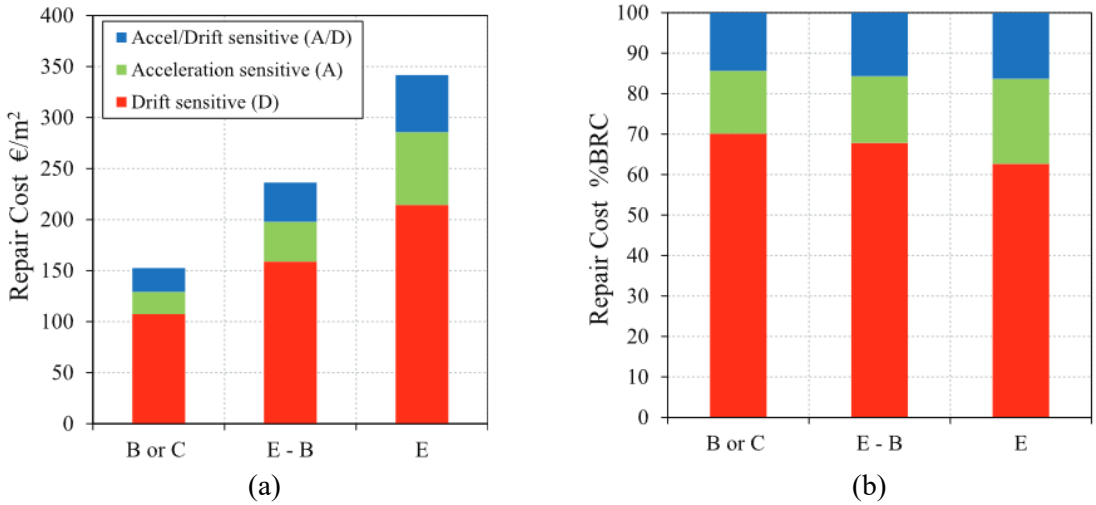

(a) (b)

Figure 2.17: Repair costs of drift and acceleration components expressed: (a) in €/m² and (b) as a percentage of the building repair costs (%BRC) [6].

2.2.6. Relationship between repair costs and building damage state

The building damage state is a function of the damage experienced by the IPs and vertical structural elements as described in AeDES forms. In addition to DS0 (null damage), there are five different DSs which includes: DS1 (slight damage, identified by fine cracking in the plaster or the IPs); DS2 (moderate damage, identified by cracking in the structural elements and IPs); DS3 (substantial to heavy damage, identified by extensive cracking of structural elements and large cracks or the failure of IPs); DS4 (very heavy damage, identified by large cracks in structural elements); and DS5 (destruction, identified by the collapse of the ground floor or other parts of a structure) [6].

Figure 2.18 shows the repair costs associated with the damage state level at the building and component level, including drift (D), acceleration (A), and acceleration/drift (A/D) sensitive component categories in terms of mean and standard deviation. It can be noted that none of the buildings experienced DS5 since they include buildings that experience partial or global collapse that commonly results in their demolition and reconstruction (E_{dem}), with the mean actual reconstruction costs equivalent to 1213.4 €/m^2 [10].

	Mean repair cost (standard deviation)				
Building damage state (DS)	0	1	2	3	4
No. of buildings	10	15	39	40	10
Component category	€/m²	€/m²	€/m²	€/m²	€/m²
(1) Structural components	1.74	4.10	8.49	6.63	10.33
	(3.10)	(6.14)	(20.73)	(9.54)	(24.27)
(2) Infills and partitions	34.48	91.34	108.30	125.44	122.01
	(35.46)	(47.93)	(73.40)	(61.78)	(37.45)
(3) Plumbing and electrical system	6.72	22.46	35.35	45.08	49.53
	(7.84)	(12.49)	(32.86)	(36.11)	(33.01)
(4) Windows/doors	4.42	10.51	23.03	34.21	40.16
	(6.07)	(16.87)	(21.21)	(24.43)	(22.68)
(5) Other non-structural components[a]	14.25	21.20	39.01	50.85	68.83
	(8.82)	(17.72)	(30.93)	(43.14)	(27.08)
Building Repair Cost	75.54	149.62	214.17	262.21	290.86
(BRC = (1) + (2) + (3) + (4) + (5)[b]	(84.65)	(65.50)	(134.76)	(149.28)	(82.02)
(6) Other costs[c]	28.53	50.58	60.13	63.02	73.87
	(28.09)	(26.68)	(45.89)	(55.82)	(34.22)
(7) External works	2.41	5.97	7.93	4.93	8.20
	(5.39)	(16.23)	(16.66)	(10.84)	(8.97)
(8) Repair costs for strengthening interventions	2.10	21.48	23.73	42.33	107.08
	(4.70)	(35.84)	(38.81)	(52.34)	(74.10)
Total Repair Cost	94.45	227.65	305.97	372.49	480.01
(TRC = BRC + (6) + (7) + (8))	(83.31)	(103.23)	(181.91)	(218.75)	(116.26)
Drift-sensitive (D)	41.13	107.08	142.09	167.47	176.81
	(43.86)	(53.67)	(90.50)	(81.69)	(40.94)
Acceleration-sensitive (A)	13.76	20.08	36.05	47.81	64.52
	(8.39)	(17.44)	(30.98)	(42.40)	(22.93)
Acceleration- and drift-sensitive (A/D)	6.72	22.46	35.40	44.60	49.53
	(7.84)	(12.49)	(32.83)	(35.83)	(33.01)

Note that these costs can be normalised by the reconstruction costs of RC buildings divided by 1213.4 €/m².
BRC: building repair cost; TRC: total repair cost.
[a]This includes: stair finishes; floor finishes; roofs and chimneys; sanitary equipment; and communication and security.
[b]This is the sum of the repair costs of all the building components: (1)–(5).
[c]This includes: general costs for construction field installation, safety measures, and professional fees related to repair actions.

Figure 2.18: Repair costs of drift and acceleration components of the 120 subset buildings in terms of damage states [6].

It can be shown from **Figure 2.19** that there is an increase in the TRC and the BRC with DS, which can also be seen in the drift, acceleration, and drift/acceleration sensitive-components categories. **Figure 2.19b** shows that the repair costs of all the building components increase with an increase in DS level. Meanwhile, the repair costs related to IPs for DS3 are almost the same as those of DS4, since, according to the classification adopted for earthquake damage, the collapse of IPs, which results in the highest repair costs, happens in DS3.

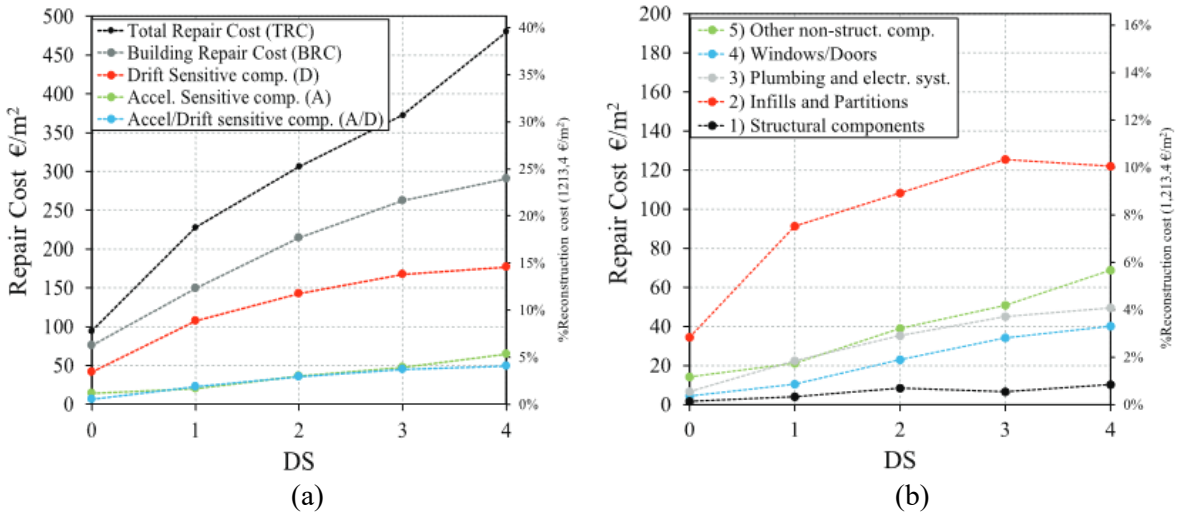

(a) (b)

Figure 2.19: Repair costs in terms of the building damage states at: (a) building level and (b) component category level [6].

A further analysis of the 120 buildings was carried out since there is high dispersion in the previous analysis, as shown in **Figure 2.20a**. This is done by carrying out a detailed analysis of the reports, drawings, and pictures of the damage available in the funding applications for each building and definition of the DSs for IPs (known as DS_{IP}) as proposed by [23] and [24]. Therefore, a further classification of the 120 buildings is divided into: $DS_{IP}1$, known as light cracking; $DS_{IP}2$, known as extensive cracking; and $DS_{IP}3$, known as partial collapse, merged with $DS_{IP}4$, known as global collapse, since there is no marked difference between their respective repair actions and costs, as demonstrated in **Figure 2.21**. The damage extent, q, of the infill walls (expressed in linear meters) of the panels for each of the 120 subsets of buildings belonging to each DS was calculated by summing the total length of each of the damaged panels (i.e., the RC frame clear bay length).

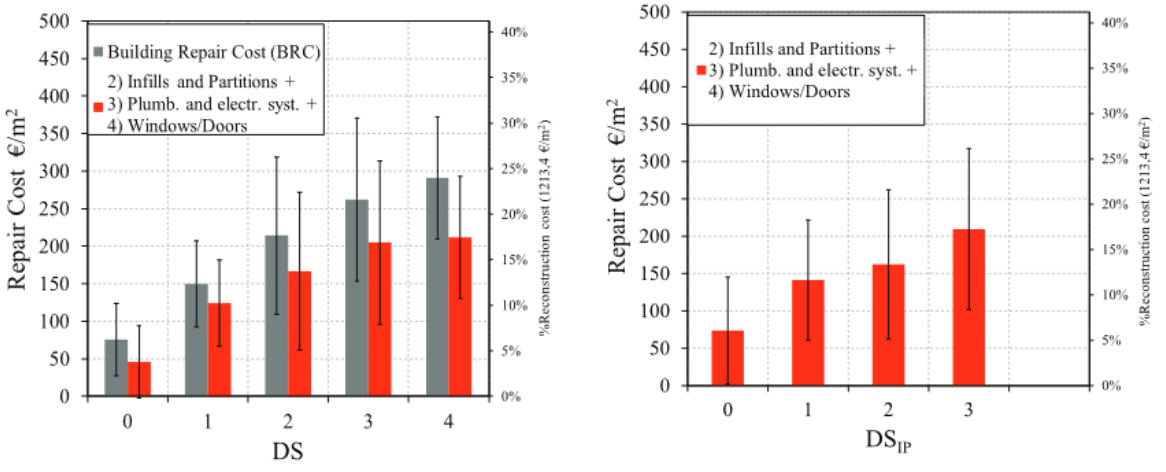

(a) (b)

Figure 2.20: Repair costs infills and partitions at: (a) building damage state level and (b) component category level [6].

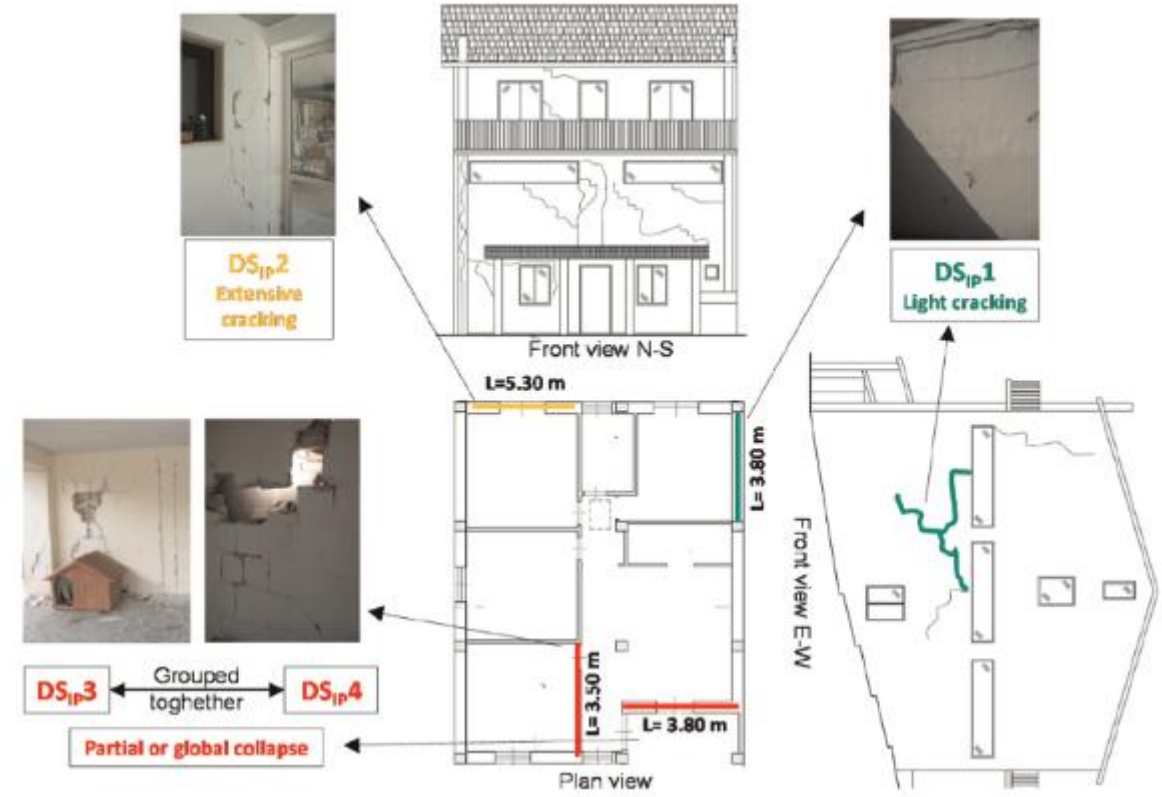

Figure 2.21: Damage category and measured damage severity for infills and partitions acquired from damage reports submitted for funding applications [6].

Considering the repair operations at the panel level, the available cost estimates are analyzed to determine the repair costs necessary to restore the component's functionality. Therefore, the repair costs in relation to repair actions for one part of the panel (replacement of some damaged brick) and the cost related to the full infill panel (such as painting or wall finishes) are summed. As a result, the costs associated with repairs that only involve a part of the panel, for example, replacing a few damaged bricks, as well as those associated with activities that involve the entire infill panel, for example, painting or wall finishes, are added up. Next, each panel in the same DS has its TRC added together and normalized by the overall length of the damaged panel. [6]. Further details can be found in [6].

2.3. Cost and Effectiveness of Fiber Reinforced Polymer (FRP)

Del Vecchio [1] focuses on developing a simple cost analysis tool that best analyzes and quantifies the cost related to the use of FRP materials for seismic strengthening of existing RC structures that suffered during the L'Aquila earthquake (large scale) because the initial costs based on the price lists might lead to significant estimates of the actual costs. This tool, therefore, can be used for assessing the cost-benefit for other retrofit interventions after seismic events.

It was discovered that FRP-strengthening was the technique used the most (34 and 56% of the buildings were subjected to repairs or global retrofitting, respectively) to conduct effective and rapid repairs and achieve an improved seismic performance.

Del Vecchio [1] discovered that the technique most commonly employed was FRP-strengthening, with 34% and 56% of the structures undergoing repairs or global retrofitting, respectively. This method was used to carry out effective and swift repairs while enhancing seismic performance [1]. The expense of putting these solutions into practice was approximately 94.4 €/m^2 for local strengthening and 281.1 €/m^2 for global retrofitting. These costs are less than those linked to alternative strengthening methods. The method most employed was enhancing the shear capacity of unconfined beam-column joints, together with upgrading the connections between infills and the perimeter structure using FRCM. This is since FRPs primarily function by increasing the displacement capacity of the structural framework. As a result, further measures are necessary to safeguard the infills and partitions [1].

It was also discovered that the direct costs incurred for joint shear strengthening typically average around 2051.5 €/member (38.4% RC) for systems focused on local strengthening, and 2939.2 €/member (55.0% RC) for those designed as part of a global retrofit approach. The differences in costs arise from variations in the number of members that are strengthened and the layers used on the joint panels [1].

However, for regular structures with adequate lateral stiffness, FRP strengthening solutions can serve as efficient solutions for seismic strengthening. In fact, this research demonstrated an enhancement of the safety index, ζ_E, from an average value of 0.3 to approximately 0.7 [1].

The findings of this study could be highly beneficial for both researchers and practitioners working to generate initial insights regarding the advantages and associated expenses of seismic-risk mitigation strategies for individual structures or large-scale existing reinforced concrete buildings.

2.4. Structural Strengthening Schemes

Studies [3] focused on enhancing the seismic performance of reinforced concrete exterior beam-column joints (BCJs) through the use of fiber-reinforced polymer (FRP) materials that can be installed from outside the structure, thus reducing the impact on occupants and the overall disruption. The role of FRP wrapping or the use of code-compliant internal reinforcement only acts at reducing the probability of collapse by avoiding the local failures of RC members.

A new innovative strengthening approach, referred to as MinInv, is introduced, which utilizes a blend of carbon fiber-reinforced polymer (CFRP) fabrics and spike anchors. The main outcomes of this research can be summarized as follows:

- Specimen T_1L_12A was reinforced using a single layer of CFRP fabric and 12 anchors, with 2 placed on each side of the columns and beams. This enhancement improved its strength by approximately 12% compared to the original specimen. However, the premature debonding at the beam's end restricted the capacity to fully utilize the CFRP fabric, leading to a joint panel shear failure without the beam's longitudinal reinforcement reaching yielding.
- By employing 16 anchors, i.e. 4 at the ends of each beam and 2 on each side of the columns, the bond was notably enhanced, resulting in the CFRP fibers fracturing in the joint panel. This greater contribution from the FRP system resulted in significant increases in strength, with energy dissipation improved by roughly 24% and 17% in the reference specimen.
- The same number of anchors was insufficient to meet the demands imposed by two layers of CFRP fabric, leading to debonding at the end of the beam in Specimen T_2L_16A. This occurred after the beam’s longitudinal reinforcement had yielded, thus limiting the potential to exploit its full ductile capacity. An observed strength increase ranged from 17% to 25%, alongside a 41% rise in energy dissipation. The existing capacity models for the shear strength of spike anchors effectively predicted the failure mode witnessed (i.e., fiber rupture at the anchor bends). Nonetheless, significant uncertainties arise regarding the accurate assessment of shear demand on the anchors, prompting this paper to suggest a preliminary (and conservative) approach.

- Since most of the damage occurred at the BCJs and top of the columns, the type of strengthening that can be employed is as shown in **Figure 2.22** and **Figure 2.23** respectively.

It should therefore be noted that for the purpose of this thesis, steel fiber reinforced polymer (SFRP), single layer carbon fiber reinforced polymer (SL_CFRP), and double layer carbon fiber reinforced polymer (DL_CFRP) were employed.

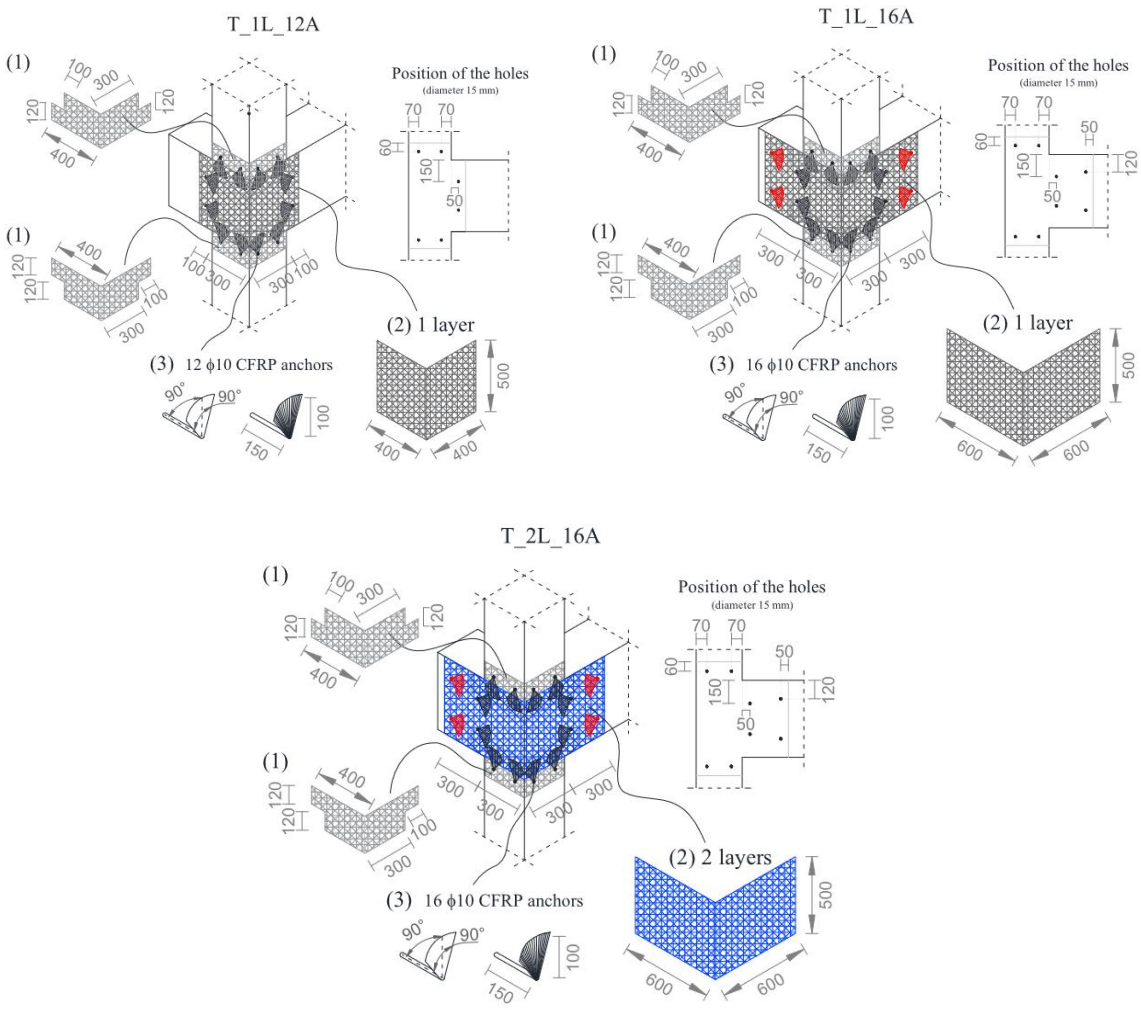

Figure 2.22: FRP strengthening techniques for the BCJs layouts (dimensions in mm) [3].

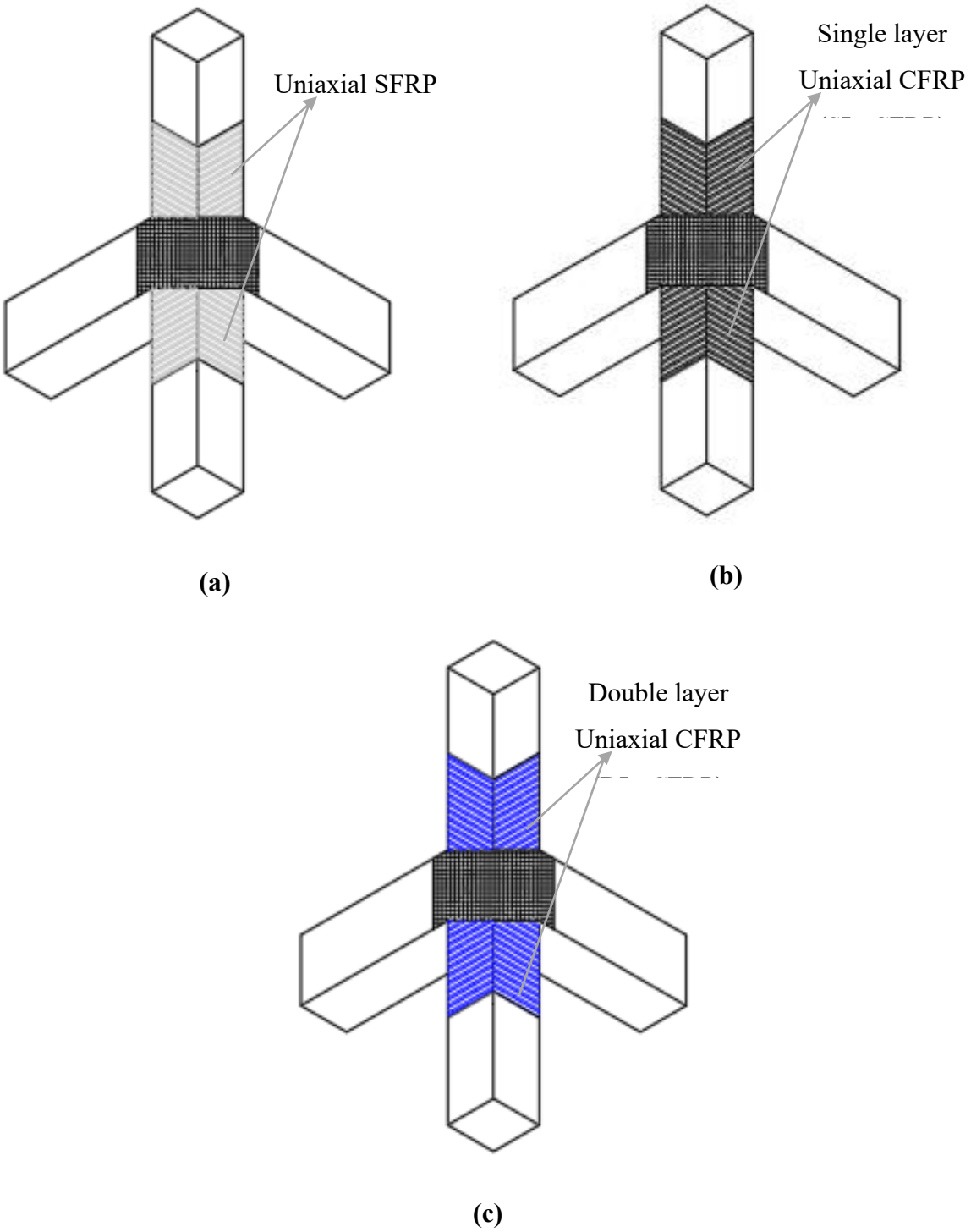

Figure 2.23: FRP strengthening techniques for the column ends **(a)** SFRP, **(b)** SL_FRP**,** and **(c)** DL_FRP

THIS PAGE WAS INTENTIONALLY LEFT BLANK

3. SIMPLIFIED LOSS ASSESSMENT FRAMEWORK

This section presents the method implemented in the framework for loss assessment at the regional scale as shown in **Figure 3.1**. This framework has been developed in MATLAB and was used to perform analysis of 3 case study building (i.e. 2,3 and 4-storey buildings) extracted from L'Aquila database in the as built and FRP strengthened configuration. The FRP strengthening solutions considered include the use of steel fiber reinforced polymer (SFRP), single layer fiber reinforced polymer (SL_FRP) and double layer fiber reinforced polymer (DL_FRP). It should therefore be noted that this analysis is based on seismic and gravity-load designed building cases (i.e. SLD and GLD).

Firstly, a non-linear history analysis (NLTHs) was performed in order to account for the engineering demand parameters which gives an idea on the seismic response of the building. In order to perform this analysis, inputs such as material properties (concrete, steel, FRP), geometrical characteristics (building plan dimension, number of floors, interstorey height, column section sizes, length of infills, and length and height of beam), mass on each floor. **Table 3.1** shows the 7 set of records with the associated scaling factors which depend on the 9-return period T_R both in the X and Y direction. In addition to the mass defined, the strength and stiffness of the hysteretic pivot is also defined as a simplified model for the analysis.

Secondly, using the results obtained from the NLTHs in terms of the EDPs, loss analysis according to FEMA P-58 component-based framework was done using the fragility function and consequence functions which has been developed for both the as-built and FRP strengthened configuration to predict the damage state of the structural exterior, interior and non-conforming beam column joints (BCJs). In particular, three different DSs, namely, light damage (DS1), moderate damage (DS2), and heavy damage (DS3) are considered and adopted for the classification according to [6], [25], [26]**.** With this, the damage state of as-built and effectiveness of the FRP configuration is evaluated.

Table 3.1: Accelerogram and return periods used for analysis.

Direction	Records \ Return period	1	2	3	4	5	6	7	8	9
X	1	0.48	0.63	0.73	0.83	0.96	1.11	1.39	1.66	1.98
	2	0.91	1.18	1.37	1.57	1.78	2.09	2.62	3.13	3.74
	3	5.28	6.86	7.97	9.13	10.35	12.14	14.91	18.18	21.70
	4	1.29	1.67	1.94	2.22	2.52	2.95	3.70	4.42	5.28
	5	2.72	3.53	4.10	4.70	5.33	6.25	7.82	9.36	11.17
	6	3.69	4.78	5.56	6.37	7.22	8.47	10.60	12.68	15.14
	7	0.20	0.26	0.31	0.35	0.40	0.47	0.58	0.70	0.83
Y	1	0.39	0.51	0.59	0.68	0.77	0.91	1.13	1.36	1.62
	2	0.89	1.15	1.34	1.53	1.74	2.04	2.55	3.05	3.64
	3	4.03	5.23	6.08	6.96	7.89	9.25	11.38	13.86	16.54
	4	1.18	1.53	1.78	2.04	2.31	2.71	3.39	4.06	4.84
	5	1.94	2.51	2.92	3.35	3.79	4.45	5.57	6.66	7.95
	6	2.71	3.52	4.09	4.69	5.31	6.23	7.80	9.33	11.14
	7	0.23	0.30	0.35	0.40	0.45	0.53	0.66	0.79	0.94

In the same vein, the probability of collapse and analysis of cost is assessed by arranging the costs in ascending form for all the number of realizations (i.e. 500) to understand the evolution of the total mean costs for each return period. It should therefore be noted that any cost value greater than reconstruction costs assigns the value of the reconstruction cost signifying a collapse. This shows the costs associated with each realization considering the influence of the probability of collapse on these costs for the as-built and FRP configurations.

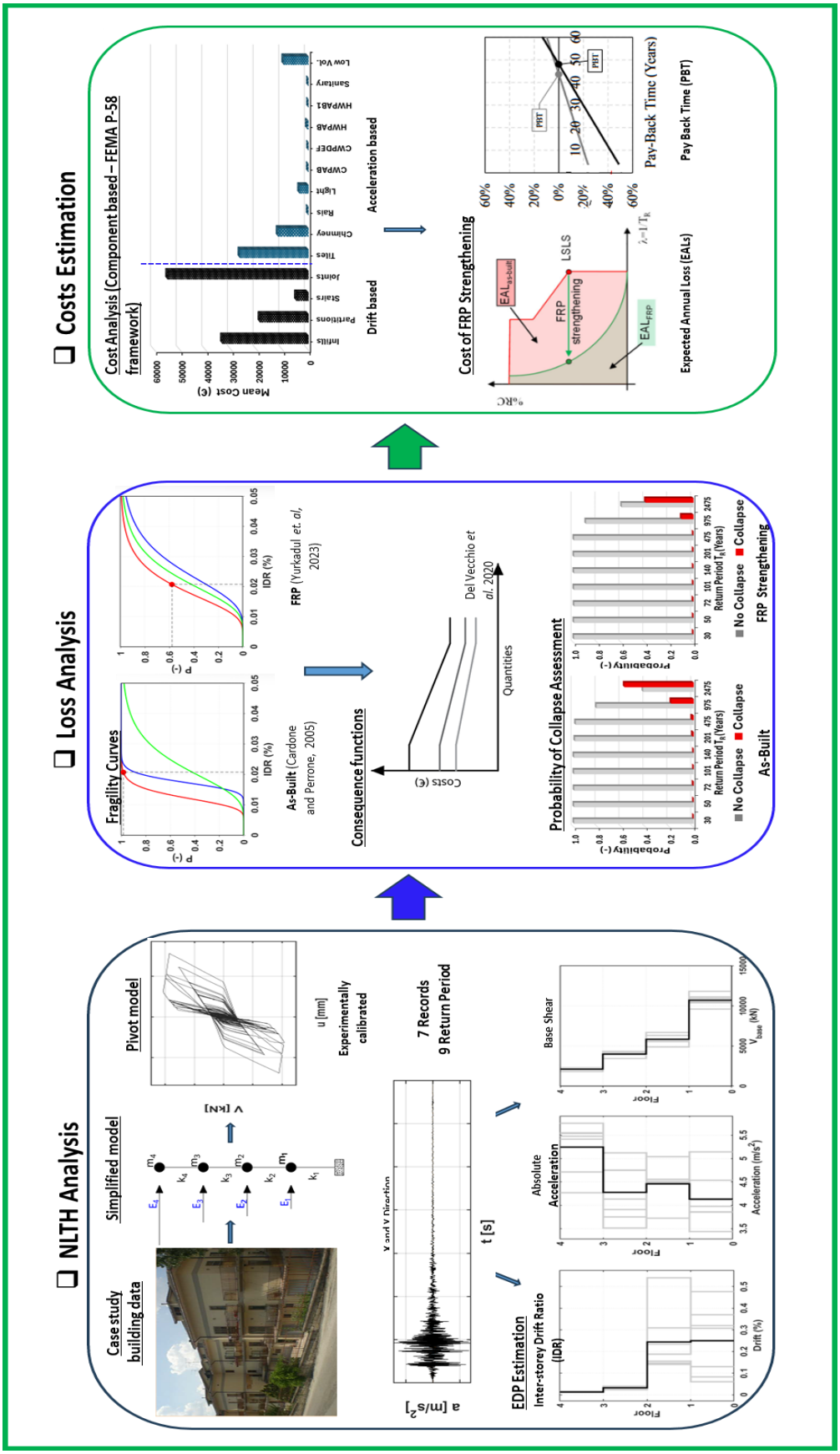

Figure 3.1: Framework for analysis and quantification of the benefit of FRP retrofitting solution.

Lastly, the cost analysis is done using FEMA P-58 component-based framework which classifies the components into drift and acceleration sensitive based components. The drift components consist of the joints (exterior, interior, non-conforming); exterior infill walls (with / without openings and with French windows (Fw); interior partitions (with/without openings and stairs). For the acceleration-based components, it consists of the clay tile roof, masonry chimney, raised access floors, independent lightning, cold water piping (A, B, D, E, F), hot water piping (A, B, B1), sanitary waste and low voltage. This is done for both the as-built and FRP configurations (i.e. SFRP, SL_CFRP and DL_CFRP). Therefore, the repair cost associated with each component and at each return period for the configurations are generated after this analysis.

This framework has been entirely implemented in MATLAB to facilitate loss assessment and reduce the computational demand that can be used as simplified tool by the practitioners and engineers.

As mentioned earlier, some input datas are necessary to be implemented in framework in order to perform the seismic analysis and account for the loss incurred in the as-built and FRP strengthened configurations for both the SLD and GLD cases. This input data contains the main characteristics of the building obtained from the documents obtained from the practitioners during assessment after the seismic event. The characteristics extracted and used as the input data are as follows:

- Building plan dimension (x and y direction): the length in the x direction is associated with the longer direction, and the y in the shorter direction of the building.
- Mass of each floor: the mass of each floor takes into consideration the mass of the beam, columns, floors, infills, stairs, and balcony. This mass is assumed to be 2 tons/m^2 on each floor.
- Number of floors: this is important to account for the number of degrees of freedom required for the analysis.
- Inter-storey height: this is taken as the distance between beam centers on each floor. It is necessary to determine the stiffness of the columns and infill members.
- Numbers, length, and clear height of infills (x and y direction): this is necessary to evaluate the stiffness and the maximum capacity required.
- Column section (minor/base and major/height): this is required to evaluate their contribution to the stiffness (the stiffness of the beams is neglected since an infinitely rigid bending behavior is assumed) and to capacity.
- Effective length and height of the beam (x and y direction)

- Concrete and steel grade
- Reconstruction costs, which are evaluated as the surface area (m^2) x €1350/m^2

The floor includes beam, column (divided into exterior, interior and non-conforming joints), and infills which are arranged and extracted in the direction of X and Y direction as shown in the **Figure 3.2**.

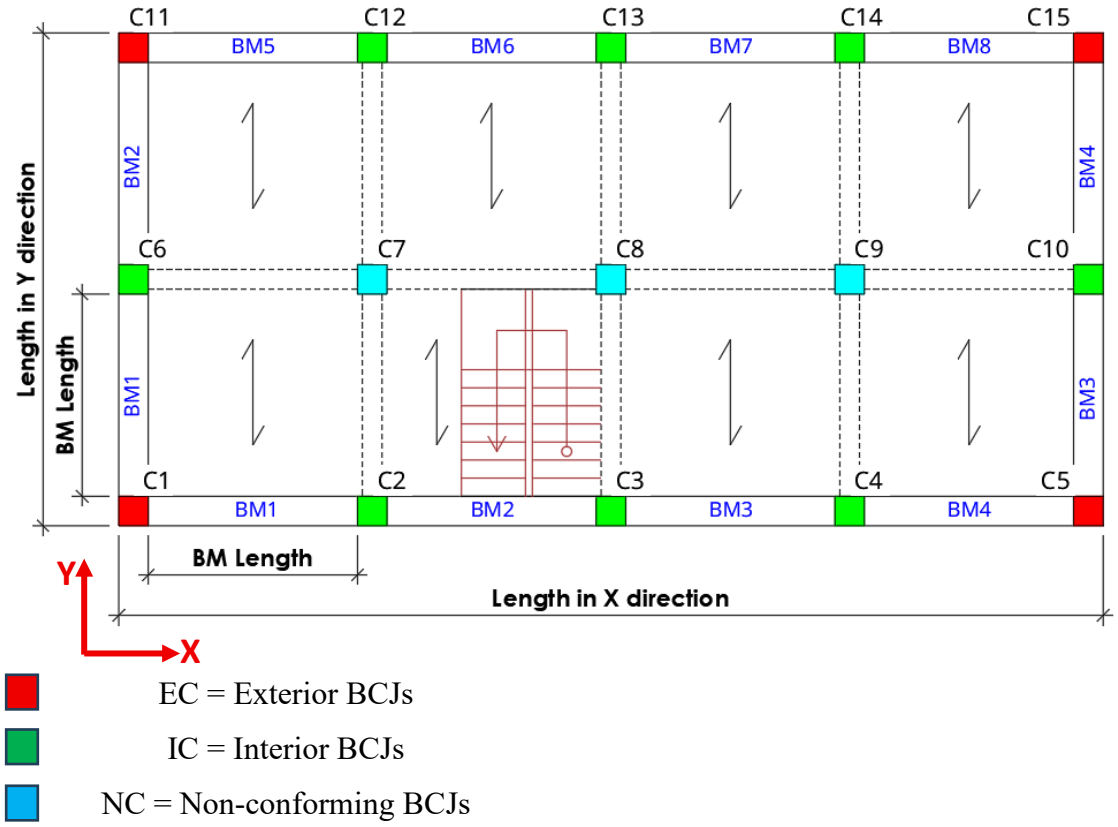

Figure 3.2: Sample of a floor plan.

3.1. Non-Linear Time History (NLTH) Analysis

The structural performance of selected buildings was assessed through nonlinear time history analysis (NLTHs). The building was modelled using a simplified nonlinear numerical model obtained as simplification of a refined model which was experimentally calibrated and validated [7]. The nonlinear response of structural (columns and beams) and non-structural elements (infill) in the refined model is reproduced using a lumped plasticity technique. This technique idealizes the response of infills with a three-strut model with the plastic hinges located at the centre of the element and the extremities of the element for the structural members [27].

In order to capture the pinching effects and stiffness degradation made with the infills (hollow clay blocks), a pivot model is suggested, which is also used to reproduce the hysteresis response of the elements.

The non-linear time history analysis is therefore used to calibrate the pivot model to have a good match with the PsD tests using the same inputs, with the damage also compared. More details on the PsD tests, refined numerical model, calibration, and damage assessment can be found in [7].

The simplified refined model developed starting from the refined model, is implemented to carry out the seismic loss assessment at the regional scale has been developed in MATLAB (The MathWorks Inc. 2022). A 2D multi-degree of freedom (MDOF) model with the number of degrees of freedom associated with the number of building floors and masses lumped at each storey is used in the framework, as shown in **Figure 3.1**. For each storey, their nonlinear response is reproduced with a single non-linear spring to reproduce the experimentally calibrated pivot model [27].

3.1.1. Assessment of Engineering Demand Parameters (EDPs)

A nonlinear time-history analysis using a set of 7 accelerogram (X and Y direction) scaled at 9 return periods is selected and used for analysis to evaluate the seismic behaviour of the selected building and further used to generate the engineering demand parameters (EDPs) in order to perform the loss analysis. The EDPs used are the inter-story drift ratio (IDRs), floor acceleration and inter-storey shear. The EDPs are evaluated for the as-built configuration only because the FRP configurations are assumed to have the same EDPs as the as-built configuration since there is no change is the dynamic properties of the structure using FRP [28]. The EDPs are calculated for the group of NLTHs in both directions, and the numerical method, α-OS SPLITTING METHOD, is employed to solve the MDOF model [29].

3.2. Vulnerability Analysis

The damage evaluation follows the methodology used in PACT some adopted simplifications [22]. The fragility curves for key components sensitive to drift and acceleration include infill, partition walls, beam-column connections, chimneys, tiles, cold/hot water pipes, raised floors, lighting, low voltage systems, and plumbing. These curves are provided along with their mean and CoV values in the PACT library and relevant literature, particularly for recent

advancements concerning infill [30] and beam-column connections [26]. Within the framework of fragility curves, the consequence curve is characterized by two values for quantity and two for cost: upper and lower limits, with a linear function applied to determine the quantity between these bounds.

After the structural analysis has been done, the assessment of damage for each component of the buildings through loss analysis is carried out in the MATLAB framework. This is carried out by using the FEMA P-58 [22] procedure implemented in the PACT software. To obtain a loss curve, a time-based performance assessment that involves different steps as described in the studies [25], is performed for the two configurations, i.e., as-built and FRP strengthened, and described below:

i) Demand simulation: The MATLAB code gives a vector output that contains the EDPs focusing on the peak floor acceleration and peak floor drift ratio at each floor in each direction, which is further compiled. It then generates a matrix that contains the results of one analysis in the rows (7 for each direction) and the values of a demanding parameter in the columns (depending on the number of floors).

   The matrix entries are assumed to be a joint lognormal distribution and are manipulated to compute a vector of median demands (the median vector derived from the set of analyses), variances (or dispersion), and a correlation matrix indicating how each demand parameter varies to the other demand parameters in the set.

ii) Collapse Assessment: The framework accounts for the probability of the collapse in the analysis of losses in order to quantify the benefits of FRP strengthening that mainly increase the performance at ultimate limit states which takes into consideration the loss of the total value of the building when there is structural collapse occurs. This is based on the interstorey drift ratio (IDR) and interstorey shear estimated from the NLTH analysis carried out using the validated simplified model. In the framework, the Sidesway Global Collapse (SGC) and Gravity Load Collapse (GLC) are considered for the assessment in the simplified model as proposed by De Risi *et al.* [31]. It should however be noted that this model only considers the infill degradation and does not explicitly consider the strength degradation in RC members. For SGC to occur, it is assumed that 50% of the RC components have failed in shear on the same floor level, taking into consideration the failures under that occurred in both the directions as shown in **Figure 3.3**.

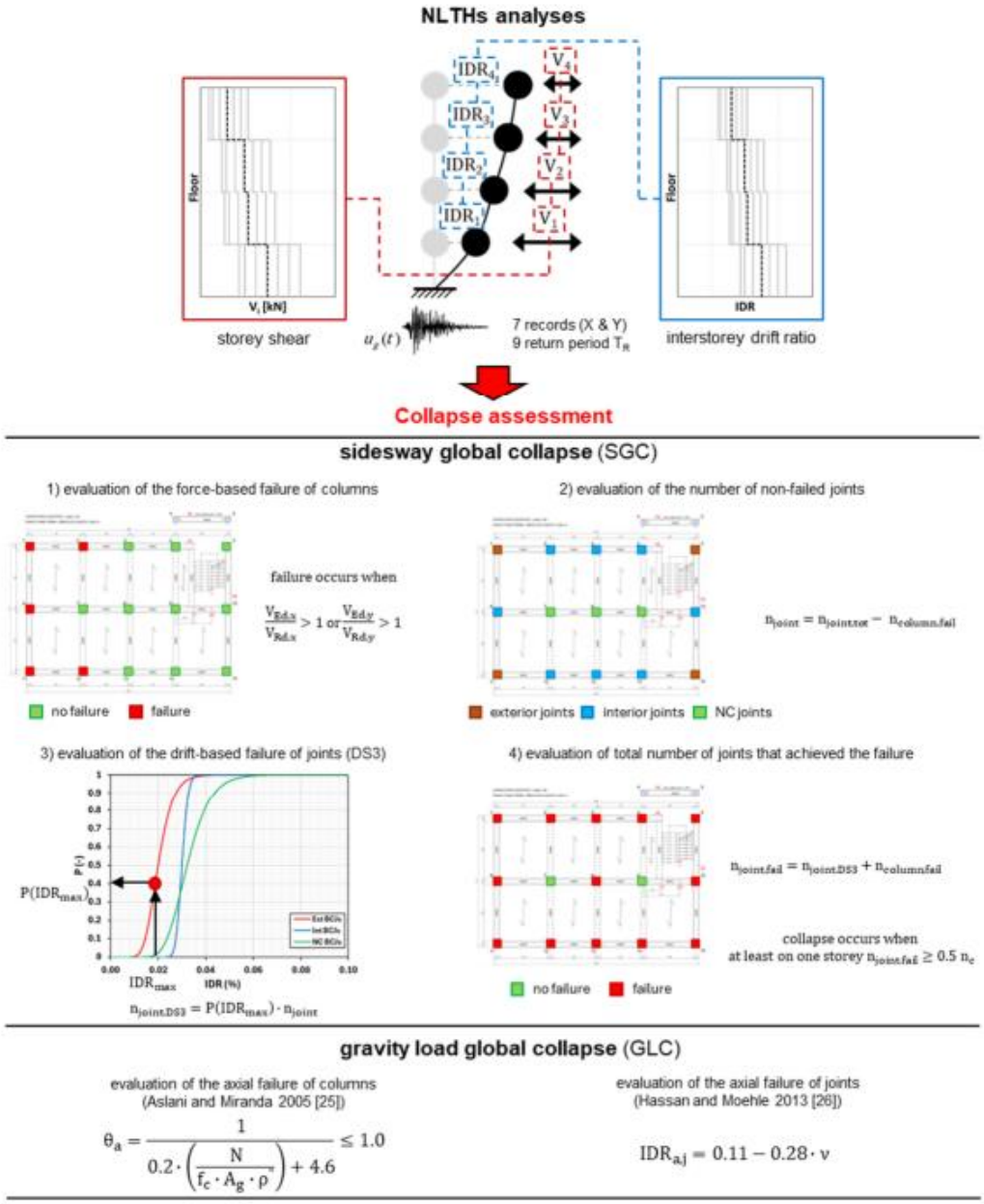

Figure 3.3: Collapse assessment approach used for Sidesway Global Collapse (SGC) and Gravity Load global Collapse (GLC) [38].

iii) Loss Calculation: The definition of DS allows one to evaluate the loss to realization using the consequence curve for each performance group uploaded in the script with the upper and lower bounds for quantity and cost (a hypothetical consequence curve is shown in Figure 60. The valuation of losses, assuming a simplified approach, is done by identifying the quantity on the curve related to the group of outputs analyzed and determining the corresponding cost value. The quantities of each performance group are identified in different ways. For the infill and beam-column joint, they are calculated from the design documents, while for the other components

used in the work, a tool provided by the ATC must be used. For a single structure, the total damage is the sum of the damage sustained by each performance group evaluated as described above. Loss distributions are developed by repeating the calculation of damage and loss for a large number of realizations and sorting the values in ascending (or descending) order to allow calculation of the probability that the total loss will be less than a given value for a given intensity of earthquake (intensity-based assessment). For example, if damage calculations are performed for 1,000 realizations and the realizations are compiled in ascending order, the repair costs with a 90% probability of exceedance are the repair costs calculated for the realization with the 100th largest cost, since 90% of the realizations had higher calculated costs (ATC - Applied Technology Council 2012a)

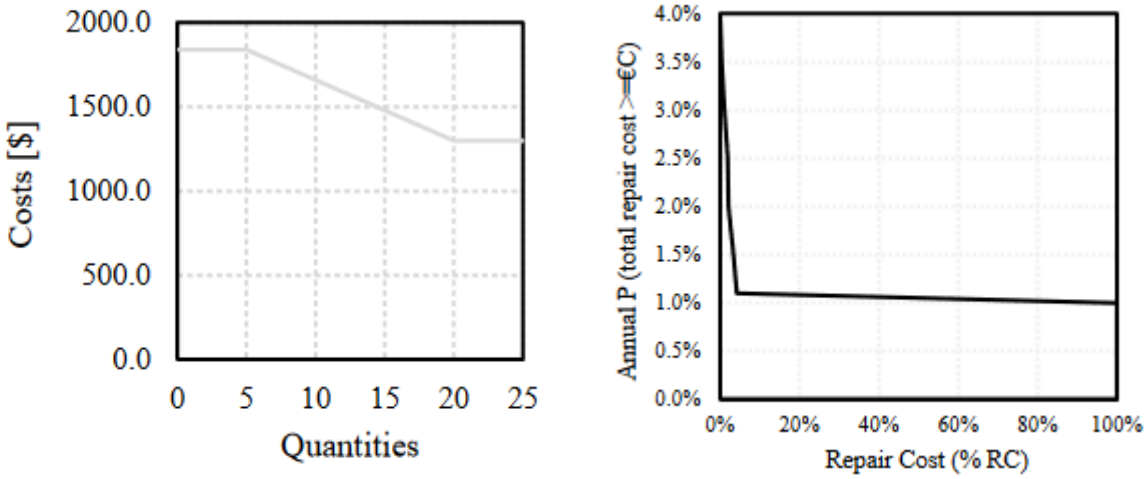

(a) (b)

Figure 3.4: Hypothetical consequence curve and loss distribution [32].

3.2.1. Design of the retrofit alternatives and collapse definition

The analysis of the shear failure of columns and beam-column joint for each direction and at each floor of buildings are performed for the as-built and FRP-strengthened configuration.
The number of failed RC members is calculated combining force and drift-based approaches. The force-based approach involves the computation of the number of columns that failed in shear by comparing the shear demand with the capacity of the cross-section. The shear capacity of as-built RC columns is computed according to Biskinis *et al.* [33], while the fib bulletin 90 [34] is used to calculate the contribution of the FRP strengthening [19]. The drift-based

approach on the other hand is used to assess the failures at beam column joint which may occur at high displacement.

From this analysis, the number of columns that did not fail in shear is estimated and the number of joints that have achieved a damage state (DS3) is evaluated according to the drift-based approach and attached with specific probability of occurrence of a DS3. The number of failed RC components is then computed using the fragility functions proposed by Cardone and Perrone [30] and Yurkadul *et al.* [26] for as built and FRP strengthened BCJs taking into the consideration the maximum IDR estimated from the NLTHs analysis.

The formular according used for the calculation of the shear capacity for both the as-built and FRP strengthening configuration is presented below:

The as-built is verified by comparing the demand evaluated through NLTHs with the capacity of the column that can be evaluated using the formula obtained from Eurocode 8 (CEN 2004a), which is also known as Bikinis' formular, shown in **Equations (3.1) to (3.6).**

$$V_R = \frac{1}{\gamma_{el}}[V_N + k_{el}(V_w + V_c)] \tag{3.1}$$

where:

V_R is the total shear capacity of the column.

γ_{el} is taken as 1.15

$$V_N = \frac{(h-x)}{2L_v} * min(N; 0.55 f_c A_c) \tag{3.2}$$

h is the total height of the cross-section.

x is the depth of the neutral axis (height of the compression part of the cross-section), assumed to be the concrete cover.

L_v is the cutting gap.

N is the axial compressive force evaluated using the area of influence of the column.

f_c is the compressive resistance of concrete.

A_c is the area of the cross-section.

$$k_{el} = 1 - 0.05 * min(5; {\mu_\Delta}^{pl}) \tag{3.3}$$

$${\mu_\Delta}^{pl} = \frac{\theta_m - \theta_y}{\theta_y} = \mu_\theta - 1 \tag{3.4}$$

where:

$\mu_{\Delta,pl}$= the ratio between the plastic part of the chord rotation and the yielding rotation.

k_{el} is assumed to be equal to 1, i.e., no deterioration in shear, as shown in **Figure 3.5** which is justified by the premature failure due to a lack of seismic details.

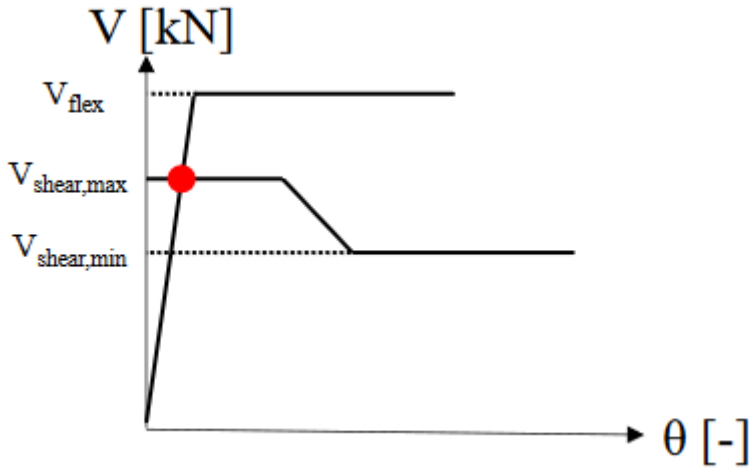

Figure 3.5: Shear behaviour for cyclic load.

$$V_w = \frac{A_{sw}}{s} f_y (h - c) \tag{3.5}$$

where:

V_w is the shear provided by transverse reinforcement.

A_{sw} is the area of stirrups.

s is the distance between two stirrups.

$$V_c = 0.16 * max\,(0.5; 100\rho_{tot}) \left(1 - 0.16 * \min\left(5; \frac{L_v}{h}\right)\right) \sqrt{f_c} A_c \tag{3.6}$$

where:

V_c is the shear resistance contributed by concrete.

ρ_{tot} is the geometrical percentage of longitudinal steel.

The analysis is performed on a set of 7 accelerogram (X and Y direction) scaled at 9 return periods. For each story, the failed columns in the x and y directions are combined to determine the total number of columns that collapsed. The collapse is determined when 50% of the element in the first return period fails on the floor. The minimum return period between all floors is the return period of the collapse of the structure.

This same procedure is followed for the FRP-strengthened configuration system, only for the columns that failed in the as-built configuration. The FRP capacity is evaluated as described in Fib Bulletin 90 [34] and the Italian guidelines, which are shown below:

$$V_{R,FRP} = t_f * f_{ffd} * w_{f,max} \quad (3.7)$$

where:

t_f is the thickness of steel fiber reinforced polymer (SFRP) and carbon fiber reinforced polymer (CFRP) equal to 0.266 mm and 0.164 mm, respectively.

f_{ffd} is the design resistance of FRP calculated as below

$$f_{ffd} = \eta * \frac{f_d}{\gamma_{FRP}} \quad (3.8)$$

where:

η is the coefficient equal to 1.

f_d is the resistance of steel fiber reinforced polymer (SFRP) and carbon fiber reinforced polymer (CFRP) equal to 2580 MPa and 4900 MPa, respectively.

γ_{FRP} is equal to 1.1.

$$w_{f,max} = B * cos\,\theta \quad (3.9)$$

where:

$w_{f,max}$ is the FRP maximum usable length.

B is the base or H, which is the height of the column, in case of the other direction.

θ is the angle of FRP application assumed to be 45°.

After the collapse is evaluated for the as-built configuration, the FRP strengthened solutions only consider the return period that identifies the collapse of the elements, taking into consideration that if 50% of the elements fail, the next return period is calculated just as it was done for the as-built configuration after failure occurred. This is important to obtain the safety index of the FRP strengthening techniques.

3.3.Costs Estimation

The cost estimation is calculated for both the as built and strengthened techniques (SFRP and CFRP) in terms of component level and at different return periods. This gives an idea of the cost associated with each component type, i.e., drift and acceleration-based component as well as the effects of the FRP strengthening on the costs associated to the beam column joints (BCJs). The drift element consists of the joints (exterior, interior, non-conforming); exterior infill walls (with / without openings and with French windows (Fw); interior partitions (with/without openings and stairs). For the acceleration-based elements, it consists of the clay tile roof,

masonry chimney, raised access floors, independent lightning, cold water piping (A, B, D, E, F), hot water piping (A, B, B1), sanitary waste and low voltage.
The cost for the FRP is evaluated by considering three elements: a price of 2051.5 €/element, a cost of 81.37 €/m^2 for the strengthening linked to the intervention, which is acquired from the document owner if feasible; if not, a cost equal to 40% of the total reconstruction expense is assumed, with the reconstruction valued at 1350 €/m^2.

3.4. Case Study Building

Three RC buildings selected from the database realized after the reconstruction process of the L'Aquila earthquake were used as a case study. These buildings are 2, 3, and 4 storeys, respectively and are assumed regular in plan and in height and are characterized by poor quality concrete and lack of transverse reinforcement details.

3.4.1. Four-storey building

The four-storey building selected is one of the heavily damaged buildings after the L'Aquila events. It is 39.2 m x 9.7 m in plan as shown in **Figure 3.7**. Meanwhile, since the existing MATLAB framework is developed to analyse a regular building, the case storey building is assumed to be regular by aligning the building plan to be rectangular. The total height of the building is 11.65 m with inter-storey heights of 2.65 m from the ground floor to first floor, and 3.05m for the subsequent floors to the last floor, as shown in **Figure 3.8**. This building, therefore, relies on RC moment resisting frames available in the main directions of the building, i.e., x-direction. It can be observed that the structural system consists of eleven frames in the longitudinal (x) direction, three frames in the transverse (y) direction, and a staircase to access the subsequent floors. The infill lengths are 4.5 m and 4.7 m in the y-direction and vary from 3.5 m to 4.65 m in the x-direction. The building consists of a square column cross-section of 0.4 m x 0.4 m. The beams consist of a rectangular section with the perimeter beams having a 0.15 m width and 0.45 m height, while the internal beams are of 0.15 m height.

Figure 3.6: Case study building after the L'Aquila earthquake, 2009.

Figure 3.7: Case study building first floor plan (4-storey building).

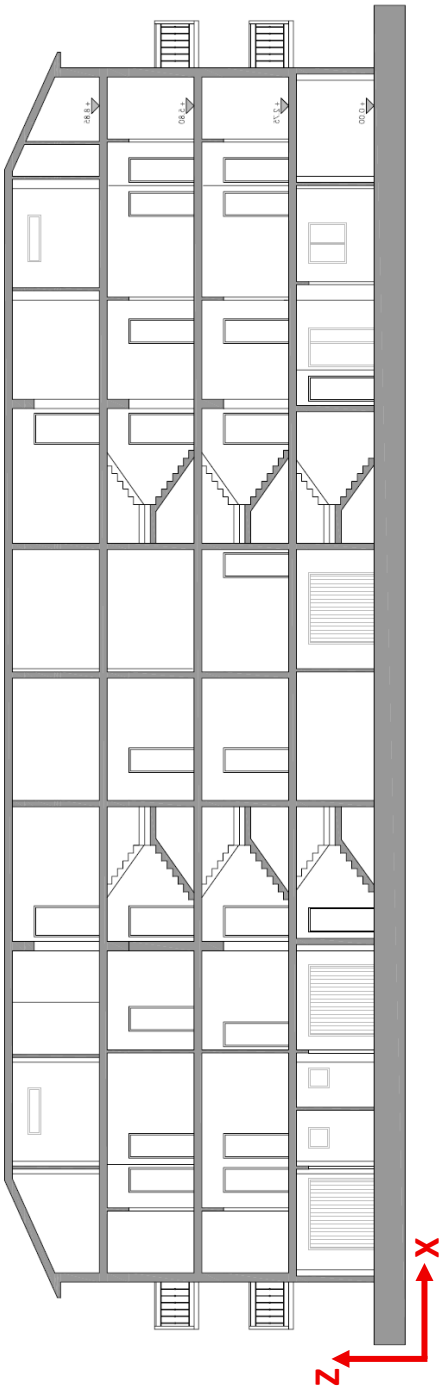

Figure 3.8: Case study building cross-section view (4-storey building).

3.4.2. Three-storey building

The three-storey buildings selected are the second case of the heavily damaged buildings after the L'Aquila events. It is 11.2 m x 9.3 m in plan as shown in **Figure 3.9**. As it was stated earlier, the MATLAB framework is designed to analyse a regular building; therefore, the case storey building ignored the part of the building with no frame to have a rectangular plan surrounded

by columns. The total height of the building is 8.75 m with inter-storey heights of 2.55 m from the ground floor to first floor, and 3.1 m from first to second floor, and from second floor to the roof floor as shown in **Figure 3.10**. It can be observed that the structural system consists of three frames in the longitudinal (x) direction (ignoring the column not aligned with the others), three frames in the transverse (y) direction, and 2 staircases to access the subsequent floors. The infill length is 4.5 m in the y-direction and varies from 4.8 m and 5.15 m in the x-direction. The building consists of rectangular columns with cross-sections of 0.3 m base (minor direction) and 0.5 m and 0.7 m in height (major direction). The beam's section is rectangular, with the perimeter beams having a 0.5 m height and the internal beams consisting of 0.2 m height.

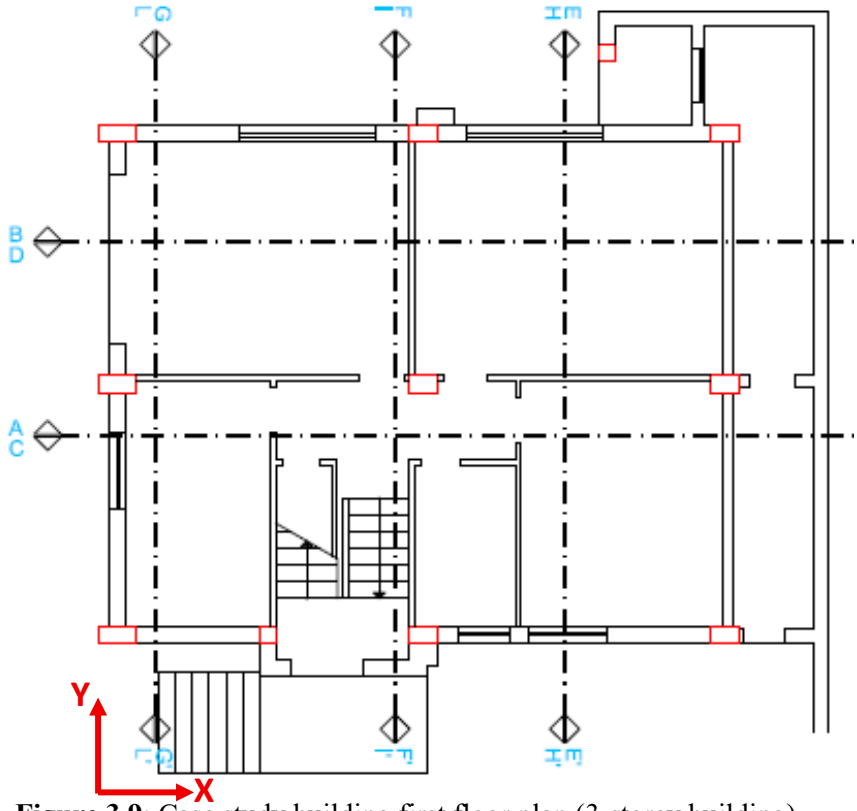

Figure 3.9: Case study building first floor plan (3-storey building).

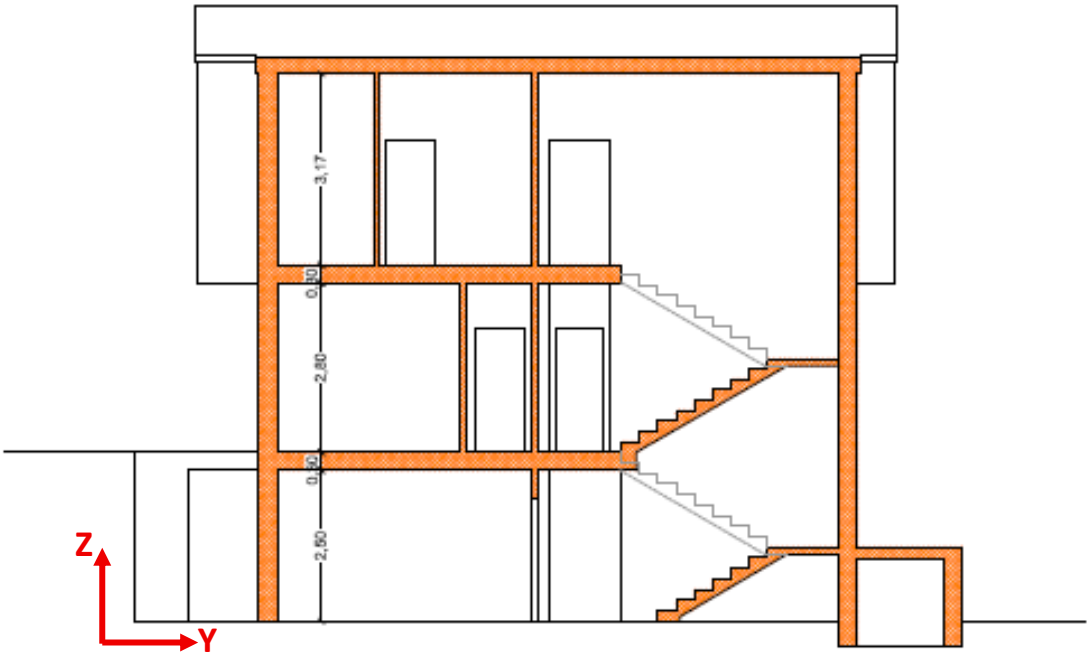

Figure 3.10: Case study building cross-section view (3-storey building).

3.4.3. Two-storey building

The two-storey buildings selected are the third case of the heavily damaged buildings after the L'Aquila events. It is 20.1 m x 11.7 m in plan as shown in **Figure 3.11**. As it was stated earlier, the MATLAB framework is designed to analyse a regular building, therefore, the case storey building is assumed to be rectangular by focusing on the longer side of the x and y directions. The total height of the building is 6.39 m with inter-storey heights of 3.15 m from the ground floor to first floor, and 3.24 m from first to the roof floor as shown in **Figure 3.12**. It can be observed that the structural system consists of five frames in the longitudinal (x) direction (ignoring the column not aligned with others), three frames in the transverse (y) direction and 1 staircase to access the other floors. The infill length varies from 5.7 m to 6.05 m in the y-direction and varies from 3.9 m and 5.15 m in the x-direction. The building consists of square and rectangular columns with cross-sections of 0.4 m base (minor direction) and of 0.4 m and 0.9 m in height (major direction). The beams cross section is rectangular in shape with the perimeter beams and the internal beams having 0.55 m height.

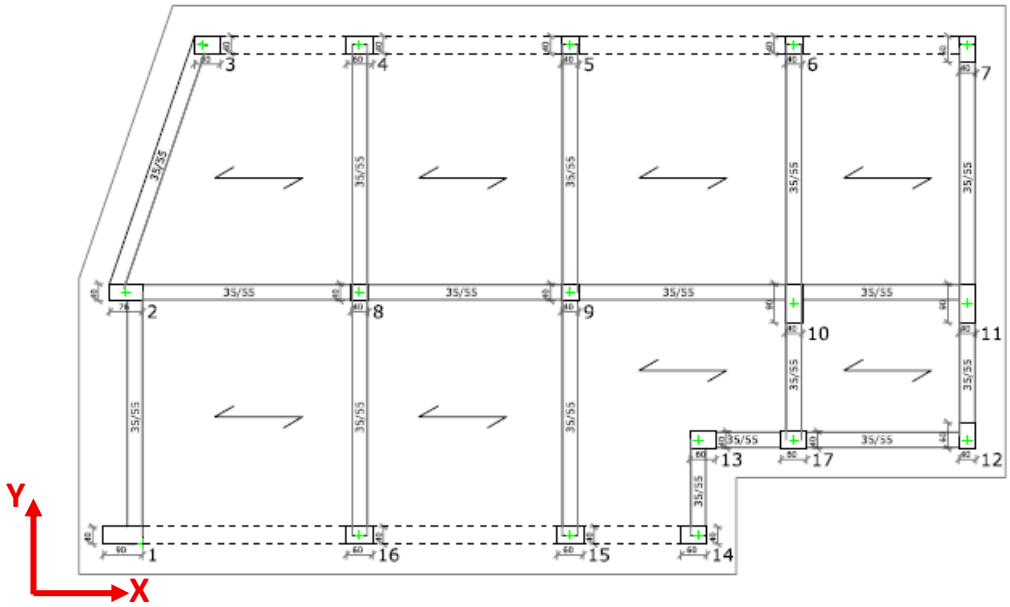

Figure 3.11: Case study building first floor plan (2-storey building).

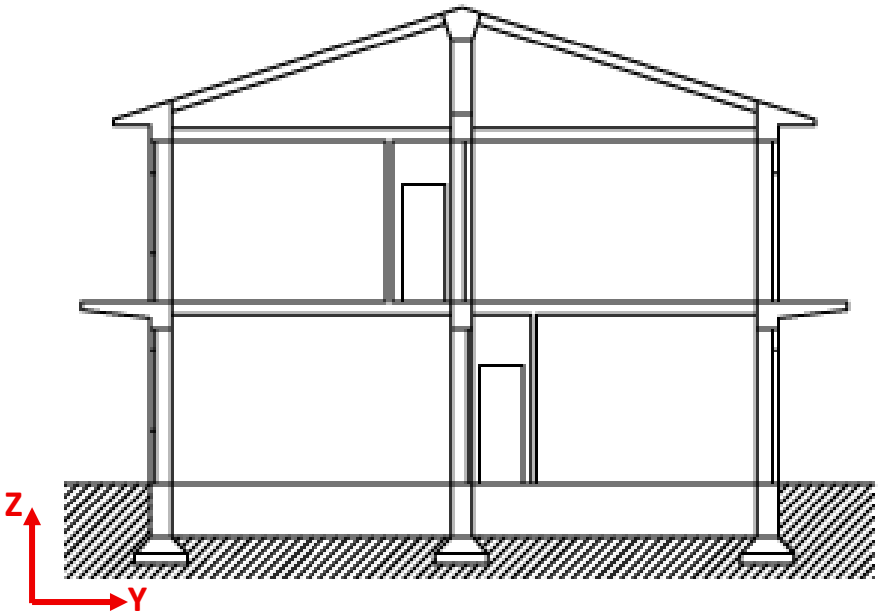

Figure 3.12: Case study building cross-section view (2-storey building).

THIS PAGE WAS INTENTIONALLY LEFT BLANK

4. ANALYSIS OF SEISMIC LOAD DESIGNED BUILDINGS

This section shows the result in terms of the result obtained from the analysis perform on the seismic load designed buildings. The results include the engineering demand parameters (i.e. interstory drift ratio, peak floor accelerations, and interstorey shear) which is used in determining the collapse exhibited by the beam column joints. In addition, the probability of collapse in relation to the cost of the strengthening was also discussed. Also, the repair cost at component level which help to understand the component that is most affected during the seismic event is also analysed and discussed. Lastly, the repair cost at each return period is determined and analysed for the as-built and FRP strengthened configuration of the three case study buildings. With this, the effectiveness of FRP for strengthening is evaluated to in terms of reduction in collapse and cost of the seismic load designed buildings.

4.1. Engineering Demand Parameters (EDPs)

The simplified nonlinear model implemented in the seismic loss assessment framework was validated by comparing the results of the case study buildings. The seismic performances of the case study buildings were simulated utilizing the nonlinear time history analyses. The NLTH analyses is performed on set of 7 accelerogram (X and Y direction) scaled at 9 return periods. This has been modified to perform the analysis in the two directions with the AQG signal scaled from 10% to 150%. For each of the return period, the EDPs result are obtained in terms of the in terms of inter-storey drift (IDR), acceleration, and interstorey shear which are necessary to for the loss- assessment analyses. The choice of these picked EDPs is because most of the fragility curves in literatures used this for intensity measures and collapse predictions.

The seismic analysis consists of a nonlinear time-history analysis performed using as input the original signal of the 2009 L'Aquila earthquake (PGA of 0.45 g) recorded by the AQG station in the E-W direction.

The results obtained from the analysis performed with the proposed framework for the three buildings were compared in terms of inter-storey drift (IDR), acceleration, and interstorey shear in both directions and picked for the maximum record which the 3rd records with its corresponding return period of 475 years (LSLS) and 2475 years i.e. 7th and 9th return period. These results are described as follows.

4.1.1. Interstorey Drift Ratio (IDR)

The result in terms of IDR obtained from the analysis performed for the selected buildings modelled using a nonlinear simplified model are shown in **Figure 4.1**. It can be shown that the maximum mean drift (indicated with a black line on the graph) is concentrated on the first floor for all the case study buildings (4, 3, and 2 storey buildings) in the X direction, with the maximum value of about 0.25% IDR achieved in the 4-storey building type. In the Y direction, the drifts are also concentrated on the first floor except for the 4-storey building type, which was concentrated on the second floor with 1.36% drift. This is due to the higher stiffness observed on the first floor due to a shorter height on the ground floor.

On the other hand, at a higher return period of 2475 years, the drift behaviour was the same as for 475 years, but with a maximum value increasing by about 68% for the 4-storey building type in the X direction. Meanwhile, for the Y direction, there was an increase of about 40% for the maximum drift observed on the second floor of the 4-storey building type. This is as shown in **Figure 4.2**.

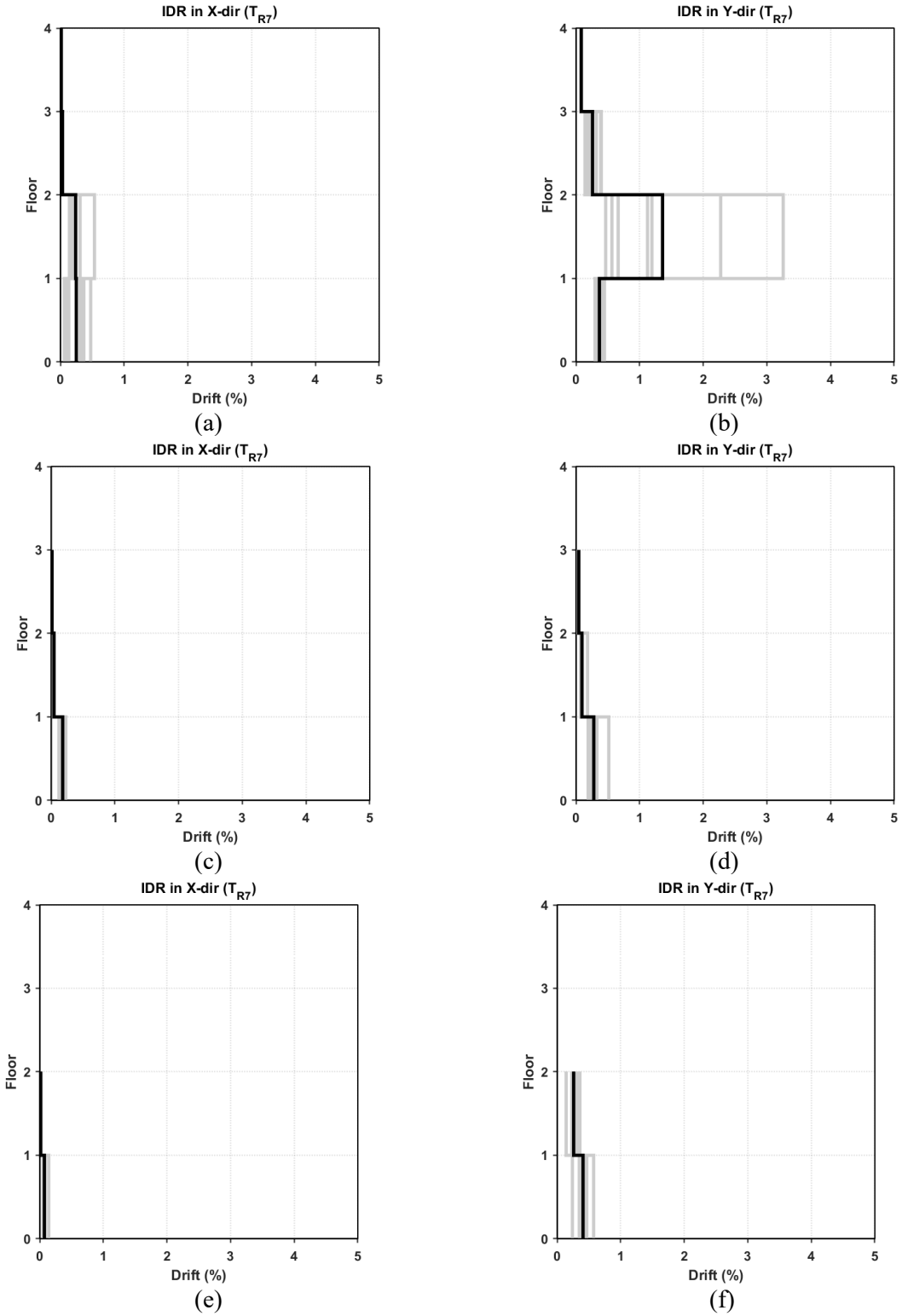

Figure 4.1: Inter-storey drift ratio (IDR) for seismic design buildings at a 475-year return period in X and Y direction: **(a)** and **(b)** 4 storey, **(c)** and **(d)** 3 storey, and **(e),** and **(f)** 2 storey.

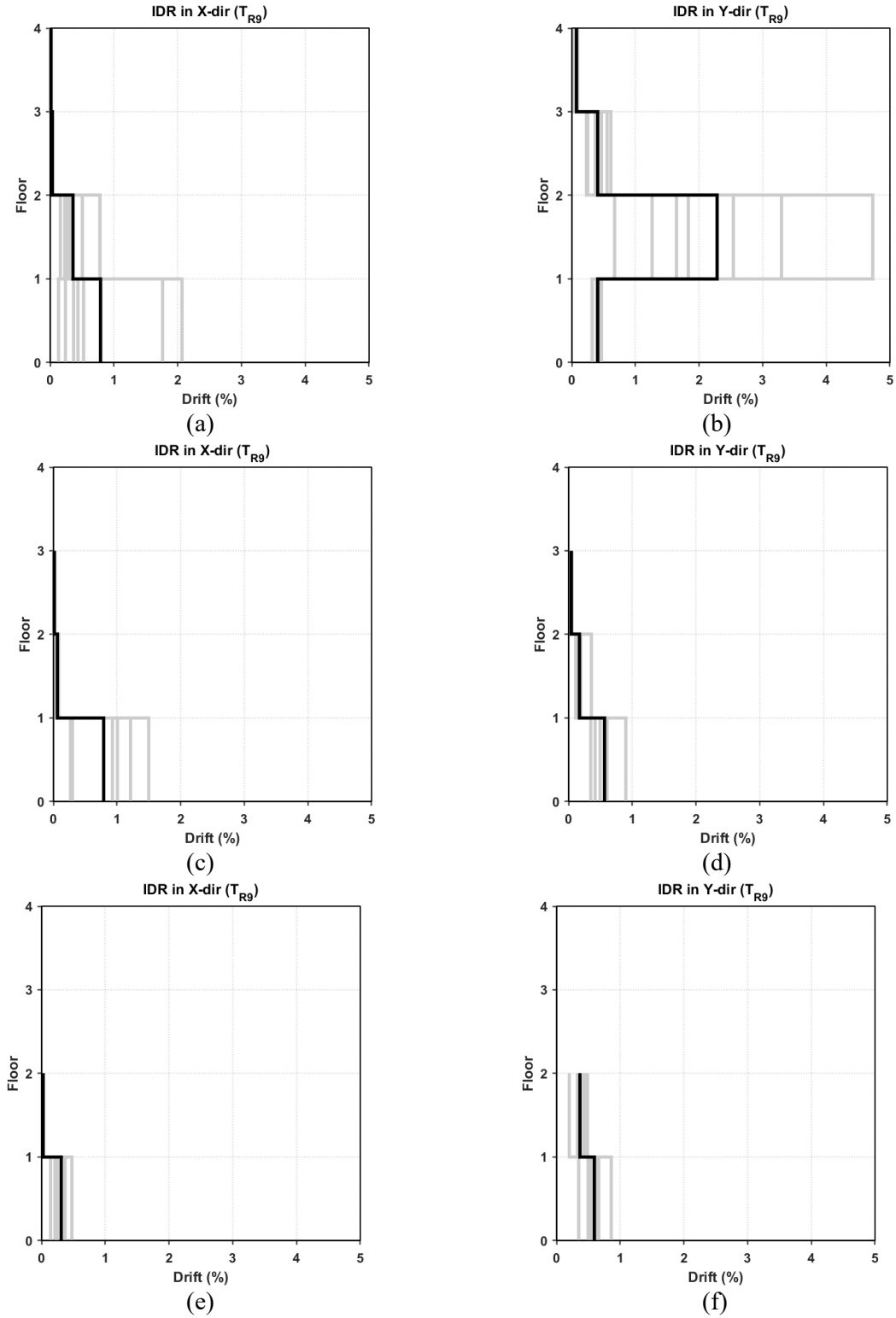

Figure 4.2: Inter-storey drift ratio (IDR) for seismic design buildings at a 2475-year return period in X and Y direction: **(a)** and **(b)** 4 storey, **(c)** and **(d)** 3 storey, and **(e),** and **(f)** 2 storey.

4.1.2. Peak Floor Acceleration (PFA)

The result in terms of PFA obtained from the analysis performed for the selected buildings modelled using a nonlinear simplified model are shown in **Figure 4.3**.

The higher acceleration shows that the higher numbers of floors result in amplification at the last floor. In the Y direction, there was a higher acceleration of about 4.2 m/s^2 on the first floor in the case of 4-storey building, which might be due to more amplification experienced in that direction. For the 3 and 2-storey, the last floor experiences higher floor accelerations. This can be seen on **Figure 4.3**.

At a higher return period of 2475 years, the floor acceleration increases to 5.6 m/s^2, 5.6 $m/s^{2,}$ and 6 m/s^2 for the 4, 3, and 2 storey building types, respectively, in the X-direction. In the Y direction, there was a higher acceleration on the first floor in the case of 4 4-storey building of about 5.7 $m/s^{2,}$ as it was in the X direction. Meanwhile, for the 3 and 2-storey buildings, there was also about a 10-25% increase in the floor acceleration on the last floor. This is as shown on **Figure 4.4**.

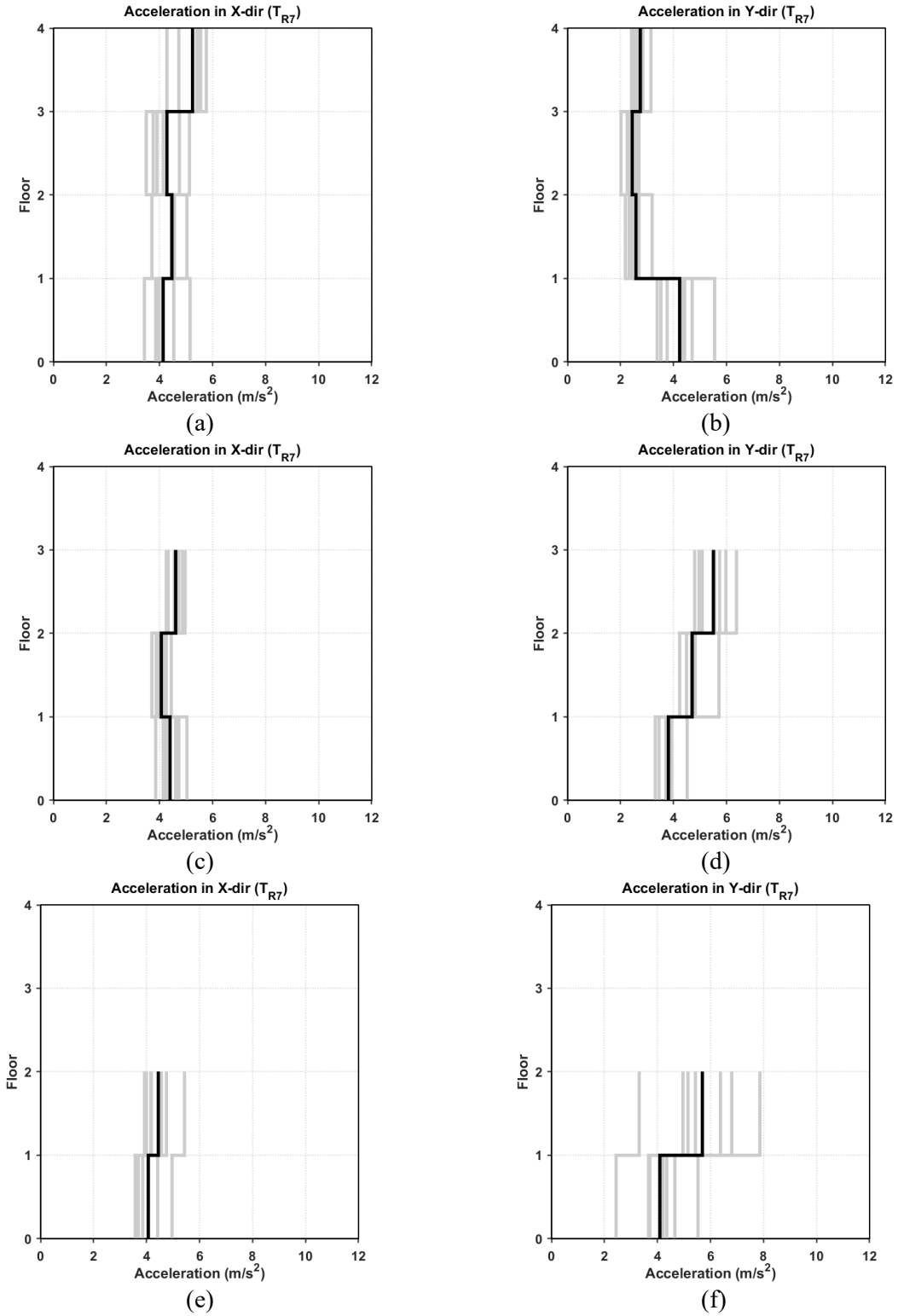

Figure 4.3: Peak floor acceleration (PFA) for all the case study seismic design buildings at 475 years return period: **(a)** and **(b)** 4 storey, **(c)** and **(d)** 3 storey, and **(e),** and **(f)** 2 storey.

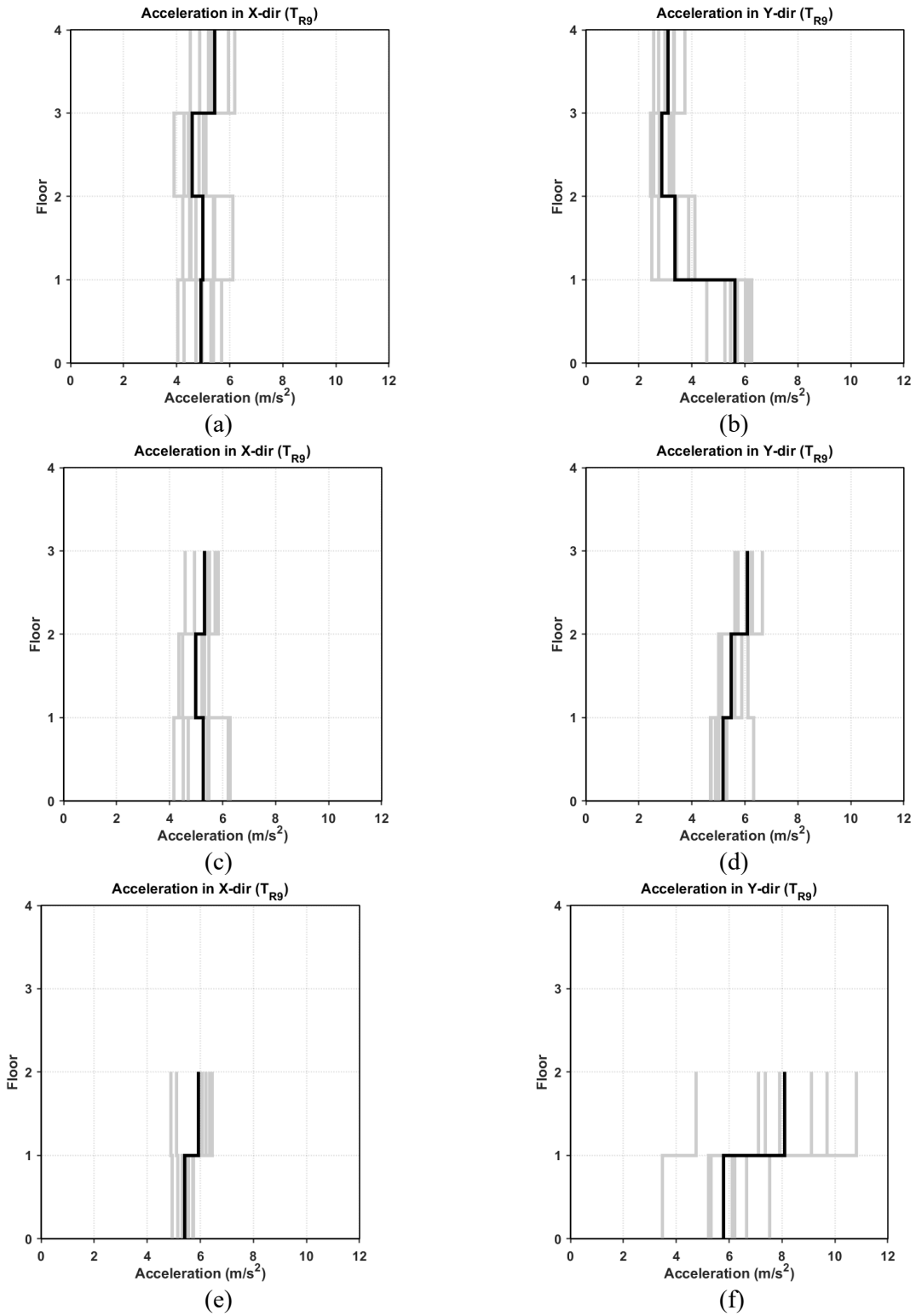

Figure 4.4: Peak floor acceleration (PFA) for all the case study seismic design buildings at a 2475-year return period: **(a)** and **(b)** 4 storey, **(c)** and **(d)** 3 storey, and **(e),** and **(f)** 2 storey.

4.1.3. Interstorey Shear Distribution

The results in terms of inter-storey shear distribution are reported in **Figure 4.5**. It can be shown that the maximum mean inter-storey shear (indicated with black line on the graph) are concentrated on the first floor for all the case study buildings (4, 3 and 2 storey buildings) in the X direction with the maximum value of about 15000kN achieved in 4 storey building type which is almost 5 times higher than the 3 and 2 storey buildings which is a function of the size in plan of the case study buildings. In the Y direction, the inter-storey shear has the same behaviour as the X-direction, with the maximum value on the first floor for all storey building types, with about 8900kN in the 4-storey building type. It is therefore expected that the first-floor experience shear value is the same for all building types.

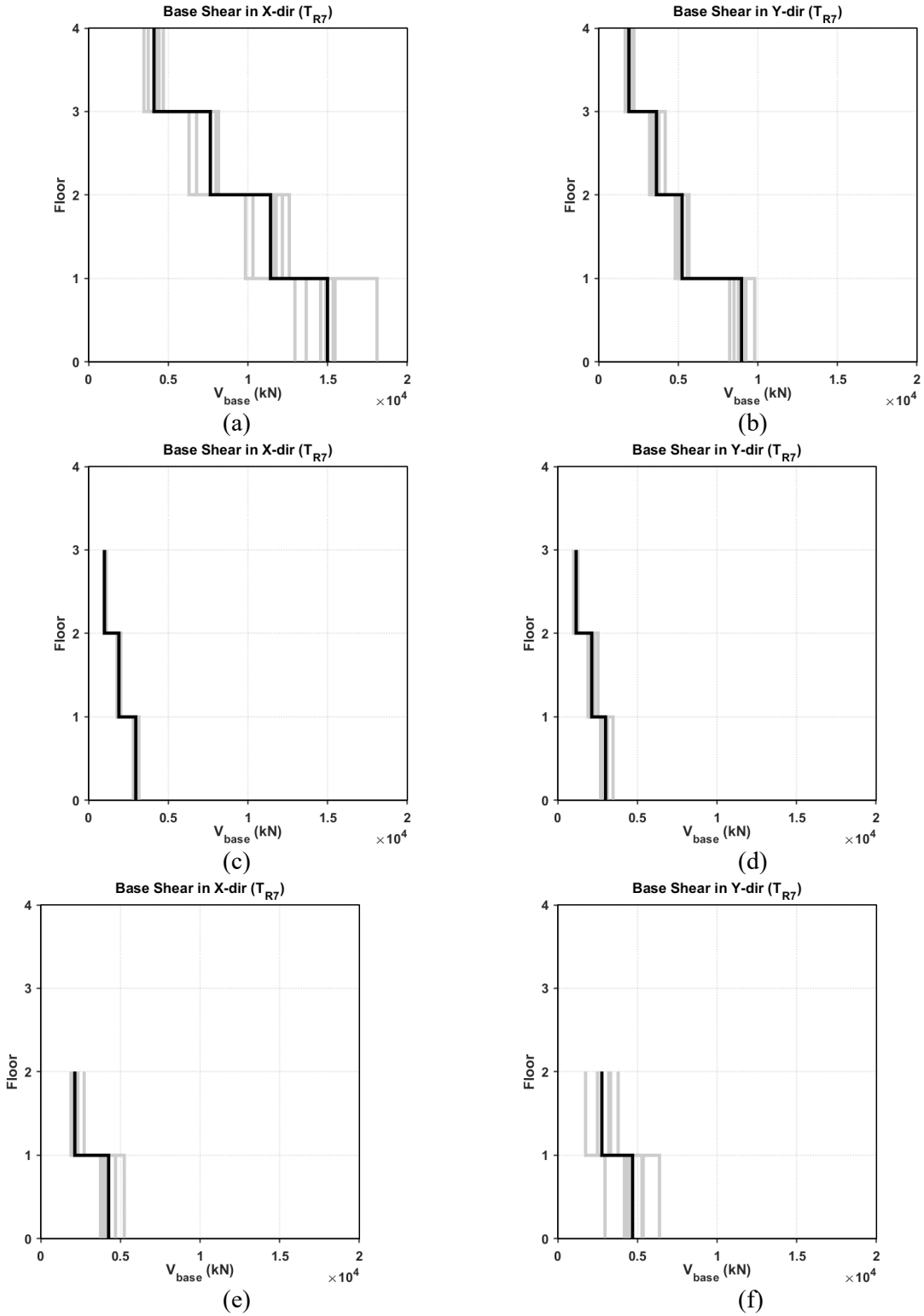

Figure 4.5: Interstorey shear for all the case study seismic design buildings at 475 years return period in **(a)**, **(b),** and **(c)** X direction and **(d)**, **(e),** and **(f)** Y direction.

On the other hand, as shown in **Figure 4.6**, at a higher return period of 2475 years, the inter-storey shear increases by about 8% for the 4-storey building type in the X direction. Meanwhile,

for the Y direction, there was an increase of about 17% for the maximum drift observed on the first floor of the 4-storey building type.

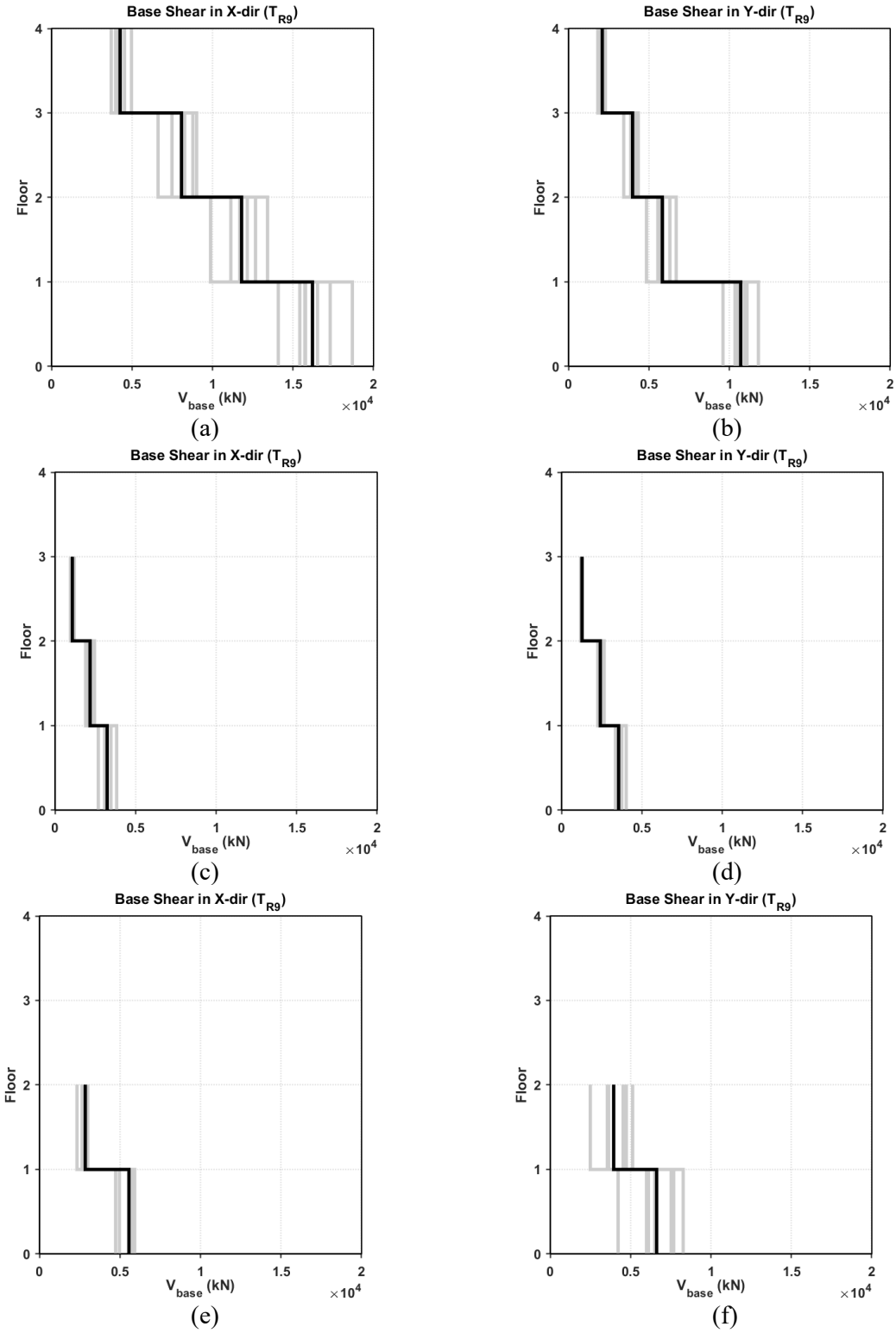

Figure 4.6: Interstorey shear for all the case study seismic design buildings at a 2475-year return period in **(a)**, **(b),** and **(c)** X direction and **(d)**, **(e),** and **(f)** Y direction.

4.2. Vulnerability Analysis

4.2.1. Fragility curves

This section shows the result of the fragility curves for the as-built and FRP-strengthened RC exterior, interior and non-conforming BCJs with the first two being the most vulnerable joint types in a moment-resisting frame. The fragility function is based on the mean maximum IDR obtained from the NLTHs performed for each building type in the previous section. Three different DSs, namely, light damage (DS1), moderate damage (DS2), and heavy damage (DS3), are considered according to widely recognized damage classifications which is obtained for the as-built and FRP-strengthened configuration. Moving forward, each storey building type is discussed below taking into consideration the IDR in X direction only (which is lower than the Y direction) in order to have an idea of the fragility curves at a lower IDR.

- **Four-storey buildings**

For the four-storey building type with the EDP that has been discussed earlier, the probability of occurrence of joint damage states in X direction is shown for both as-built and FRP configurations for the 2475 return period which as shown in **Figure 4.7**.

For the as-built configuration, at the maximum IDR, none of the joints except the non-conforming joint (i.e., exterior and interior joints) achieved light damage (DS1) at about 0.6 probability of occurrence, as shown in **Figure 4.7a.** It can be observed that the exterior joints achieved heavy damage, i.e., DS3 at the return period with a probability of occurrence of about 0.55, while the interior joint achieved medium damage (DS2) at a higher probability at the maximum drift, as shown in **Figure 4.7c and e.**

With FRP strengthened, there is a reduction in the probability of occurrence for the exterior joint at DS3 to a lower value of about 0.13, therefore making the FRP effective. At DS2, the probability of occurrence for the interior joint was reduced to about 0.3. Meanwhile, for the non-conforming joints, the FRP isn't expected to be effective since they are confined. This is as shown in **Figure 4.7b, d, and f.**

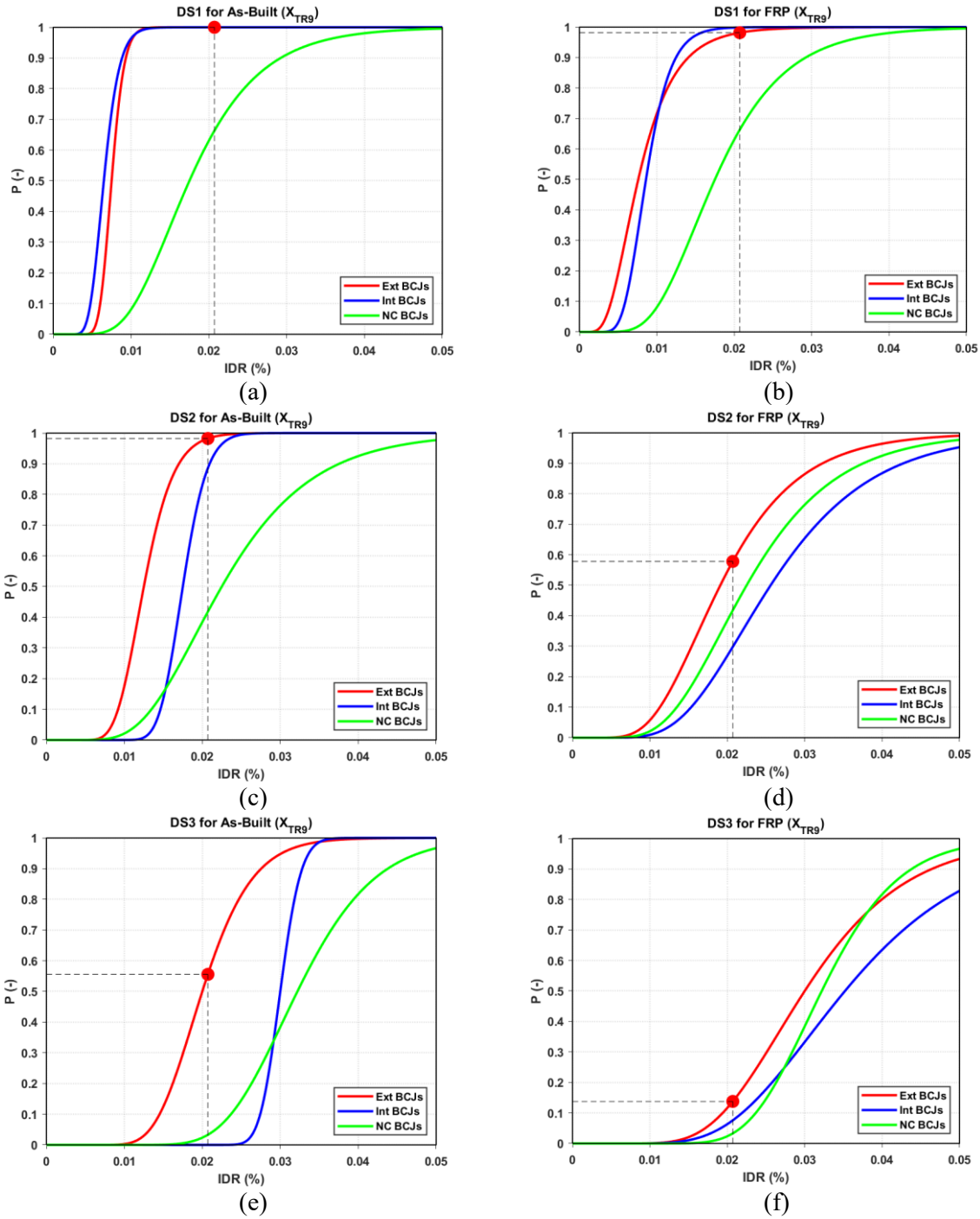

Figure 4.7: Fragility curves in X direction at 2475 years return period for 4-storey seismic design building: **(a)**, **(c)** and **(e)** As-Built and **(b)**, **(d)** and **(f)** FRP strengthened.

- **Three-storey buildings**

The probability of occurrence in X direction is shown for both as-built and FRP configurations for the 3-storey building type at a 2475 return period is as shown in **Figure 4.8**.

For the as-built configuration, at maximum IDR, none of the joints except the non-conforming joint (i.e., exterior and interior joints) achieved light damage (DS1), which is the same for the 4-storey building type at about 0.37 probability of occurrence, as shown in **Figure 4.8a.** It can be observed that the exterior joints achieved heavy damage, i.e., DS3 at the return period with a probability of occurrence of about 0.13, while the interior joint achieved medium damage (DS2) at about 0.13 probability at the maximum drift, as shown in **Figure 4.8c, and e.**

With FRP strengthened, there is a reduction in the probability of occurrence for the exterior joint at DS3 to a lower value of about 0.02, therefore making the FRP effective. At DS2, the probability of occurrence for the interior joint was reduced to about 0.08. Meanwhile, for the non-conforming joints, the FRP isn't expected to be effective since they are confined, as it was discussed earlier. This can be observed in **Figure 4.8b, d, and f.**

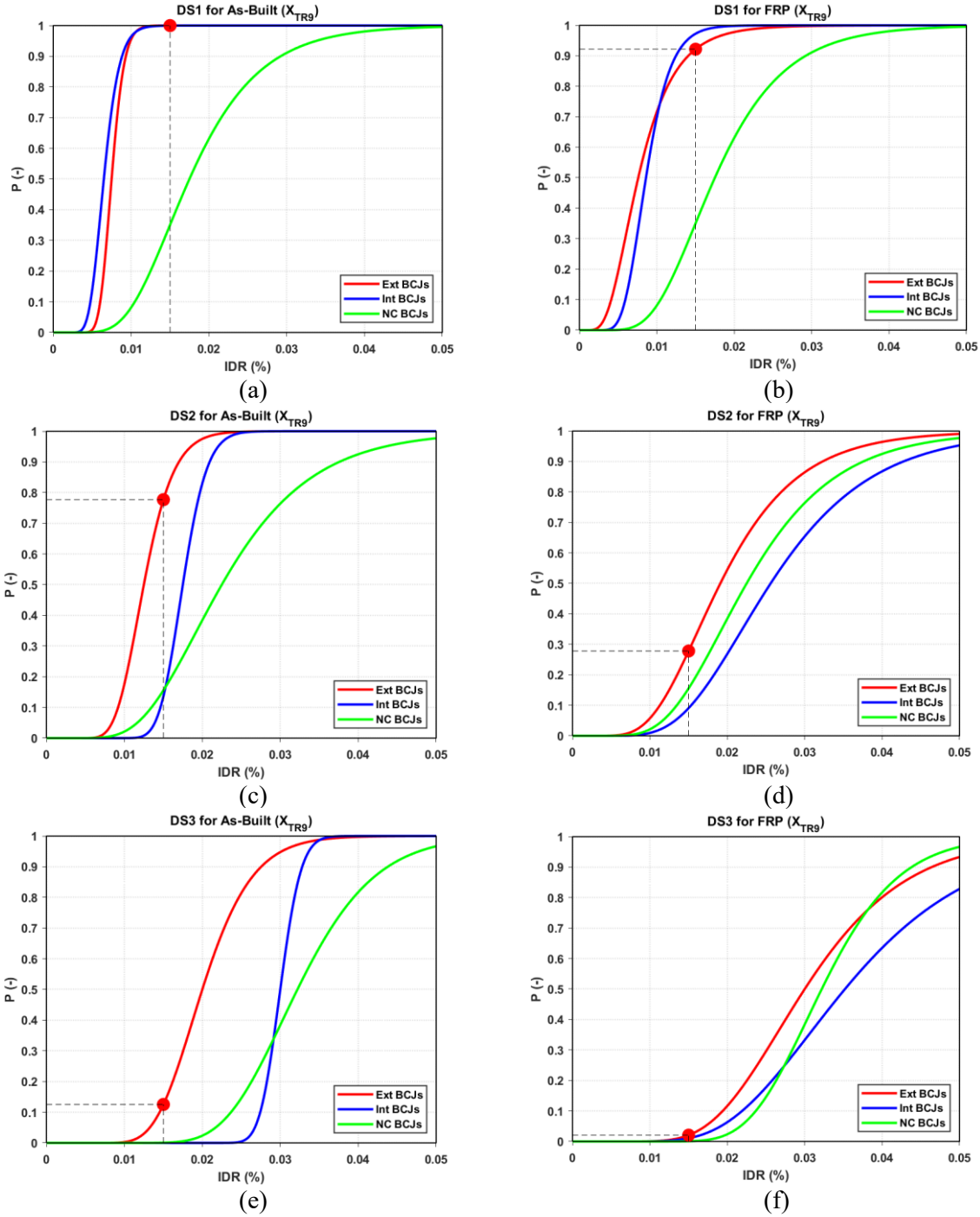

Figure 4.8: Fragility curves in X direction at 2475 years return period for 3-storey seismic design buildings: **(a)**, **(c)** and **(e)** As-Built and **(b)**, **(d)** and **(f)** FRP strengthened.

- **Two-storey buildings**

Also, for the 2-storey building type, the probability of occurrence in X direction is shown for both as-built and FRP configurations at a 2475 return period is as shown in **Figure 4.9**.

For the as-built configuration, at the maximum IDR, none of the joints achieved DS1, DS2, and DS3, as shown in **Figure 4.9c, and e.** This is because the building exhibits a lower drift ratio compared to the other building types.

With FRP strengthened, there is no reduction in the probability of occurrence for all the joints at different damage states because FRP only becomes effective when the RC member cracks at DS1.

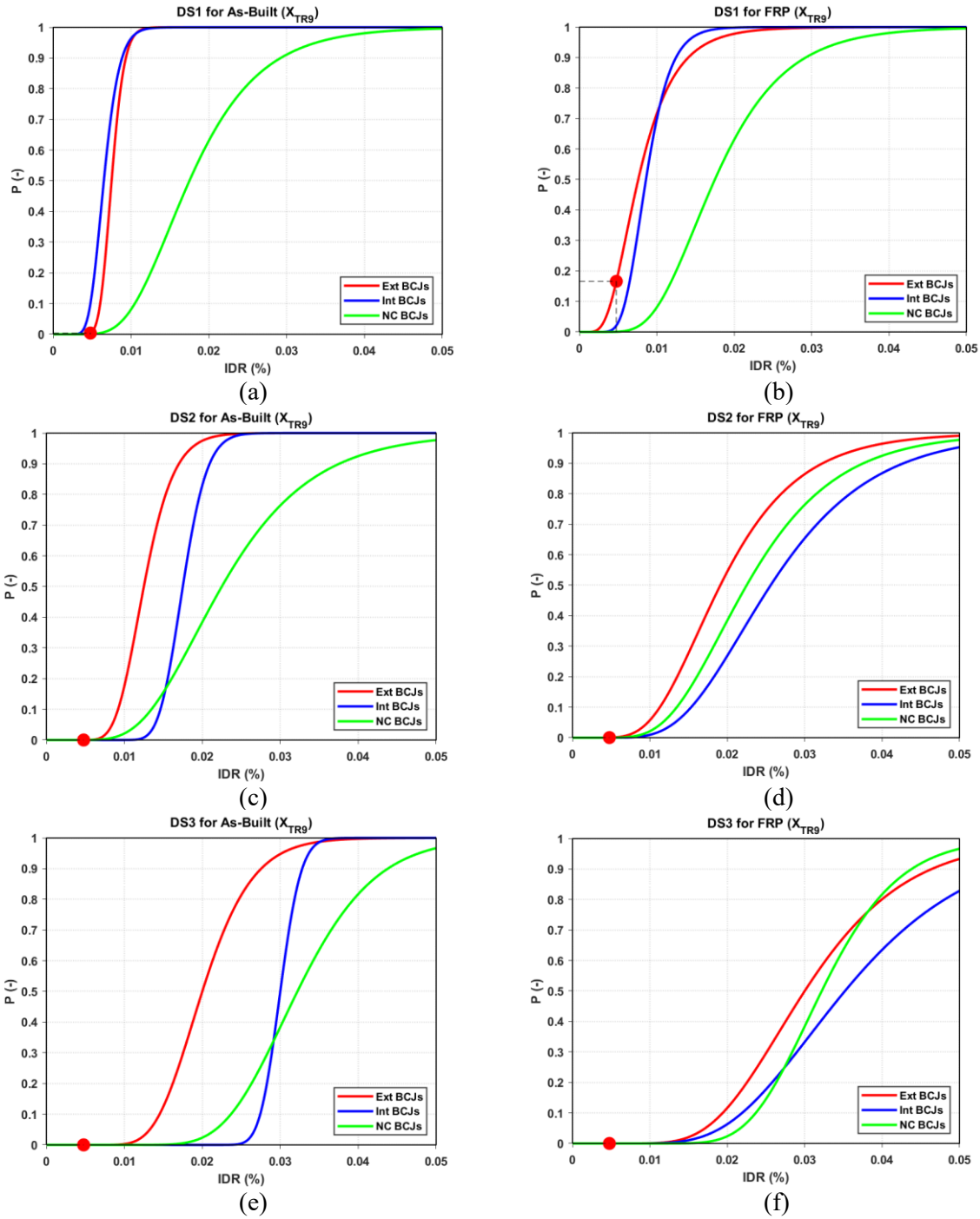

Figure 4.9: Fragility curves in X direction at 2475 years return period for 2-storey seismic design building: **(a)**, **(c)** and **(e)** As-Built and **(b)**, **(d)** and **(f)** FRP strengthened.

4.2.2. Probability of Collapse Assessment and Analysis of Costs

As was discussed earlier, the costs which are arranged in ascending form for the all the number of realizations (i.e. 500) were used to understand the evolution of the total mean costs for each return period in which any value greater than reconstruction costs assigns the value of the

reconstruction cost which signifies a collapse. This section shows the costs associated with each realization considering the influence of the probability of collapse on these costs for the as-built and FRP configurations.

- **Four storey buildings**

For the 4-storey building type, the total number of collapses observed are 65 to 153 with a probability of collapse of 0.13 and 0.31 respectively from return period T_{R7} to T_{R9} as shown in **Figure 4.10a**. In addition to this, higher costs are associated with the return period that exhibits this collapse (i.e. 475 to 2475 years) for the as-built configuration as shown in **Figure 4.11a**.

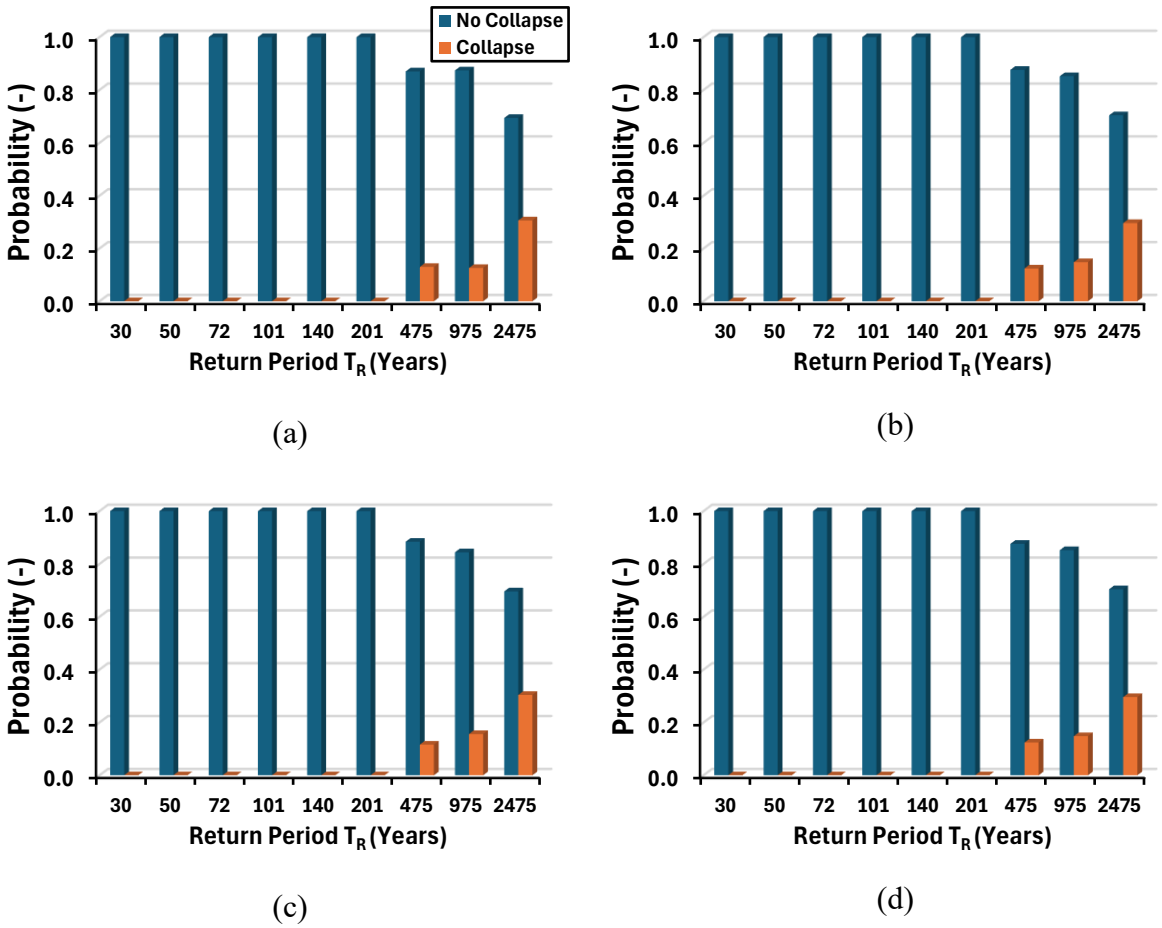

Figure 4.10: Probability of collapse for 4-storey building: **(a)** As-built, **(b)** SFRP, **(c)** SL_CFRP strengthened, and **(d)** DL_CFRP strengthened.

On the other hand, for the SFRP configuration, there was a slight reduction in the costs, but the collapse remains from return period T_{R7} to T_{R9} (i.e. 475 to 2475 years). This can be observed in the flatten shape compared to the as-built configuration as shown in **Figure 4.11b**. This can

be related to the number of collapses that reduced in the associated return period to 62 and 148 with a probability of collapse of 0.12 and 0.30. This is as shown in **Figure 4.10b**.

Further strengthening with single layer of CFRP (SL_CFRP) and double layer of CFRP (DL_CFRP) shows the slight reduction of the costs from T_{R7} to T_{R9} but with number of collapses of 58 to 148 having almost the same probability of collapse as it was for the SFRP case. This is attributed to their capacity not enough to erase the collapse, rather it reduced the cost slightly. This can be observed on **Figure 4.11c-d** and **Figure 4.10c-d.**

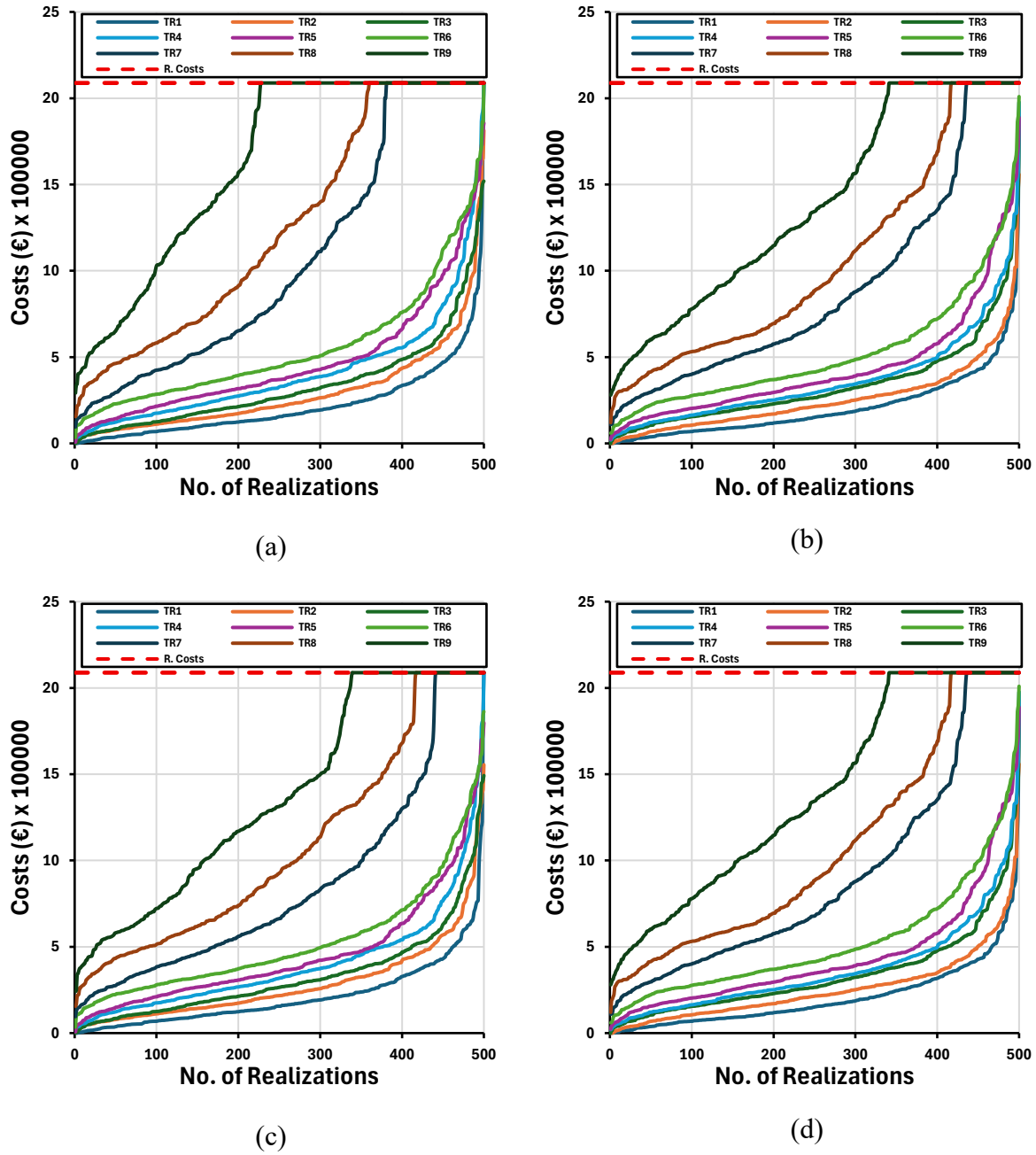

Figure 4.11: Cost vs realizations for all return periods (4-storey seismic design building): **(a)** As-Built, **(b)** SFRP, **(c)** SL_CFRP, and **(d)** DL_CFRP strengthened.

- **Three-storey buildings**

For the 3-storey building type, it can be observed that collapse occurs for all the return periods T_{R1} to T_{R9} (i.e., 30 to 2475 years) for the as-built configuration, as shown in **Figure 4.13a**. The total number of collapses observed is 74 to 500 with a probability of collapse of 0.15 to 1, i.e., total collapse. This is as shown in **Figure 4.12a**.

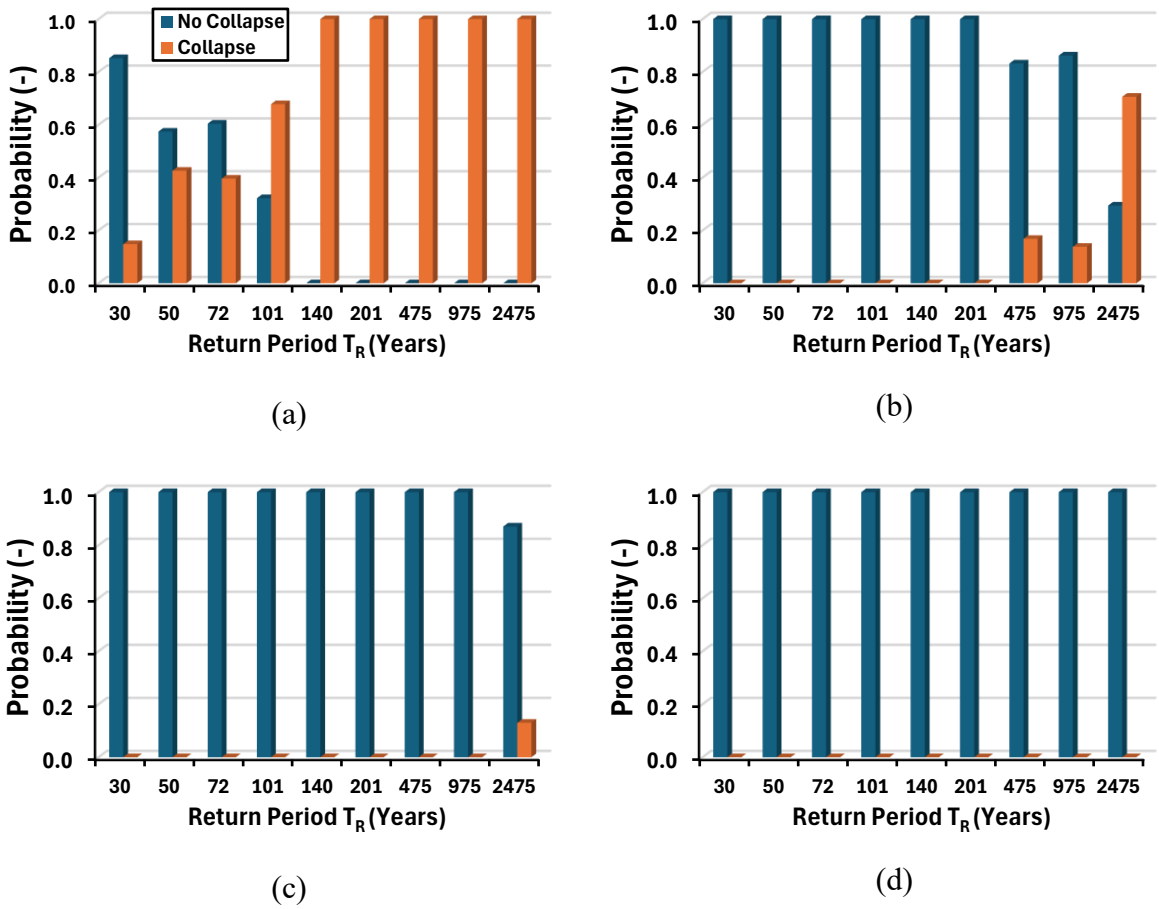

Figure 4.12: Probability of collapse for 3-storey seismic design building: **(a)** As-built, **(b)** SFRP, **(c)** SL_CFRP strengthened, and **(d)** DL_CFRP strengthened.

Using SFRP strengthening, there was a reduction in all costs, leading to no collapse from T_{R1} to T_{R6}, but the collapse remains from return period T_{R7} to T_{R9}, at a reduced collapse probability. This is as shown in **Figure 4.13b**. This can be related to the number of collapses that reduced in the associated return period to 0 for T_{R1} to T_{R6} and 84 to 353 for the remaining return period, with probability of collapse of 0.17 and 0.79 for the latter. This is as shown in **Figure 4.12b**. With SL_CFRP and DL_CFRP, there was a shift in collapse to T_{R9} and no further collapse, respectively. This is related to the number of collapses being 65 (0.13 collapse probability) and

zero collapses for each strengthening technique used. This shows a great effectiveness of the CFRP capacity that was able to erase the collapse of the structure completely, especially with DL_CFRP. This can be seen in **Figure 4.13c-d** and **Figure 4.12c-d.**

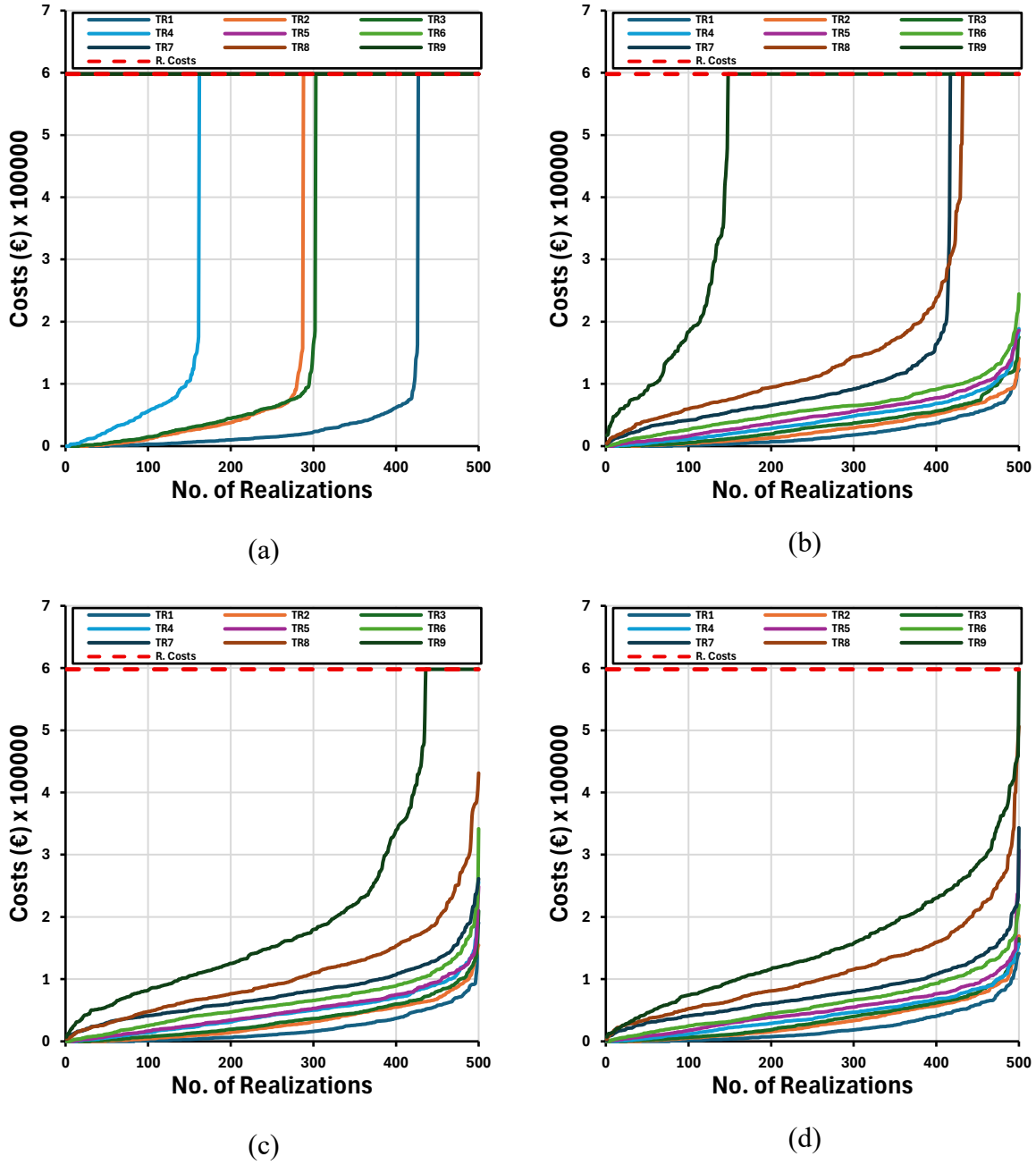

Figure 4.13: Cost vs realizations for all return periods (3-storey seismic design building): **(a)** As-Built, **(b)** SFRP, **(c)** SL_CFRP, and **(d)** DL_CFRP strengthened.

- **Two-storey buildings**

Lastly, for the 2-storey building type, it can be observed that collapse occurs for the return period T_{R8} to T_{R9} (i.e., 975 and 2475 years) for the as-built configuration, as shown in **Figure 4.15a**. The total number of collapses observed is 73 and 285, with a probability of collapse of 0.15 and 0.57, as shown in **Figure 4.14a**.

Using SFRP, SL_CFRP, and DL_CFRP strengthening, there was a reduction in all costs, leading to no collapse for the T_{RS} that suffered collapse in the as-built configuration, which is shown in **Figure 4.15b-d**. This can be related to the number of collapses that reduced in the associated return period to 0 for this $T_{RS,}$ with a probability of zero collapse. This can be observed in **Figure 4.14b-d**.

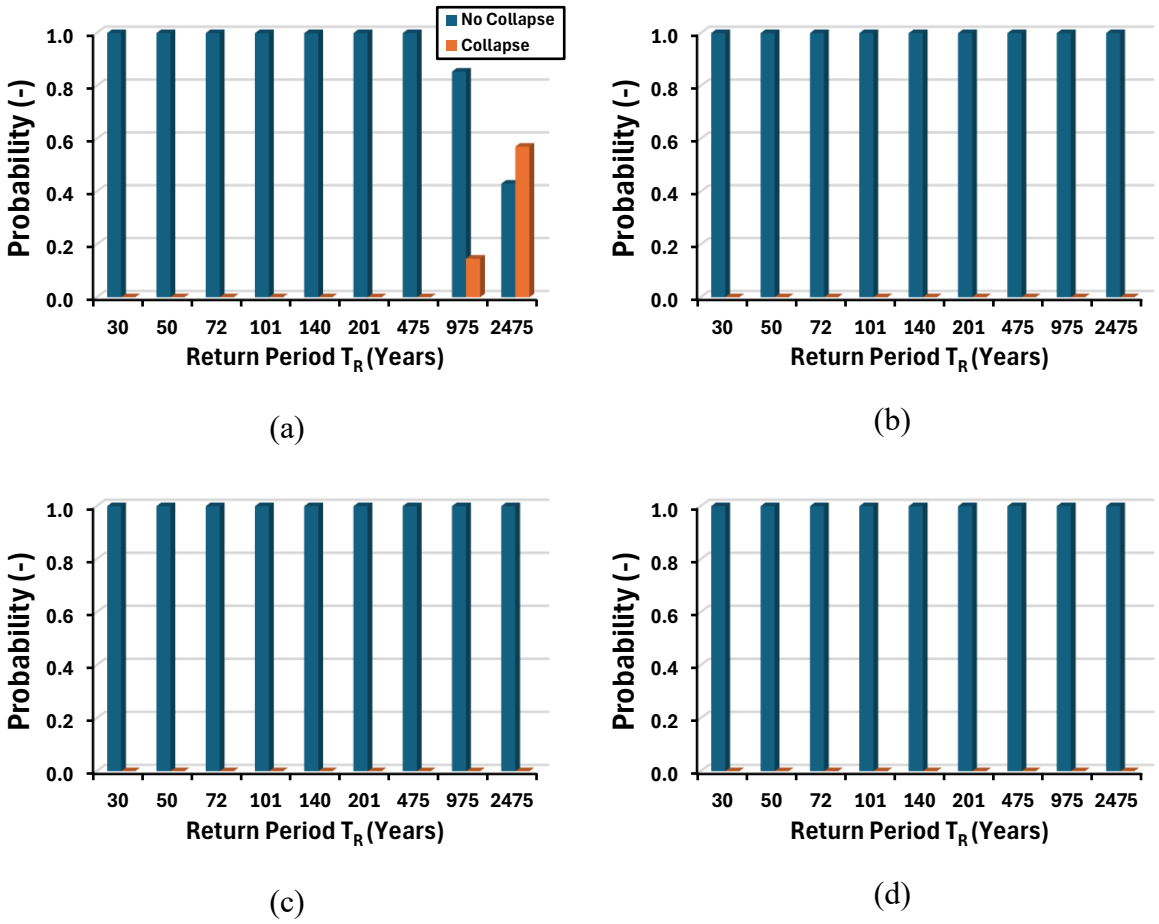

Figure 4.14: Probability of collapse for 2-storey seismic design building: **(a)** As-built, **(b)** SFRP, **(c)** SL_CFRP strengthened, and **(d)** DL_CFRP strengthened.

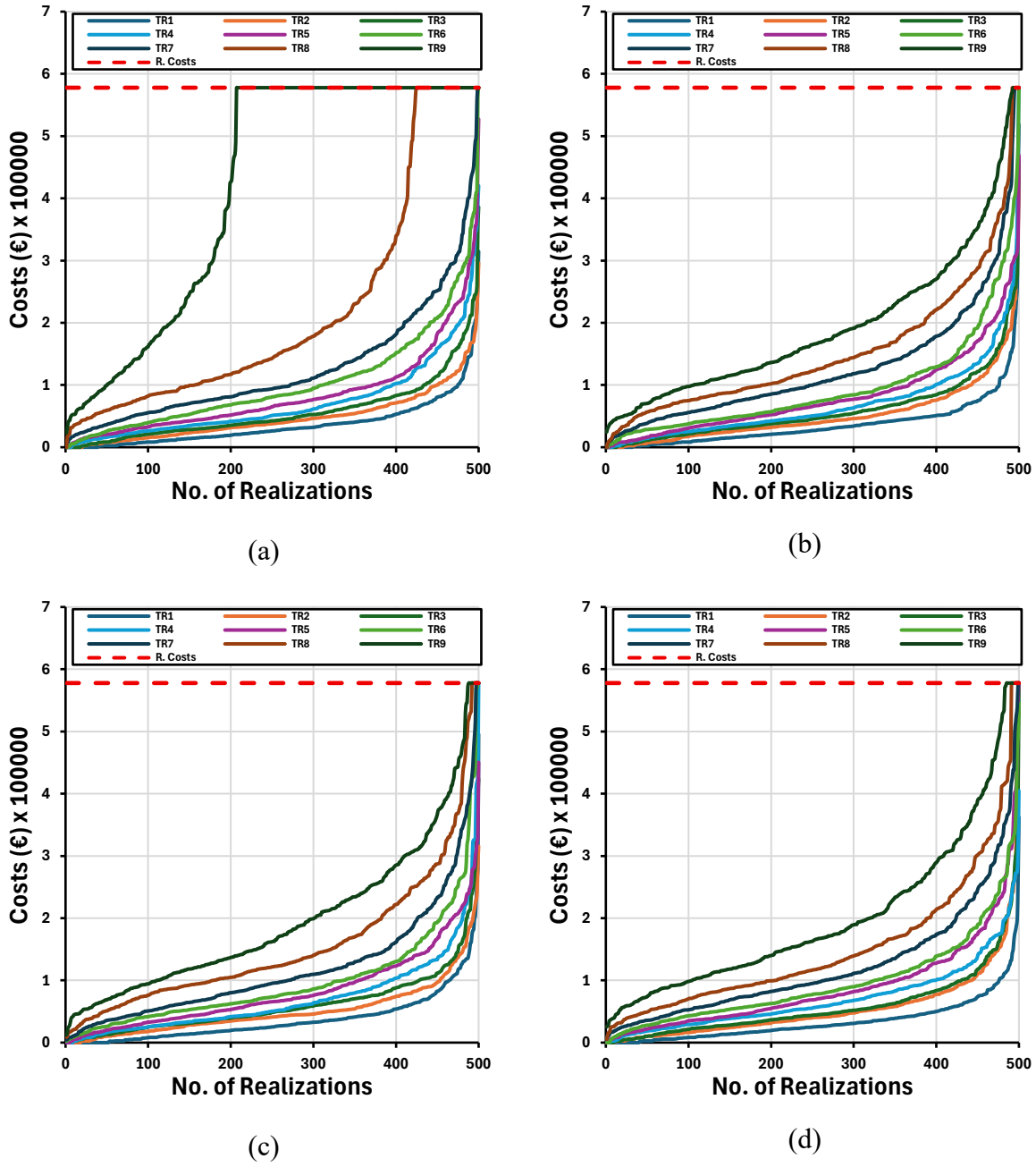

Figure 4.15: Cost vs realizations for all return periods (2-storey seismic design building): **(a)** As-Built, **(b)** SFRP, **(c)** SL_CFRP, and **(d)** DL_CFRP strengthened.

4.3. Costs Comparison

The cost comparison for the as-built and strengthened techniques (SFRP and CFRP) in terms of component level and at different return periods is discussed below. This gives an idea of the cost associated with each component type, i.e., drift and acceleration-based component as well as the effects of the FRP strengthening on the costs associated to the beam column joints (BCJs).

4.3.1. Repair costs at the component level

Figure 4.16 shows the summary of the building repair costs for the three case study building (i.e. as-built and strengthened configurations) evaluated for the drift (i.e. infills, partitions, stairs, and joints) and acceleration (i.e. tiles, chimney, raised access floor, lighting, cold and hot water piping, sanitary waste, and low voltage switch gear) sensitive components for return period T_{R9} (i.e. 2475 years). It should be noted however that these costs are not affected by the collapse, but the actual total cost associated to each component. It can be shown that the drift-based components take the larger percentage (70% to 90%), with BCJs taking about 20 to 50% of the building repair cost. Consequently, the acceleration-based components take a lesser percentage (10% to 30%) of the building repair costs.

However, in the case of a 2-storey building, the joint cost has a lesser cost of about 26% of the building repair costs, as shown in **Figure 4.16c.** At the T_{R9}, the influence of SFRP strengthening reduces the joint costs by 12%, 31% and 28% for the 4, 3, and 2-storey buildings, respectively, as shown in **Figure 4.16a-c**. This shows the effectiveness of SFRP before collapse. Meanwhile, the use of SL_CFRP reduces the joint cost by 13%, 21% and 14% for the 4, 3, and 2-storey buildings, respectively. Lastly, with DL_CFRP, the joint cost was reduced by 11%, 20% and 6% for the 4, 3, and 2-storey buildings, respectively. Considering the 3 strengthening techniques used, it can be noted that FRP best reduces the cost of the joint before collapse.

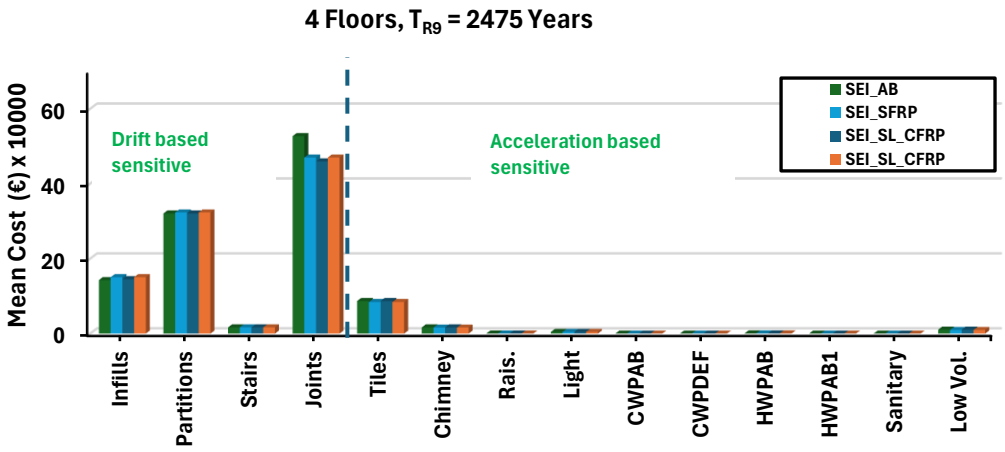

(a)

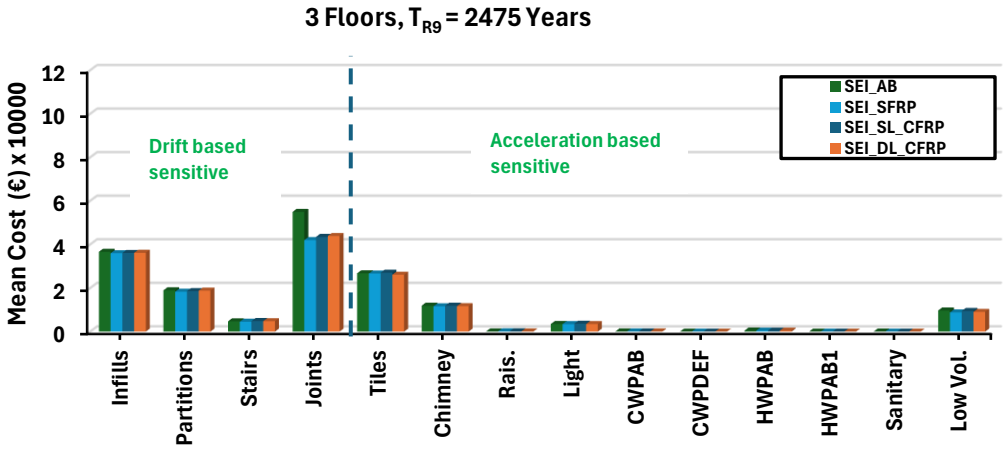

(b)

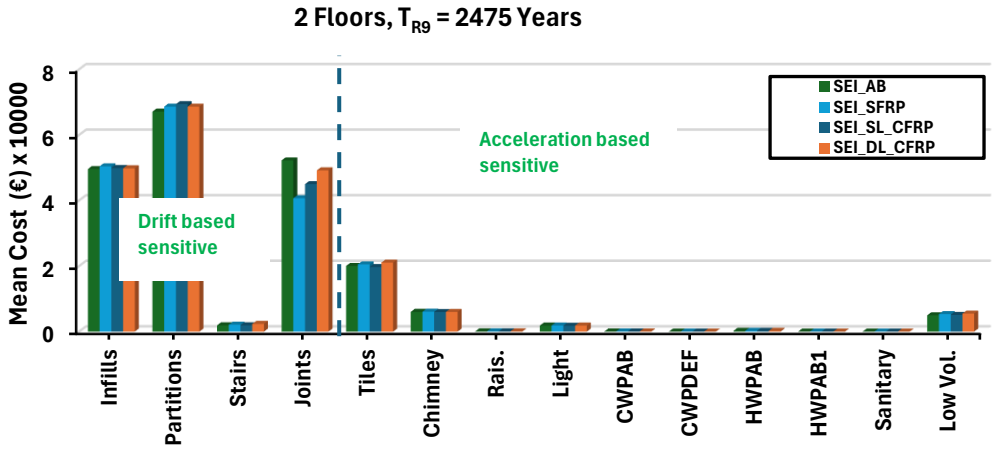

(c)

Figure 4.16: Repair cost at component level - gravity design: **(a)** 4-storey building, **(b)** 3-storey building, and **(c)** 2-storey building.

4.3.2. Repair costs at different return periods after collapse (T_{RS})

This section shows the repair costs for different return periods taking into account the collapse of the building. The cost extracted from the output and arranged in ascending order is used for this purpose. In addition, the cost of strengthening techniques at each return period is also plotted to understand their effect. **Figure 4.17a-c** shows the variation of the total repair costs associated with each T_{RS} for the 3 case study buildings. It is worth noting that, in any case the strengthening doesn't have effect at a particular T_R, therefore the cost is equal to the reconstruction cost which implies that it is better for the building to be demolished.

For the 4-storey building type, there is non-linear increment in the repair cost from the moderate earthquake to severe earthquake where the damage is more destructive. At the last return period, if the reconstruction cost wasn't reached, therefore, the structure can be strengthened else once the costs are more than 50% of the reconstruction costs, it is better to demolish the structure. There is a reduction in the as-built costs when compared to the reconstruction costs without any of the T_{RS} reaching collapse, therefore it is better to strengthening the structure. At the 9th return period (i.e. 2475 years), there is about 22% reduction of the reconstruction costs for the as-built costs. Upon the use of SFRP, SL_CFRP, and DL_CFRP, there was a reduction of 34% for all cases when compared with the reconstruction costs. Since the strengthening costs is more than 50% of the reconstruction costs, it is therefore better to demolish the building. This can be seen in **Figure 4.17a.**

Consequently, for the 3-storey building type, there is a gradual increase in the repair costs from 1st – 4th return period (i.e. 30 to 101 years) without reaching the reconstruction costs. After the 4th return period, the remaining return period therefore reaches the reconstruction costs, therefore. With SFRP, there is a reduction of the repair costs for all the return period from about 20% to 92% for the T_{RS}. At the 9th return period, there is about 22% reduction compared to the reconstruction cost. On the other end, using SL_CFRP, the cost reduced significantly for all the return periods with the 9th return period having about 64% reduction when compared with the reconstruction costs. Meanwhile, with the use of DL_CFRP, the costs were almost the same with that of the SL_CFRP up to the 8th return period but reduced slightly for the 9th return period having about 74% reduction in cost when compared to the reconstruction costs. This shows that SL_CFRP and DL_CFRP are more effective when compared to the SFRP strengthening techniques during the earthquake. This is as shown in **Figure 4.17b.**

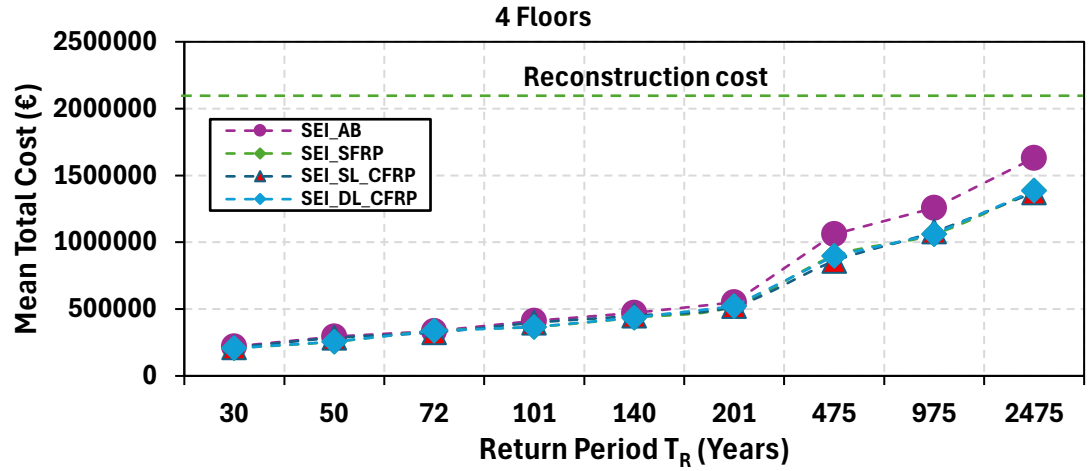

(a)

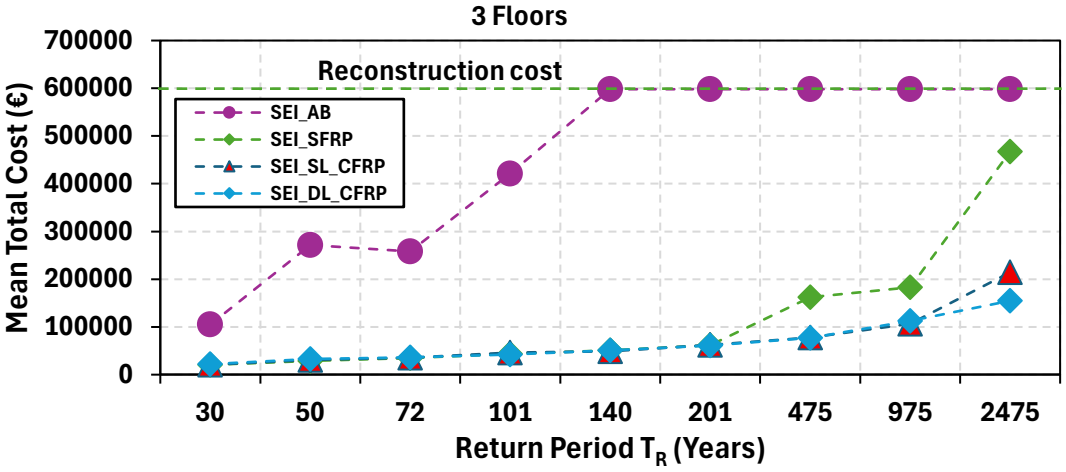

(b)

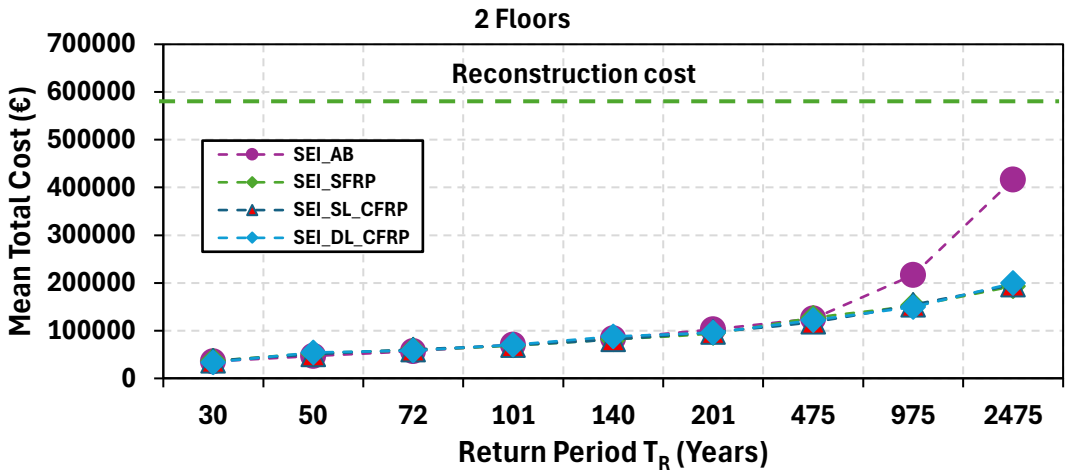

(c)

Figure 4.17: Total repair cost at each return period-seismic design: **(a)** 4-storey building, **(b)** 3-storey building, and **(c)** 2-storey building.

Lastly, for the 2-storey building type, there is a non-linear increase in the repair costs for all the return period without reaching the reconstruction costs with 9th return period having about 28% reduction in cost of the repair costs to the reconstruction cost. Meanwhile, with SFRP, SL_CFRP and DL_CFRP, the costs are similar from 1st to 6th return periods with the 9th return period having 67%, 66% and 65% reduction in cost of the repair costs to the reconstruction cost respectively. This implies the 3 strengthening techniques are effective to strengthen the structure at severe earthquake (see **Figure 4.17c).**

THIS PAGE WAS INTENTIONALLY LEFT BLANK

5. GRAVITY LOADS DESIGNED BUILDINGS (GLD)

The same analysis was repeated for the building designed according to obsolete codes to withstand gravity only (GLD). This is done by redesigning the case study buildings selected form the database according to the stress limit state prescribed in old building code (Law 5/11/1971n. 1086 and Ministerial Decree 30/5/1974) and was analysed using SAP2000 v.23. [39]. The slab weight therefore according to the code is 500kg/m^2 and 200kg/m^2 for the dead and live load respectively which is as shown on **Table 5.1**. In the same vein, the roof floor is 450kg/m^2 and 150kg/m^2 for the dead and live load, respectively and these are applied as an area load on the slab considered during the model on SAP2000. The infill walls' weight on the perimeter of the floor considered in the code, is calculated according to the **Equation (5.1).** This is then calculated for each of the case buildings and used for the analysis. The maximum axial load (unfactored) for each level is then extracted from the analysis and used to determine the column sections. To calculate the column sections, this is calculated using the **Equation (5.2)** and the minimum column sections are 300mm x 300mm is considered.

Table 5.1: Load used for analysis.

	Dead load (G_k) (kg/m^2)	Live load (Q_k) (kg/m^2)
Floor slab	500	200
Roof floor	400	150

$$q_{infill} = w_{infill} * h_{infill} * t_{infill} \quad (5.1)$$

where:

w_{infill} is the weight of the infills equal to 800kg/m^3

h_{infill} is the clear height of the infills

t_{infill} is the thickness of the infills equal to 0.2m

$$A_{column} = \frac{N}{\sigma_{infill}} \quad (5.2)$$

where:

A_{column} is the area of the column section

N is the axial load on the column

σ is the stress equal to 60kg/cm^2

The column section determined is then used in the input code on MATLAB, and nonlinear analysis was repeated for the 3 case building types. Therefore, the results for each building type are extracted and discussed moving forward.

5.1. Engineering Demand Parameters (EDPs)

The seismic analysis is performed as it was done for the in the previous section 4.1 of the SLD buildings. The results are also in terms of the of inter-storey drift (IDR), acceleration, and interstorey shear in both directions and picked for the maximum record which the 3rd records with its corresponding return period of 475 years (LSLS) and 2475 years i.e. 7th and 9th return period for the 3 case buildings. This is discussed below.

5.1.1. Interstorey Drift Ratio (IDR)

The results in terms of IDR are shown in **Figure 5.1**. It can be shown that the maximum mean drift (indicated with a black line on the graph) is concentrated on the first floor for all the case study buildings (4, 3, and 2 storey buildings) in the X direction, as it was for the seismic designed building. The maximum value, therefore, is about 0.6% IDR, which is 58% greater than the seismic design building for the 4-storey building type. In the Y direction, the drifts are also concentrated on the first floor except for the 4-storey building type, which was concentrated on the second floor with about 1.86% drift, which is about 24% higher than the seismic designed type. This is due to the higher stiffness observed on the first floor due to a shorter height on the ground floor, as mentioned earlier.

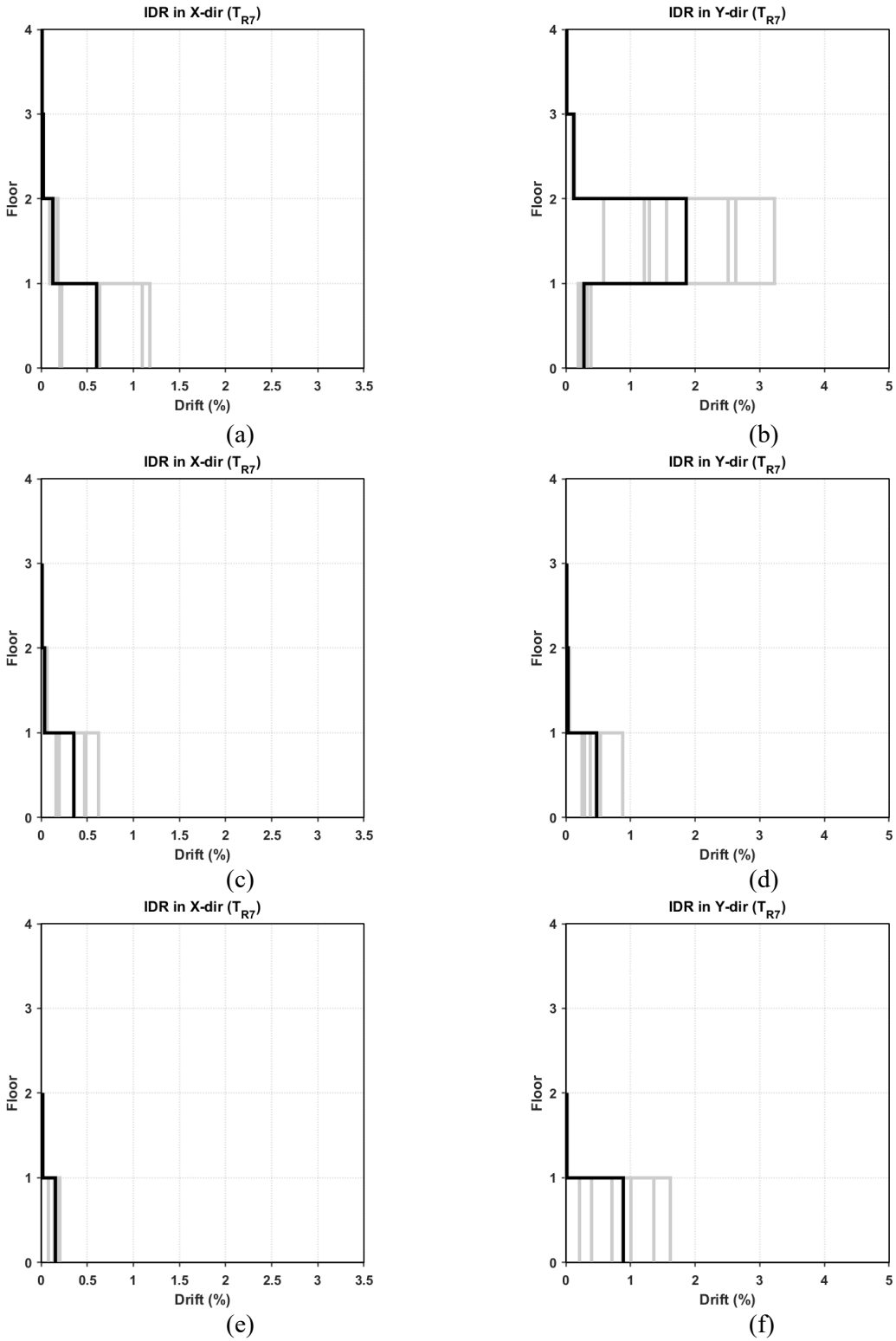

Figure 5.1: Inter-storey drift ratio (IDR) for gravity design buildings at a 475-year return period in X and Y direction: **(a)** and **(b)** 4 storey, **(c)** and **(d)** 3 storey, and **(e),** and **(f)** 2 storey.

On the other hand, at a higher return period of 2475 years, the drift behaviour was the same as for 475 years, but with the maximum value increasing by about 63% for the 4-storey building type in the X direction. Meanwhile, for the Y direction, there was an increase of about 40% for

the maximum drift observed on the second floor of the 4-storey building type. This is as shown on **Figure 5.2**.

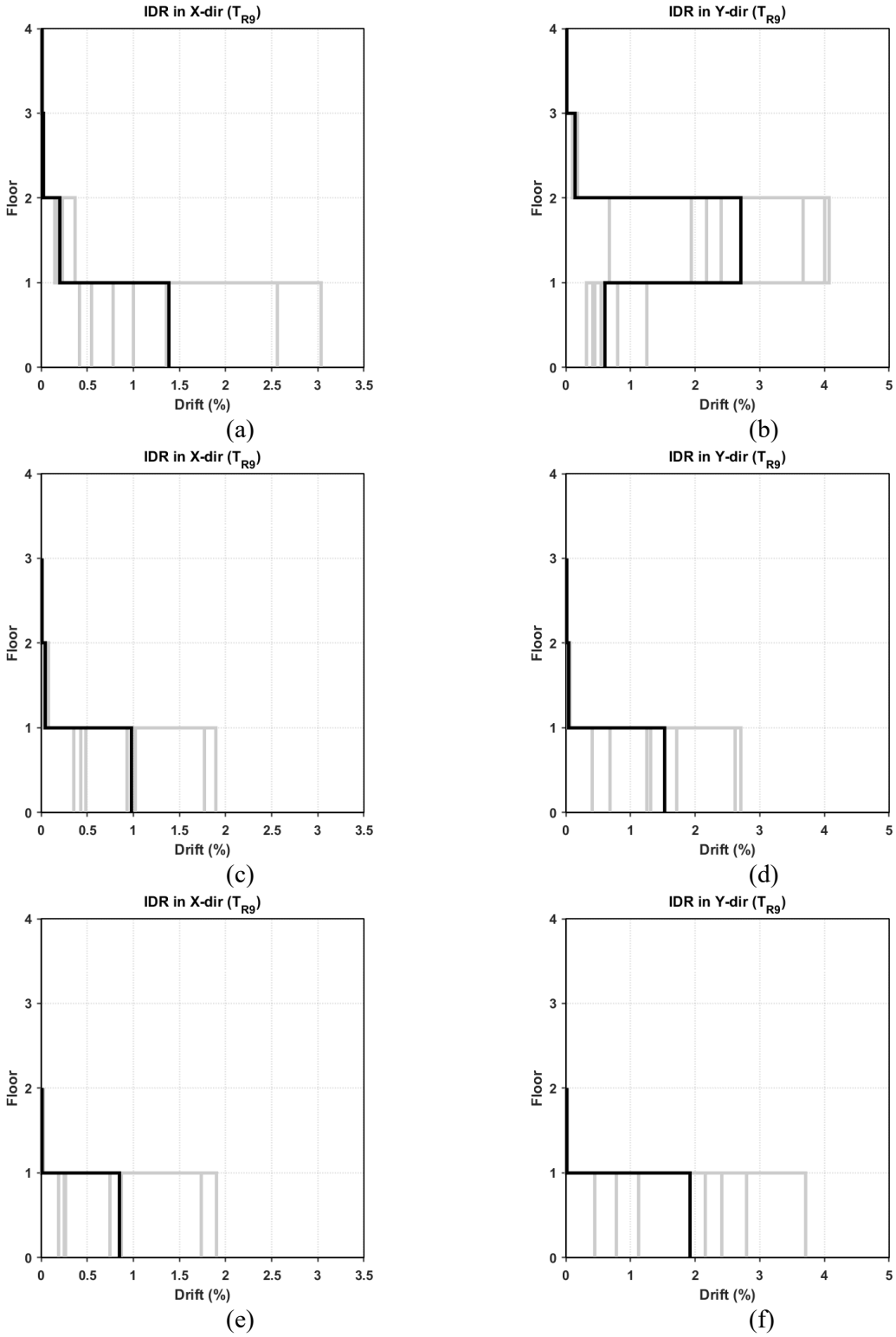

Figure 5.2: Inter-storey drift ratio (IDR) for gravity design buildings at a 2475-year return period in X and Y direction: **(a)** and **(b)** 4 storey, **(c)** and **(d)** 3 storey, and **(e),** and **(f)** 2 storey.

5.1.2. Peak Floor Acceleration (PFA)

In **Figure 5.3**, the results in terms of mean peak floor acceleration are reported. It can be shown that the mean acceleration (indicated with a black line on the graph) increases as the floor progresses for all the case study buildings, with a reduction compared to the seismic design buildings. The maximum acceleration, therefore, is 4.3 m/s^2, 4.2 $m/s^{2,}$ and 4.2 m/s^2 for the 4, 3, and 2-storey building types, respectively. In the Y direction, there was higher acceleration on the first floor in the case of 4-storey building, which might be due to more amplification experienced in that direction. For the 3 and 2-storey, the last floor experiences higher floor accelerations.

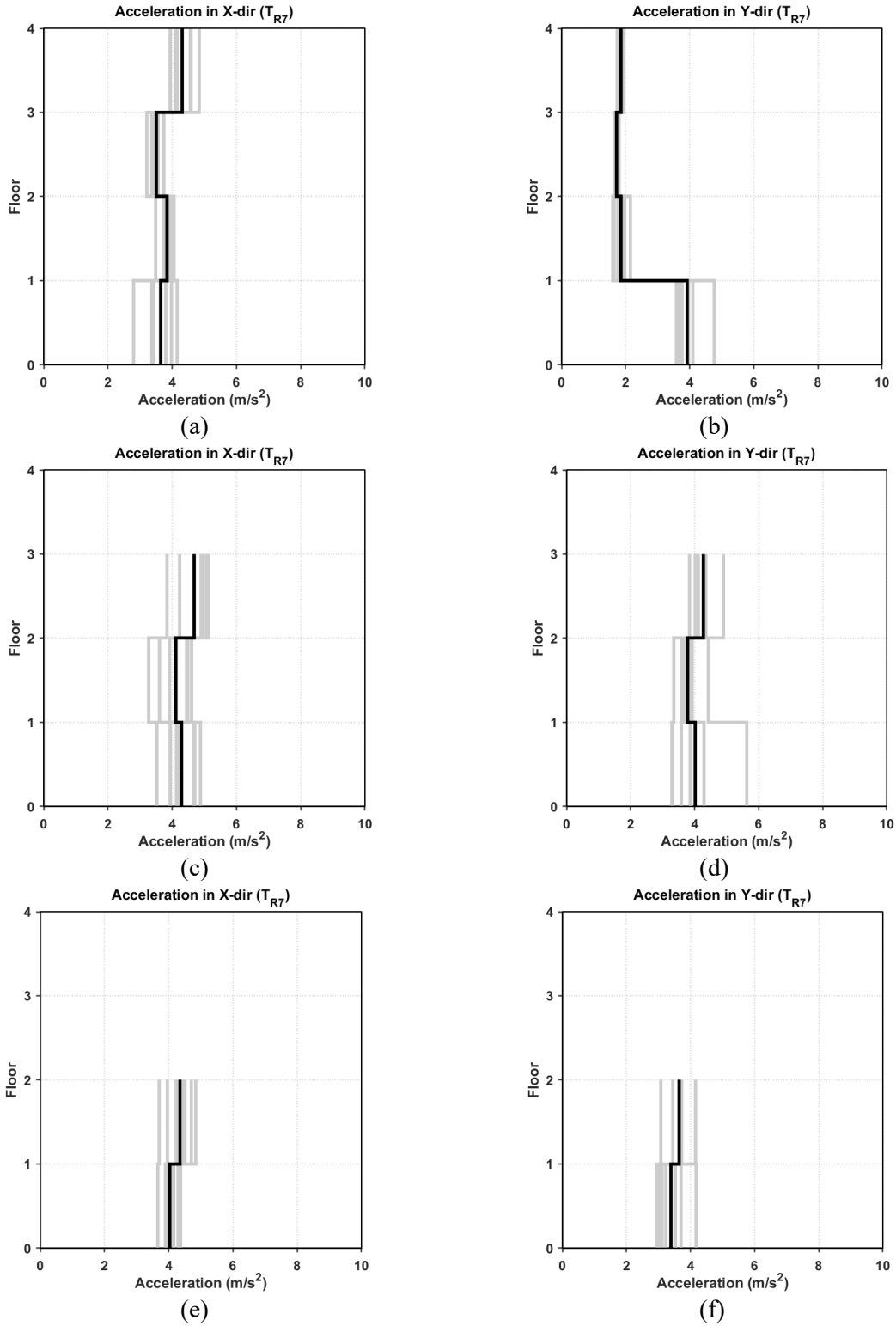

Figure 5.3: Peak floor acceleration (PFA) for all the gravity case study buildings at 475 years return period: **(a)** and **(b)** 4 storey, **(c)** and **(d)** 3 storey, and **(e),** and **(f)** 2 storey.

At a higher return period of 2475 years, the floor acceleration increases to 4.5 m/s^2, 5.1 m/s^{2,} and 5.2 m/s^2 for the 4, 3, and 2 storey building types, respectively, in the X-direction. In the Y direction, there was a higher acceleration on the first floor in the case of a 4-storey building of

about 5.2 m/s^{2,} as there was in the X direction. Meanwhile, for the 3 and 2-storey buildings, there was also about a 10-15% increase in the floor acceleration on the last floor. This is as shown on **Figure 5.4**.

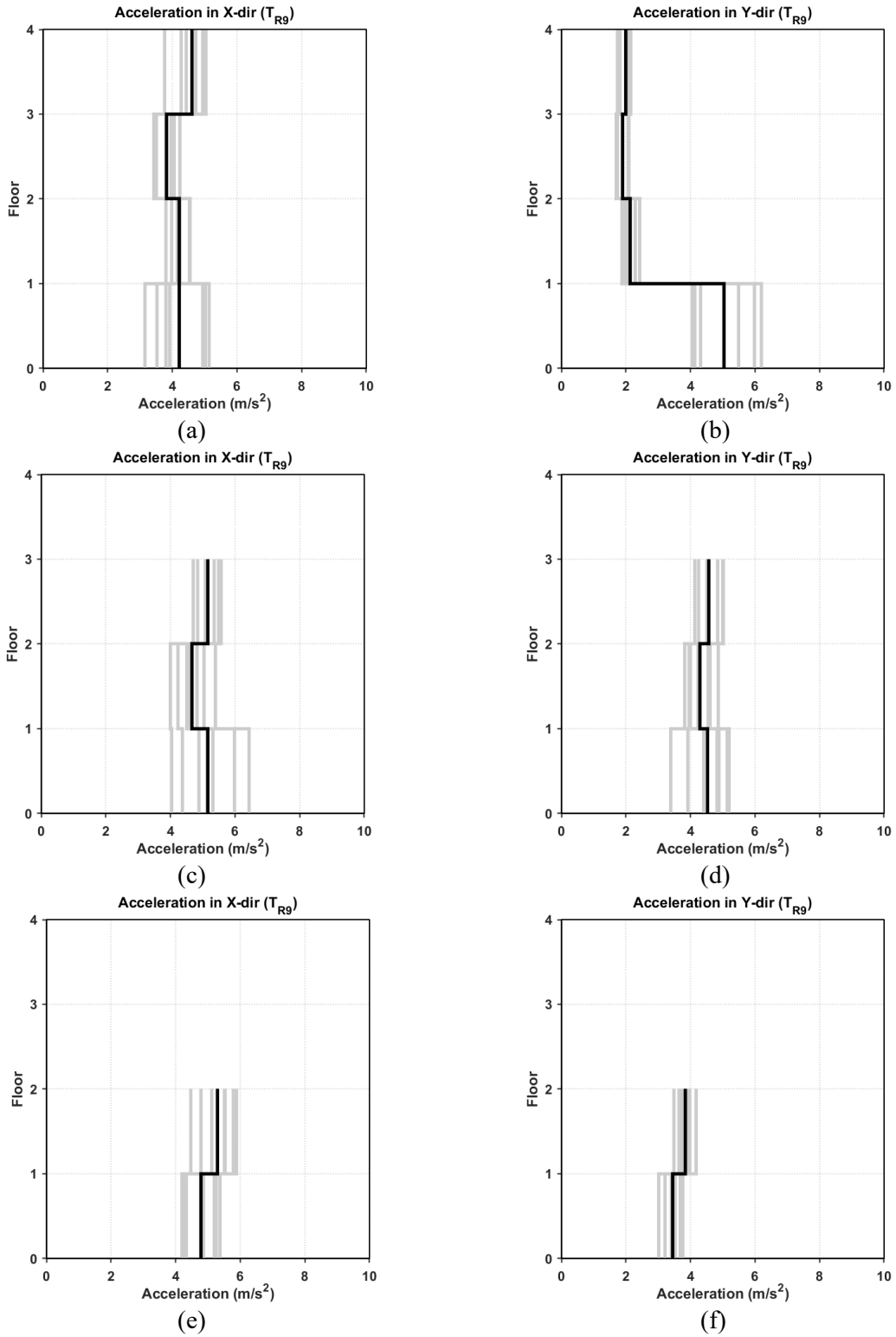

Figure 5.4: Peak floor acceleration (PFA) for all the gravity case study buildings at a 2475-year return period: **(a)** and **(b)** 4 storey, **(c)** and **(d)** 3 storey, and **(e),** and **(f)** 2 storey.

5.1.3. Interstorey shear Distribution

In Figure 5.5 the results in terms of interstorey shear are reported. It can be shown that the maximum mean interstorey shear (indicated with black line on the graph) are concentrated on the first floor for all the case study buildings (4, 3 and 2 storey buildings) in the X direction with the maximum value of about 12500kN (about 17% lesser than the seismic designed buildings) achieved in 4 storey building type which is almost 3-4 times higher than the 2 and 3 storey buildings respectively. In the Y direction, the drifts have the same behaviour as the X-direction, with the maximum value on the first floor for all storey building types, with about 7000kN in the 4-storey building type, which is about 20% less than the seismic designed type. It is therefore expected that the first-floor experience shear value is the same for all building types.

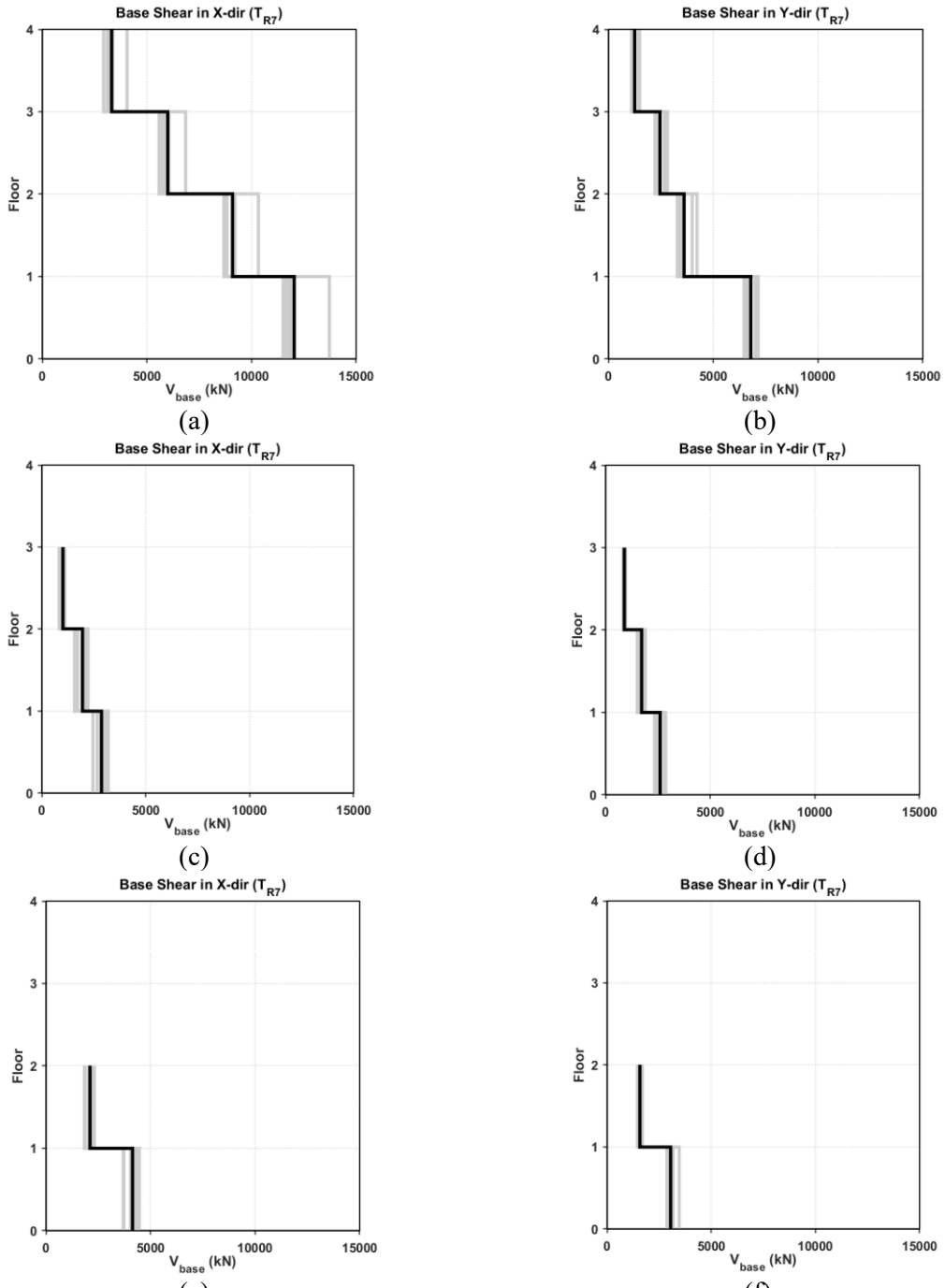

Figure 5.5: Interstorey shear for all the gravity case study buildings at 475 years return period: **(a)** and **(b)** 4 storey, **(c)** and **(d)** 3 storey, and **(e),** and **(f)** 2 storey.

On the other hand, at a higher return period of 2475 years, the interstorey shear increases slightly for all building types in the X direction and Y direction of about 5% maximum. The 4-storey building type maintained the highest interstorey shear. This is as shown on **Figure 5.6**.

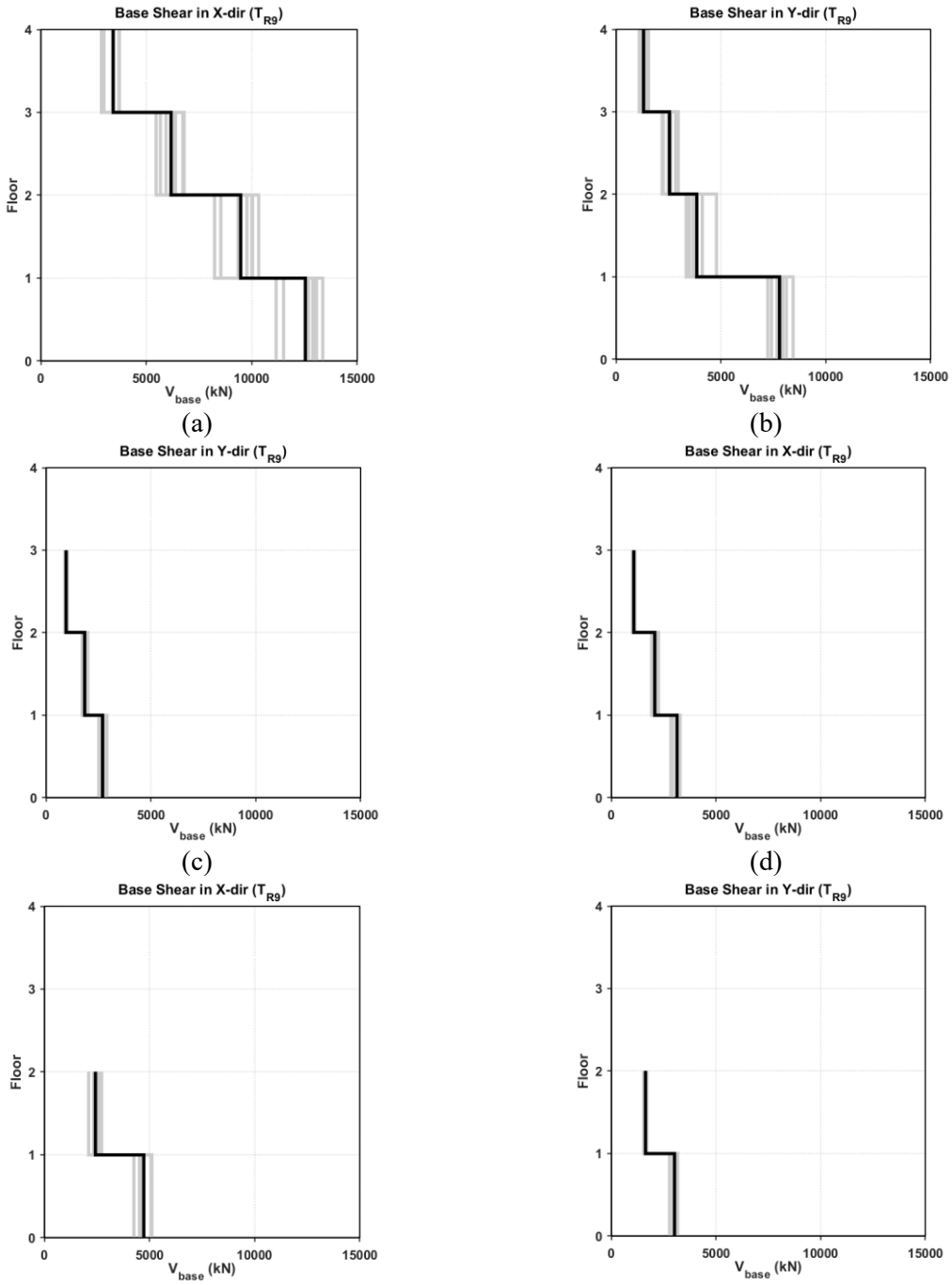

Figure 5.6: Interstorey shear for all the gravity case study buildings at a 2475-year return period: **(a)** and **(b)** 4 storey, **(c)** and **(d)** 3 storey, and **(e),** and **(f)** 2 storey.

5.2. Vulnerability Analysis

5.2.1. Fragility curves

This section shows the result of the fragility curves for the as-built and FRP-strengthened RC exterior, interior and non-conforming BCJs with the first two being the most vulnerable joint types in a moment-resisting frame. The fragility function is based on the mean maximum IDR obtained from the NLTHs performed for each building type in the previous section. Three different DSs, namely, light damage (DS1), moderate damage (DS2), and heavy damage (DS3), are considered according to widely recognized damage classifications which is obtained for the as-built and FRP-strengthened configuration. Moving forward, each gravity designed storey building type is discussed below taking into consideration the IDR in X direction only (which is lower than the Y direction) in order to have an idea of the fragility curves at a lower IDR.

- **Four-storey buildings**

For the four buildings designed to withstand gravity loads only with the EDP that has been discussed earlier, the probability of occurrence in X direction is shown in **Figure 5.7** for both as-built and FRP configurations for the 2475 return period.

For the as-built configuration, at the maximum IDR, none of the joints except the non-conforming joint (i.e., exterior and interior joints) achieved light damage (DS1) and medium damage (DS2) at about 0.9 and 0.78 probability of occurrence, respectively, as shown in **Figure 5.7a and b.** It can be observed that the exterior and interior joints therefore achieved heavy damage, i.e., DS3 at the 9^{th} return period with a probability of occurrence of about 0.96 and 0.6, respectively, at the maximum drift, as shown in **Figure 5.7c.**

With FRP strengthened, there is a reduction in the probability of occurrence for exterior and interior joints at DS3 to a lower value of about 0.51 and 0.31, respectively, therefore showing the effectiveness of FRP. At DS2, the probability of occurrence for the exterior and interior joint was also reduced. Meanwhile, for the non-conforming joints, the FRP isn't expected to be effective since they are confined. This is as shown in **Figure 5.7d, e, and f.**

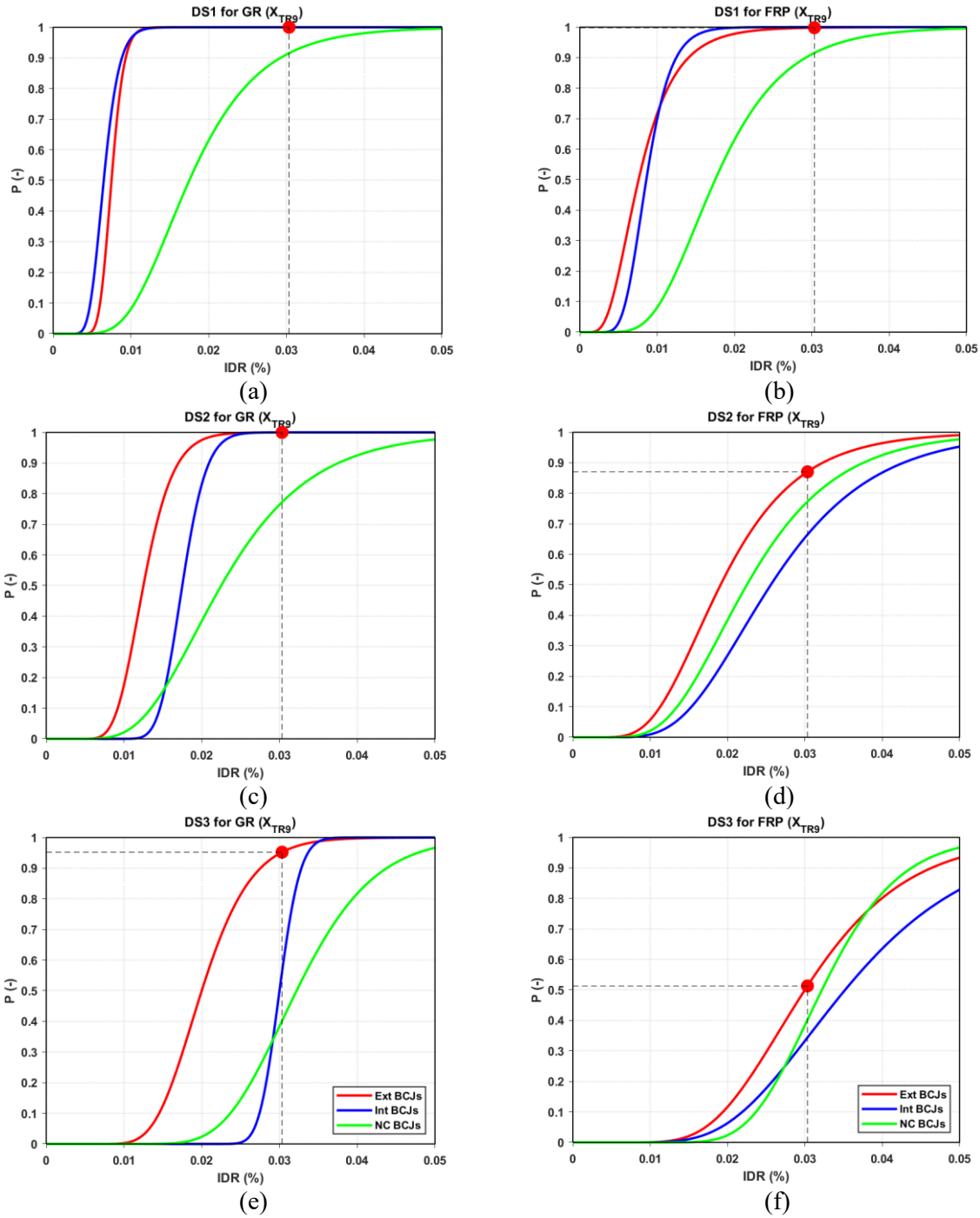

Figure 5.7: Fragility curves in X direction at 2475 years return period for 4-storey gravity building: **(a)**, **(c)** and **(e)** As-Built and **(b)**, **(d)** and **(f)** FRP strengthened.

- **Three-storey buildings**

The probability of occurrence in X direction is shown for both as-built and FRP configurations for the 3-storey gravity building type at a 2475 return period is as shown in **Figure 5.8**.

For the as-built configuration, at the maximum IDR, none of the joints except the non-conforming joint (i.e., exterior and interior joints) achieved light damage (DS1) (as it was for the 4-storey type). The exterior and interior joints achieved medium damage (DS2) at about 0.96 and 0.7 probability of occurrence, respectively, as shown in **Figure 5.8a-b.** Therefore, the interior joint achieved the DS2 state. It can be observed that the exterior joints therefore achieved heavy damage, i.e., DS3 at the 9^{th} return period with a probability of occurrence of about 0.41 at the maximum drift, as shown in **Figure 5.8c.**

With FRP strengthened, there is a reduction in the probability of occurrence for exterior and interior joints to a lower value of about 0.08 and 0.24 at DS3 and DS2, respectively, therefore showing the effectiveness of FRP. Meanwhile, for the non-conforming joints, the FRP isn't expected to be effective since they are confined. This is as shown in **Figure 5.8d, e, and f.**

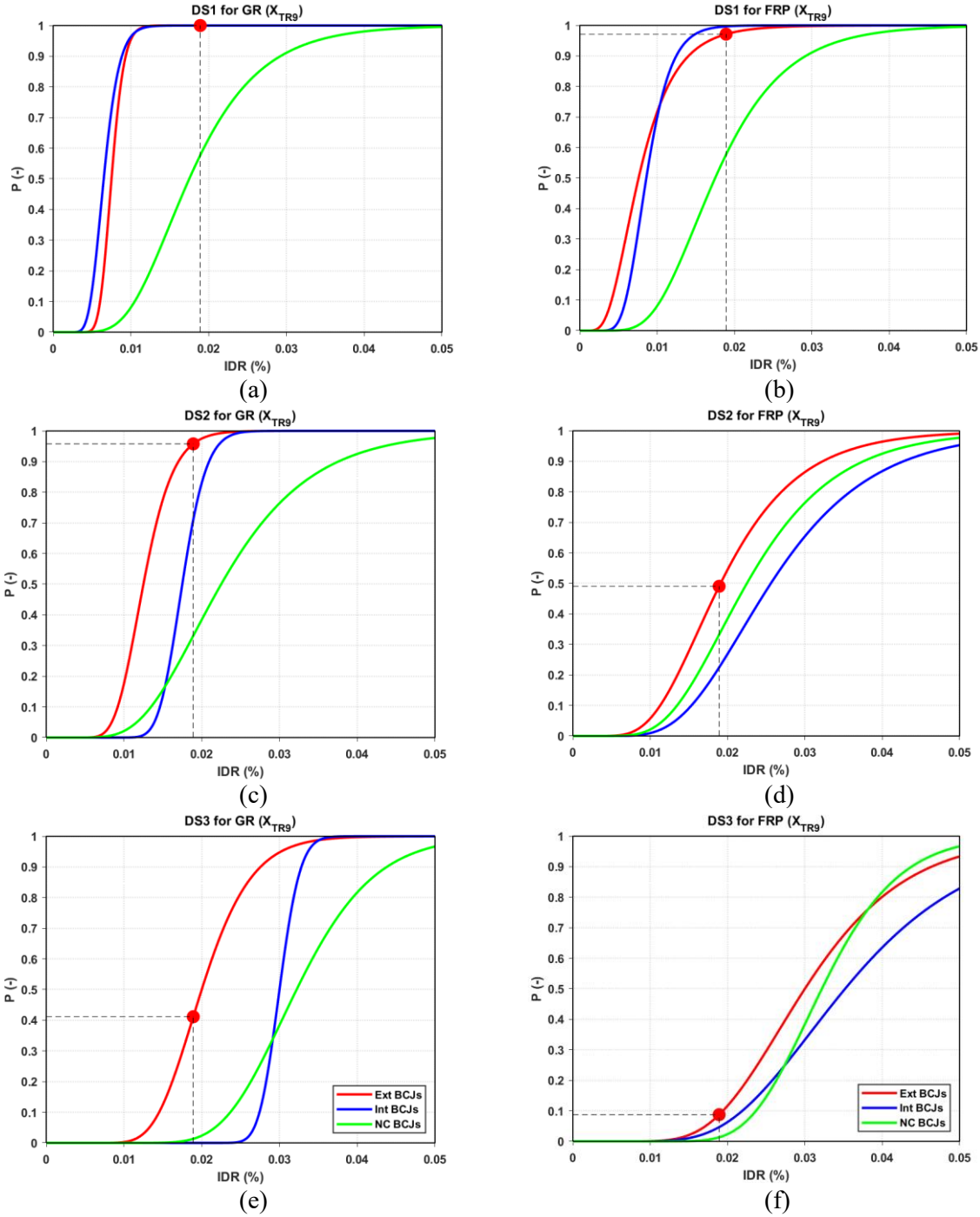

Figure 5.8: Fragility curves in X direction at 2475 years return period for 3-storey gravity building: **(a)**, **(c)** and **(e)** As-Built and **(b)**, **(d)** and **(f)** FRP strengthened.

- **Two-storey buildings**

Also, for the 2-storey building type, the probability of occurrence in X direction is shown for both as-built and FRP configurations at a 2475 return period is as shown in **Figure 5.9**.

For the as-built configuration, at the maximum IDR, none of the joints except the non-conforming joint (i.e., exterior and interior joints) achieved light damage (DS1) (as it was for the 3 and 4-storey types). The exterior and interior joints achieved medium damage (DS2) at about 0.96 and 0.7 probability of occurrence, respectively, as shown in **Figure 5.9a-b,** which is the same as the 3 floors, because they have almost the same maximum IDR. Therefore, the interior joint also achieved the DS2 state. It can be observed that the exterior joints therefore achieved heavy damage, i.e., DS3 at the 9^{th} return period with a probability of occurrence of about 0.41 at the maximum drift, as shown in **Figure 5.9c.** With FRP strengthened, it was also the same as for the 3-floor building type.

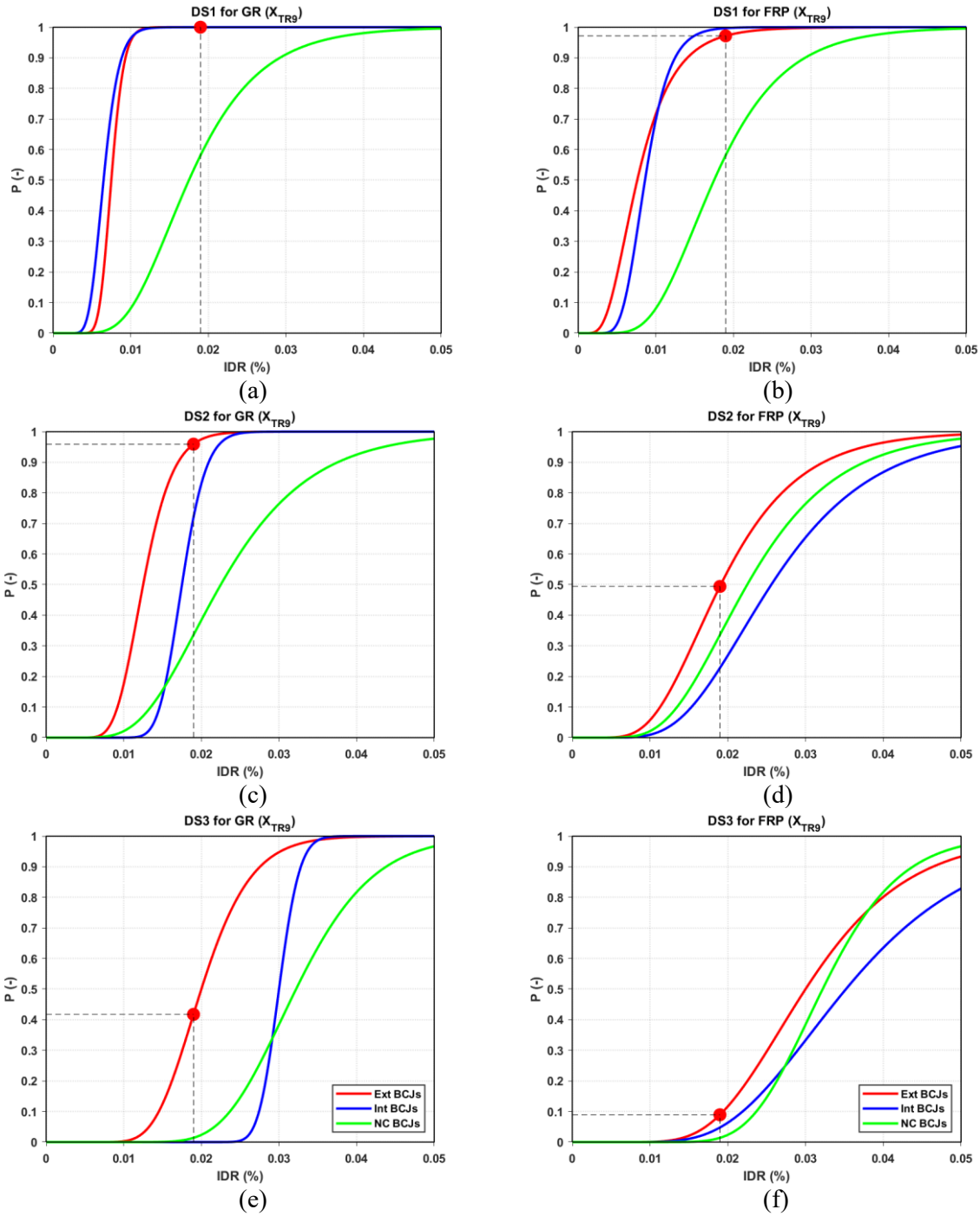

Figure 5.9: Fragility curves in X direction at 2475 years return period for 2-storey gravity building: **(a)**, **(c)** and **(e)** As-Built and **(b)**, **(d)** and **(f)** FRP strengthened.

5.2.2. Analysis of Costs and Probability of Collapse Assessment

As was done for the buildings designed to withstand to seismic loads (SLD), the costs associated with each realization considering the effect of the probability of collapse are evaluated for the as-built and FRP configuration of buildings designed to withstand gravity loads only (GLD).

- **Four-storey buildings**

For the 4-storey building type, it can be observed that collapse occurs from return period T_{R6} to T_{R9} (i.e., 201 to 2475 years) for the as-built configuration, as shown in **Figure 5.11a**. The total number of collapses observed increases from 96 to 302, with a probability of collapse of 0.19 to 0.60, respectively. This is as shown in **Figure 5.10a**.

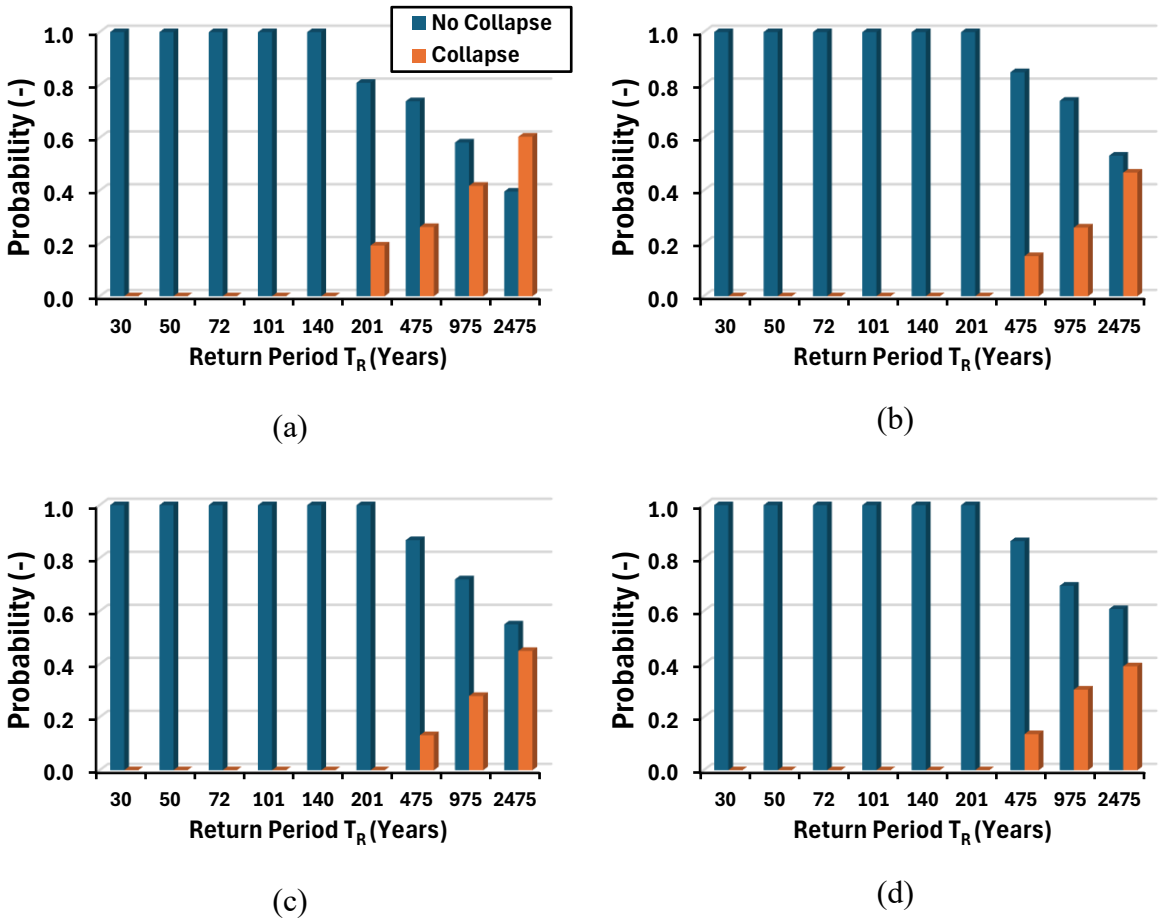

Figure 5.10: Probability of collapse for 4-storey gravity building: **(a)** As-built, **(b)** SFRP, **(c)** SL_CFRP strengthened, and **(d)** DL_CFRP strengthened.

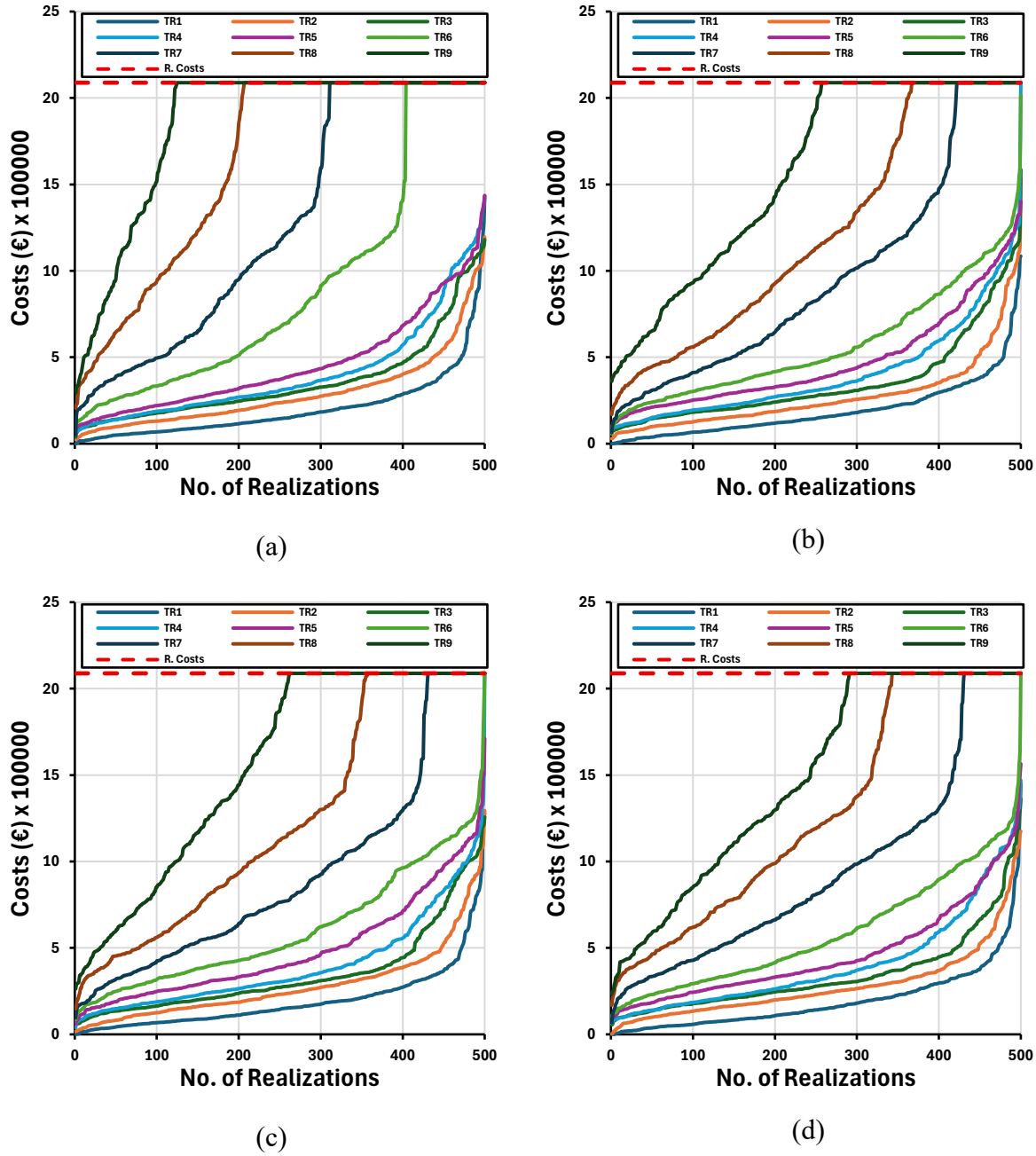

Figure 5.11: Cost vs realizations for all return periods (4-storey gravity building): **(a)** As-Built, **(b)** SFRP, **(c)** SL_CFRP, and **(d)** DL_CFRP strengthened.

On the other hand, for the SFRP configuration, there was a reduction in the costs, and the collapse occurred from return period T_{R7} to T_{R9} (i.e., 475 to 2475 years), showing the effect of the SFRP. This is as shown in **Figure 5.11b**. This can be related to the number of collapses that reduced in the associated return period, increasing from 76 to 234, with a probability of collapse of 0.15 to 0.47. This is as shown in **Figure 5.10b**.

Further strengthening with a single layer of CFRP (SL_CFRP) and a double layer of CFRP (DL_CFRP) shows the reduction of the costs from T_{R7} to T_{R9} with a lower probability of collapse of about 0.13 to 0.39 for both cases. This is attributed to their capacity not being enough to erase the collapse; rather, it reduced the cost slightly. This can be observed on **Figure 5.11c-d** and **Figure 5.10c-d.**

- **Three-storey buildings**

For the 3-storey building type, it can be observed that collapse occurs for all the return periods T_{R1} to T_{R9} (i.e., 30 to 2475 years) for the as-built configuration, as shown in **Figure 5.13a**. The total number of collapses observed increases from 145 to 500 with a probability of collapse of 0.29 to 1, i.e., total collapse. This is as shown in **Figure 5.12a**.

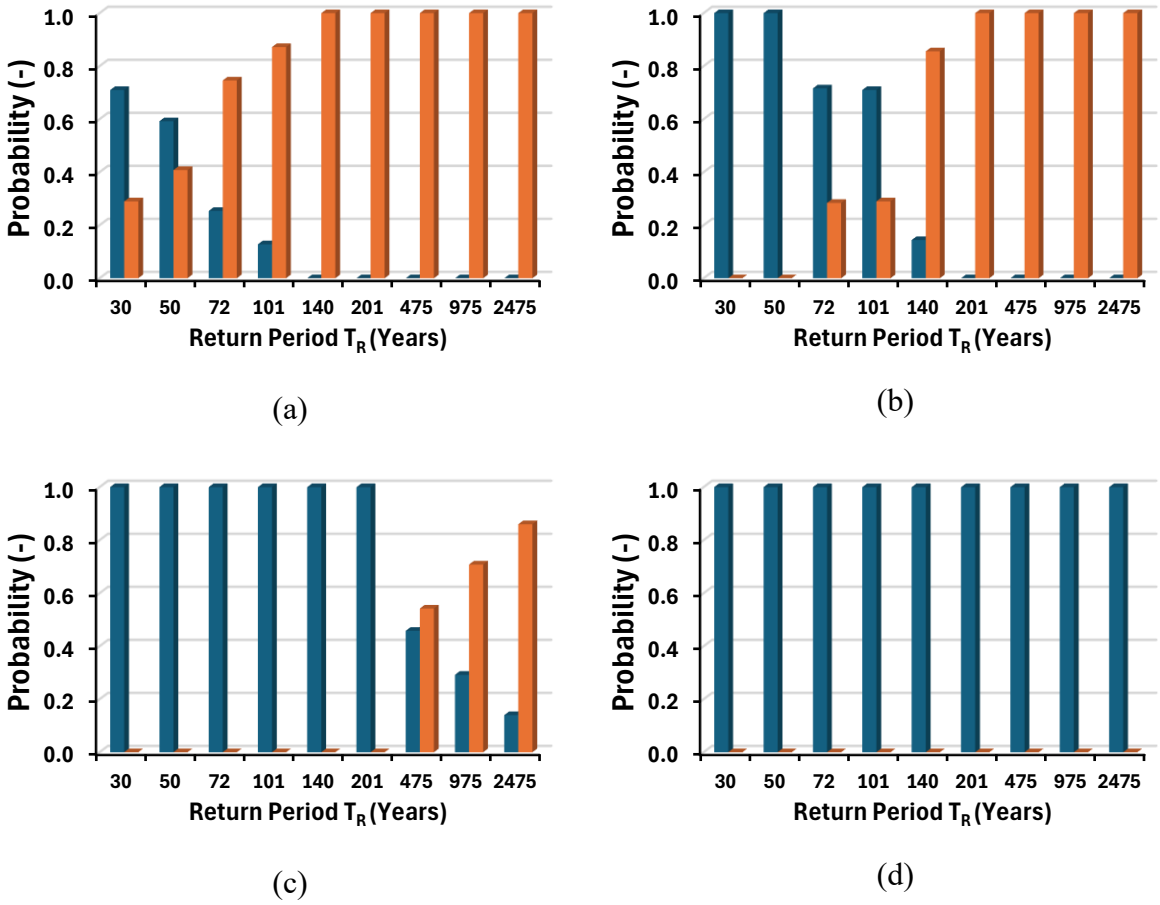

Figure 5.12: Probability of collapse for 3-storey gravity building: **(a)** As-built, **(b)** SFRP, **(c)** SL_CFRP, and **(d)** DL_CFRP strengthened.

Using SFRP strengthening, there was a reduction in all costs, leading to no collapse from T_{R1} and T_{R2}, but the collapse remains from return period T_{R3} to T_{R9}, at a reduced collapse probability. This is as shown in **Figure 5.13b**. This can be related to the number of collapses that reduced in

the associated return period to 0 for T_{R1} to T_{R2} and 142 to 500 for the remaining return period, with probability of collapse from 0.28 to 1 for the latter. This is as shown in **Figure 5.12b**.

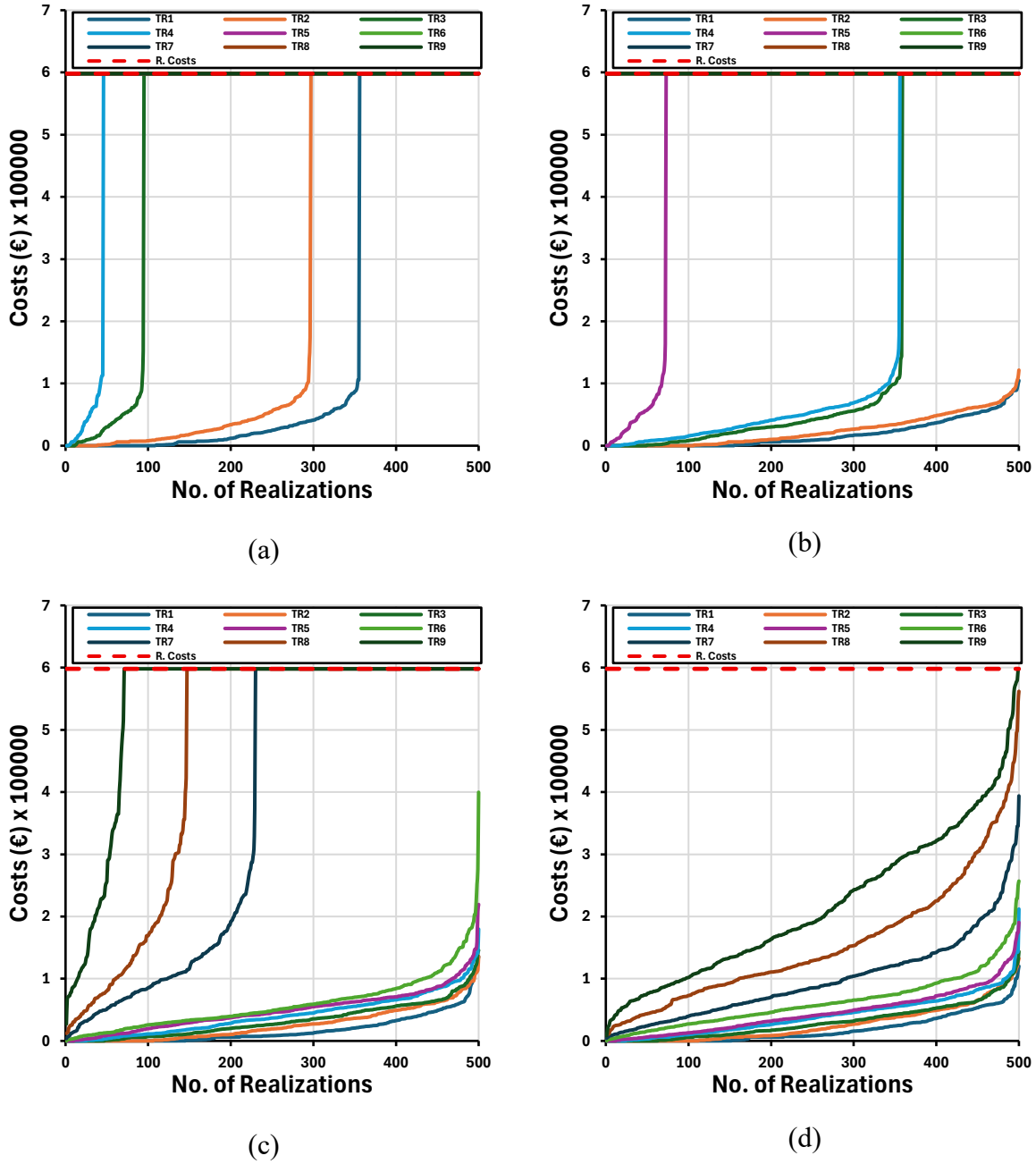

Figure 5.13: Cost vs realizations for all return periods (3-storey gravity building): **(a)** As-Built, **(b)** SFRP, **(c)** SL_CFRP, and **(d)** DL_CFRP strengthened.

With SL_CFRP and DL_CFRP, there was a shift in collapse from T_{R7} to $T_{R9,}$ and no collapse, respectively. This is related to the number of collapses ranging from 271 to 431 (0.54 to 0.860 collapse probability) and zero collapses for each strengthening technique used. This shows the

great effectiveness of the CFRP capacity that was able to erase the collapse of the structure. This can be seen in **Figure 5.13c-d** and **Figure 5.12c-d.**

- **Two-storey buildings**

Lastly, for the 2-storey building type, it can be observed that collapse occurs for all the return periods, i.e., T_{R1} to T_{R9} (i.e., 30 to 2475 years) for the as-built configuration, as shown in **Figure 5.15a**. The total number of collapses increases from 70 and 500 with a probability of collapse from 0.14 to 1 as shown in **Figure 5.14a**.

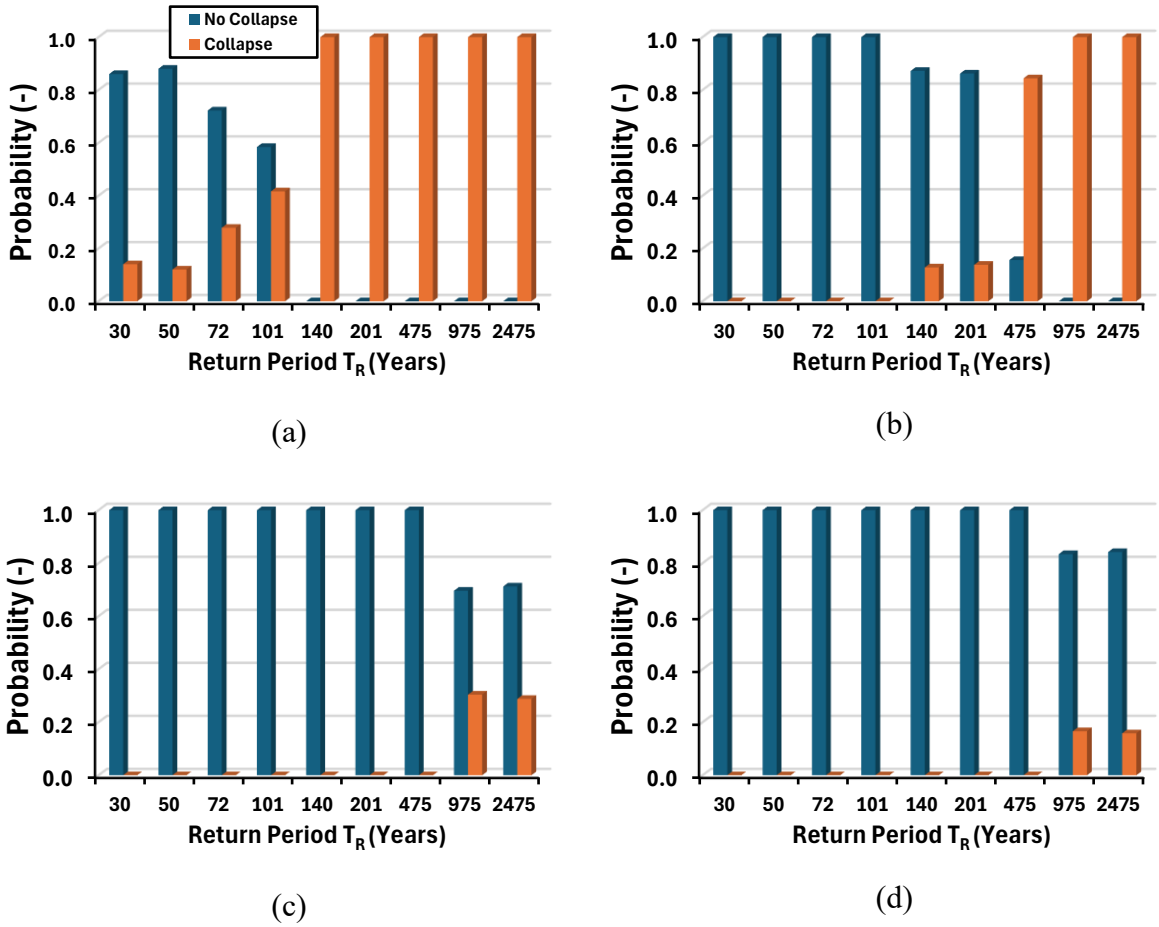

Figure 5.14: Probability of collapse for 2-storey gravity building: **(a)** As-built, **(b)** SFRP, **(c)** SL_CFRP strengthened, and **(d)** DL_CFRP strengthened.

Using SFRP strengthening, there was a reduction in all costs, leading to no collapse from T_{R1} to $T_{R4,}$ but maintained the collapse for the remaining return period (see **Figure 5.15b)** with the number of collapses being 64 to 500 (0.13 to 1 collapse probability) as shown in **Figure 5.14b**. Upon the use of SL_CFRP and DL_CFRP, there was a shift in collapse from T_{R8} to T_{R9} for both, with the number of collapses ranging from 83 to 152 (0.17 to 0.30 collapse probability). This shows the effectiveness of the CFRP capacity that was able to erase the collapse of the structure

up to the 7th return period and further reduced after doubling the CFRP. This can be seen in **Figure 5.15c-d** and **Figure 5.14c-d.**

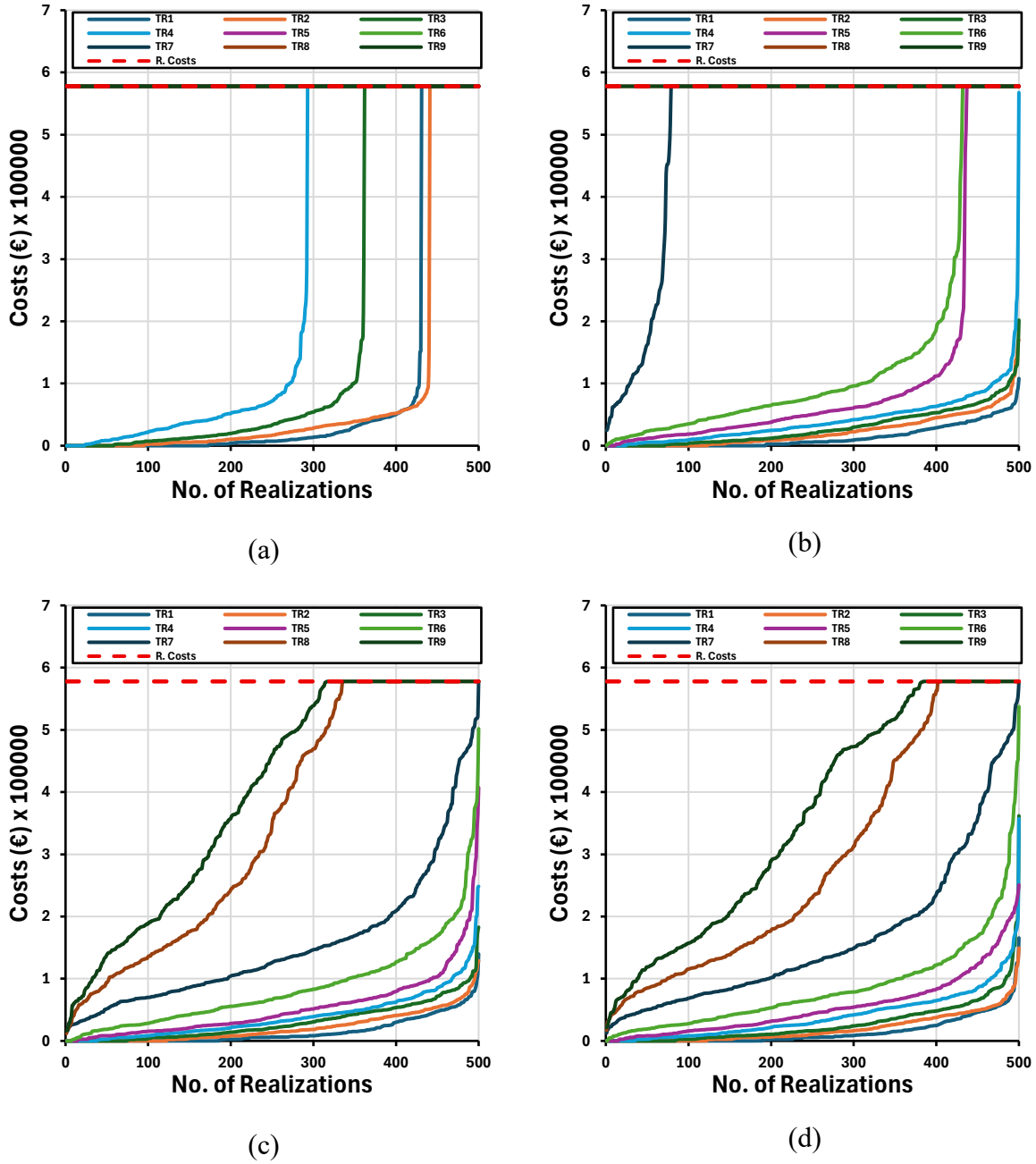

Figure 5.15: Cost vs realizations for all return periods (2-storey gravity building): **(a)** As-Built, **(b)** SFRP, **(c)** SL_CFRP, and **(d)** DL_CFRP strengthened.

5.3. Costs Comparison

In the same vein as previously done for the seismic designed buildings, the cost comparison for the as-built and strengthened techniques (SFRP and CFRP) in terms of component level and at different return periods are presented below. This gives an idea of the cost associated with each component type, i.e., drift and acceleration-based component as well as the effects of the FRP strengthening on the costs associated to the beam column joints (BCJs).

5.3.1. Repair costs at the component level

Figure 5.16 shows the summary of the building repair costs for the three case study building (i.e. as-built and strengthened configurations) evaluated for the drift (i.e. infills, partitions, stairs, and joints) and acceleration (i.e. tiles, chimney, raised access floor, lighting, cold and hot water piping, sanitary waste, and low voltage switch gear) sensitive components for return period T_{R9} (i.e. 2475 years). It can be shown that the drift-based components take the larger percentage (80% to 93%), with the joints (for all building types) taking about 50 to 55% of the building repair cost. Consequently, the acceleration-based components take a lesser percentage (7% to 20%) of the building repair costs. This is as shown in **Figure 5.16a-c.**

At the return period, the influence of SFRP strengthening reduces the joint costs by 10%, 17% and 14% for the 4, 3, and 2-storey buildings, respectively, as shown in **Figure 5.16a-c.** This shows the effectiveness of SFRP before collapse. Consequently, the use of SL_CFRP reduces the joint cost by 16%, 14% and 12% for the 4, 3, and 2-storey buildings, respectively. Lastly, with DL_CFRP, the joint cost was reduced by 14%, 10% and 12% for the 4, 3, and 2-storey buildings, respectively. Considering the 3 strengthening techniques used, it can be noted that FRP best reduces the cost of the joint before collapse.

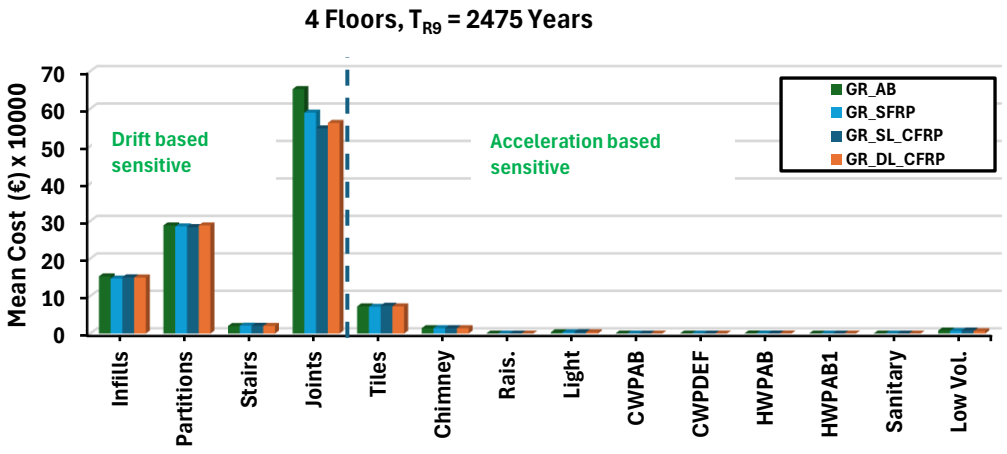

(a)

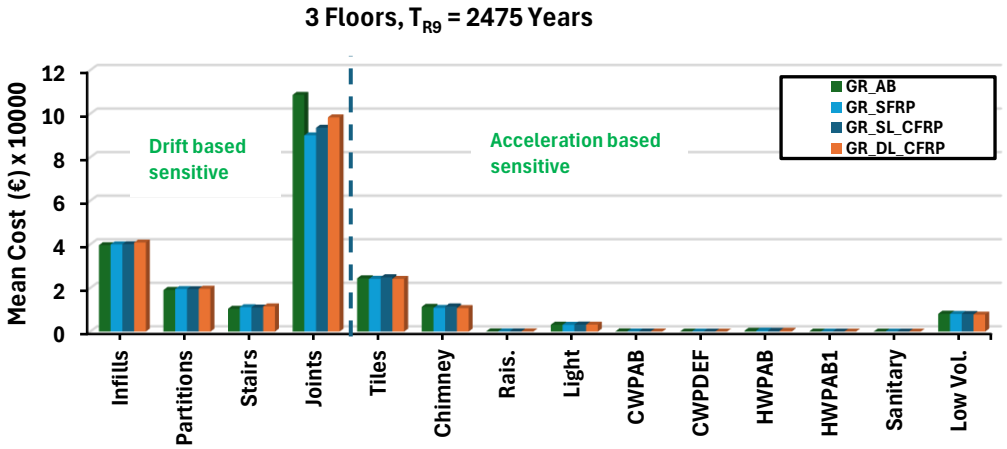

(b)

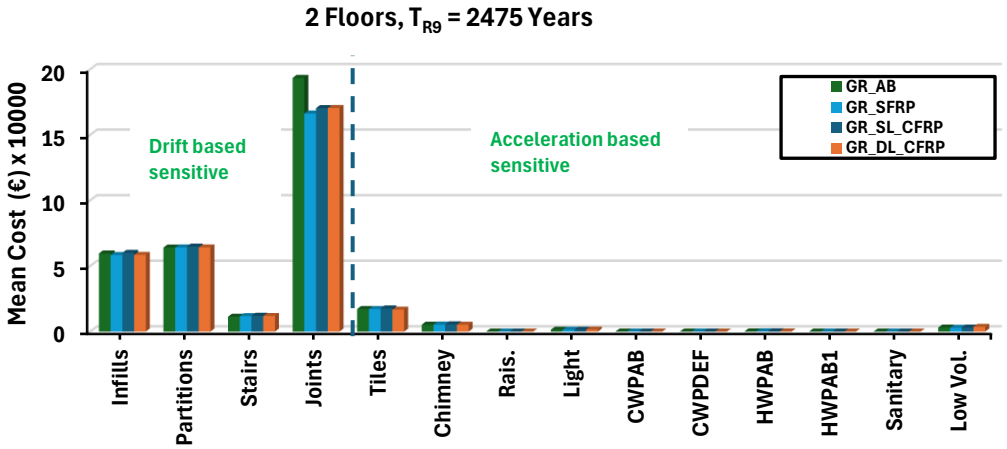

(c)

Figure 5.16: Repair cost at component level - gravity design: **(a)** 4-storey building, **(b)** 3-storey building, and **(c)** 2-storey building.

5.3.2. Repair costs at different return periods after collapse (T_{RS})

This section shows the repair costs for different return periods, considering the effect of the collapse of the building. The cost extracted and arranged in ascending order is used for this purpose. To this effect, the cost of strengthening techniques at each return period is also plotted to understand their effect. **Figure 5.17a-c** shows the variation of the total repair costs associated with each T_{RS} for the 3-case study of gravity-designed buildings. It is worth noting that, in any case, the strengthening doesn't have an effect at a particular T_R; therefore, the cost is equal to the reconstruction cost, which implies that it is better for the building to be demolished.

For the 4-storey building type, there is a non-linear increment in the repair cost from the less severe earthquake to the severe earthquake, where the damage is more destructive. At the last return period, the reconstruction cost wasn't reached; therefore, the structure can be strengthened. It is worth noting that once the costs are more than 50% of the reconstruction costs, it is better to demolish the structure. Upon the use of SFRP, SL_CFRP, and DL_CFRP, there was a reduction of 24%, 25% and 28% when compared with the reconstruction costs. Since the strengthening costs are more than 50% of the reconstruction costs, it is better to demolish the building. This can be seen in **Figure 5.17a.**

Consequently, for the 3-storey building type, there is a non-linear increase in the repair costs from the 1st – 4th return period (i.e., 30 to 101 years) without reaching the reconstruction costs. After the 4th return period, the remaining return period therefore reaches the reconstruction costs; therefore, it is necessary to strengthen the structure. With SFRP, there is a significant reduction of the repair costs up to the 5th return period (i.e., 140 years), with the remaining T_{RS} reaching the reconstruction costs. On the other hand, using SL_CFRP, the cost reduced significantly until the 6th return period and slightly for the remaining, with the 9th return period having about 9% reduction when compared with the reconstruction costs. Meanwhile, with the use of DL_CFRP, the costs were slightly the same as those of the SL_CFRP up to the 6th return period and reduced significantly for the remaining return period, with the 9th return period having about a 64% reduction in cost when compared to the reconstruction costs. This shows that DL_CFRP is more effective when compared to the other 2 strengthening techniques during a severe earthquake. This is as shown in **Figure 5.17b.**

Lastly, for the 2-storey building type, there is a non-linear increase in the repair costs from the 1st to 4th return period (i.e., 30 to 101 years) without reaching the reconstruction costs. After the 4th return period, the remaining return period therefore reaches the reconstruction costs; therefore, it is necessary to strengthen the structure. With SFRP, there is a significant reduction

of the repair costs up to the 6th return period (i.e., 201 years) and a slight reduction at the 7th return period, with the remaining T_{RS} reaching the reconstruction costs. Meanwhile, with SL_CFRP, the cost reduced significantly until the 7th return period and slightly for the remaining, with the last two with the 9th return period having about a 31% reduction when compared with the reconstruction costs. In the same vein, with the use of DL_CFRP, the costs were slightly the same as those of the SL_CFRP up to the 7th return period and reduced slightly for the remaining return period, with the 9th return period having about a 37% reduction in cost when compared to the reconstruction costs. This implies that both SL_CFRP and DL_CFRP are more effective when compared to the SFRP strengthening techniques during the earthquake (see **Figure 5.17c).**

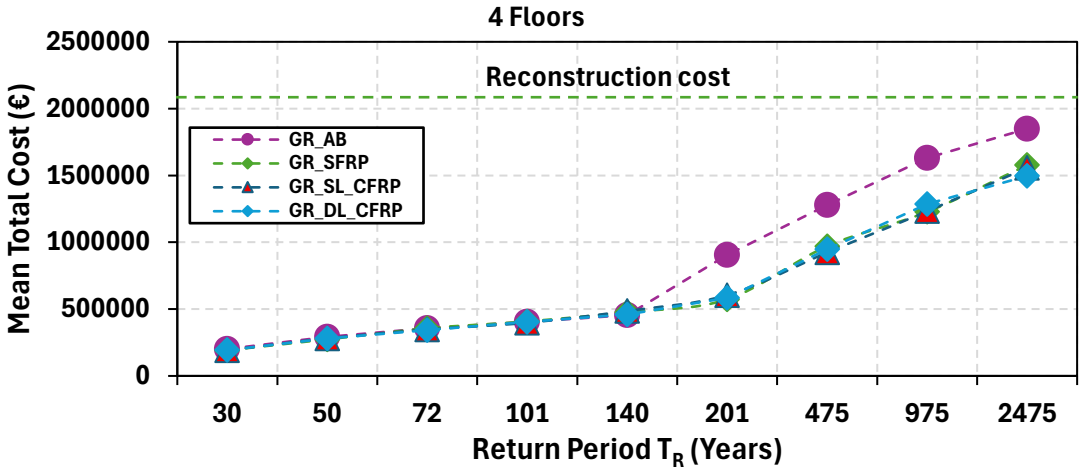

(a)

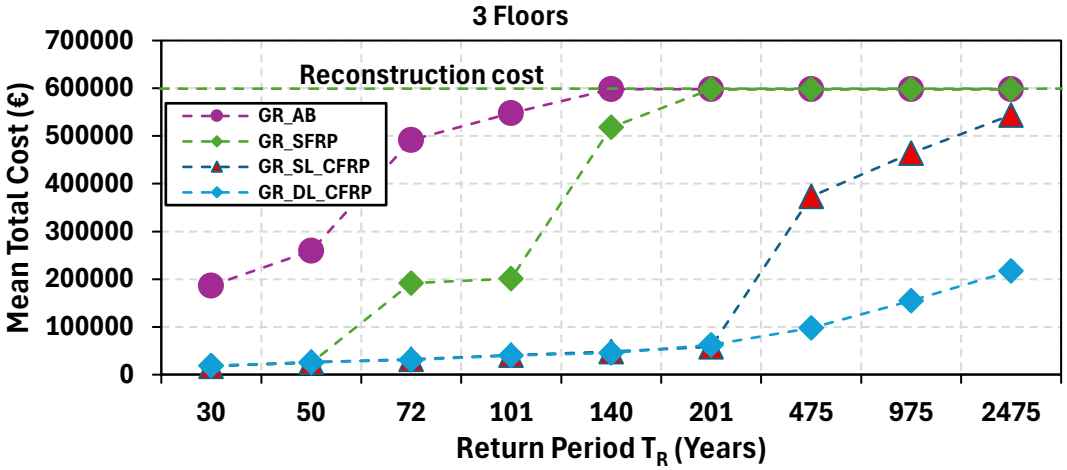

(b)

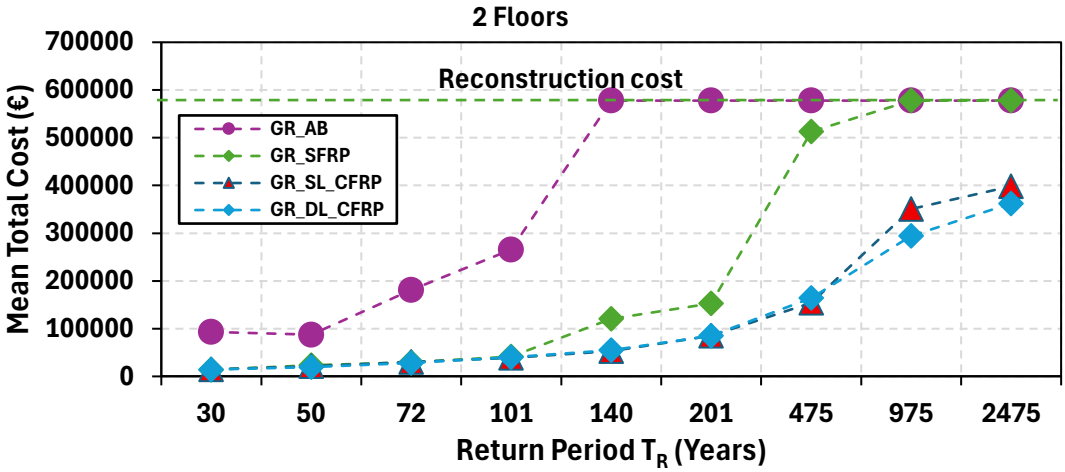

(c)

Figure 5.17: Total repair cost at each return period-gravity design: **(a)** 4-storey building, **(b)** 3-storey building, and **(c)** 2-storey building.

THIS PAGE WAS INTENTIONALLY LEFT BLANK

6. CONCLUSION AND FURTHER DEVELOPMENTS

The thesis presents the results of research work aimed at assessing the benefits of FRP strengthening on the seismic performance of RC buildings through a framework for regional scale simulations. To this end, a PBEE-based seismic loss-assessment framework developed at the University of Napoli Federico II was used and adapted for the specific scope of this work. To assess the sensitivity of simulations to main structural parameters, three reinforced concrete buildings with different floors were selected as case study from the database of existing building repaired and retrofitted during the L'Aquila reconstruction process. The seismic response of buildings was modelled using a simplified nonlinear numerical model experimentally calibrated and validated. The simplified model is implemented in a novel seismic loss-assessment framework. This framework is used to conduct nonlinear analysis to assess the structural performance of the selected buildings, evaluate the losses, the probability of collapse and quantify the cost and the benefits of FRP strengthening account for the variability of characteristics of buildings. The FRP strengthening techniques used therefore show its effectiveness in terms of reducing the strengthening cost and probability of collapse.
The main findings can be summarized as follows:

1. The proposed framework shows clear sensitivity to variations in building geometry and typology when evaluating engineering demand parameters (EDPs) in terms of interstorey drift (IDR), interstorey shear and floor acceleration. Buildings with higher number of floors designed for gravity loads (GLD) exhibit significantly larger drifts and seismic demands compared to buildings designed to withstand moderate seismic loads (SLD), confirming that the capacity of framework to properly captures the influence of structural characteristics;
2. The gravity-load designed 4-storey building experienced IDRs at return period of 475 years 58% and 24% greater than the buildings designed with moderate seismic actions in X and Y direction respectively;
3. FRP strengthening significantly reduces the probability of collapse in GLD 2- and 3-storey buildings. Strengthening solutions with Single Layer and Double Layer of Carbon Fiber (i.e., SL_CFRP and DL_CFRP) results more effective if compared to the strengthening solution realized with one layer of Steel Fiber (SFRP). In contrast, the 4-storey designed for both GLD and SLD already exhibited a low collapse probability in

the as-built configuration due to some geometric characteristics. Thus the benefit provided by CFRP strengthening solutions are limited;

4. At the 9th return period, under severe earthquake loads, exterior joints mainly achieved DS3 and interior joints DS2 across all SLD and GLD buildings (except GLD 2-storey). The probabilistic analysis highlights that FRP strengthening considerably reduces the probability of BCJs to achieve higher damage states. In particular, the probability of joints attaining DS3 decreased significantly, with reductions of about 20–40% for SLD buildings and around 60% for GLD buildings;
5. For GLD buildings, as-built EALs were 1.27%, 1.97%, and 0.66% for the 2-, 3-, and 4-storey cases. With SFRP strengthening on column and CFRP on BCJs, they dropped to 0.41%, 0.97%, and 0.57%, respectively. In 4-storey buildings, SL_CFRP and DL_CFRP gave no further reduction, but for 2- and 3-storey cases, they lowered EALs to 0.25%/0.24% and 0.30%/0.20%, respectively;
6. The analysis of costs confirms that FRP strengthening reduces total costs, especially for GLD buildings at higher return periods. For 2- and 3-storey cases, CFRP solutions consent to reduce the costs of about 60% - 90% at high seismic intensities (i.e. at return period from 7th to 9th). For 4-storey cases, SFRP already provides significant cost reductions, and other techniques may not always yield proportional benefits;
7. Overall, the effectiveness of FRP depends strongly on the strengthening solution adopted. SFRP on columns is sufficient where demand due to the infill-to-structure interaction is not very high, but single- or double-layer CFRP is recommended for GLD low- to mid-rise buildings where seismic vulnerability is higher. In addition, there is a substantial reduction in total cost upon the usage of these techniques;

In conclusion, this research confirms the reliability of the proposed framework in the assessment of the effectiveness of FRP strengthening as local retrofit for existing RC buildings. It is noteworthy noting that the data gathered pertains specifically to the selected case study buildings and further analyses and validations are needed to extend at regional scale.

REFERENCES

[1] C. Del Vecchio, M. Di Ludovico, and A. Prota, "Cost and Effectiveness of Fiber-Reinforced Polymer Solutions for the Large-Scale Mitigation of Seismic Risk in Reinforced Concrete Buildings," *Polymers*, vol. 13, no. 17, p. 2962, Aug. 2021, doi: 10.3390/polym13172962.

[2] D. A. Pohoryles, J. Melo, T. Rossetto, H. Varum, and L. Bisby, "Seismic Retrofit Schemes with FRP for Deficient RC Beam-Column Joints: State-of-the-Art Review," *J. Compos. Constr.*, vol. 23, no. 4, p. 03119001, Aug. 2019, doi: 10.1061/(ASCE)CC.1943-5614.0000950.

[3] C. Del Vecchio, M. Di Ludovico, A. Balsamo, and A. Prota, "Minimally Invasive FRP Strengthening of External Beam–Column Joints," *J. Compos. Constr.*, vol. 28, no. 4, p. 04024026, Aug. 2024, doi: 10.1061/JCCOF2.CCENG-4525.

[4] İ. E. Bal, H. Crowley, R. Pinho, and F. G. Gülay, "Detailed assessment of structural characteristics of Turkish RC building stock for loss assessment models," *Soil Dynamics and Earthquake Engineering*, vol. 28, no. 10–11, pp. 914–932, Oct. 2008, doi: 10.1016/j.soildyn.2007.10.005.

[5] X. Lu, F. McKenna, Q. Cheng, Z. Xu, X. Zeng, and S. A. Mahin, "An open-source framework for regional earthquake loss estimation using the city-scale nonlinear time history analysis," *Earthquake Spectra*, vol. 36, no. 2, pp. 806–831, May 2020, doi: 10.1177/8755293019891724.

[6] C. Del Vecchio, M. D. Ludovico, and A. Prota, "Repair costs of reinforced concrete building components: from actual data analysis to calibrated consequence functions," *Earthquake Spectra*, vol. 36, no. 1, pp. 353–377, Feb. 2020, doi: 10.1177/8755293019878194.

[7] C. Molitierno, C. Del Vecchio, M. Di Ludovico, and A. Prota, "Pseudodynamic Tests and Numerical Modelling for Damage Analysis of Infilled RC Frames," *Journal of Earthquake Engineering*, vol. 27, no. 16, pp. 4549–4574, Dec. 2023, doi: 10.1080/13632469.2023.2183048.

[8] M. Di Ludovico, A. Prota, C. Moroni, G. Manfredi, and M. Dolce, "Reconstruction process of damaged residential buildings outside historical centres after the L'Aquila earthquake: part I—"light damage" reconstruction," *Bull Earthquake Eng*, vol. 15, no. 2, pp. 667–692, Feb. 2017, doi: 10.1007/s10518-016-9877-8.

[9] C. Baggio *et al.*, "Field Manual for post-earthquake damage and safety assessment and short term countermeasures (AeDES)".

[10] M. Di Ludovico, A. Prota, C. Moroni, G. Manfredi, and M. Dolce, "Reconstruction process of damaged residential buildings outside historical centres after the L'Aquila earthquake: part II—'heavy damage' reconstruction," *Bull Earthquake Eng*, vol. 15, no. 2, pp. 693–729, Feb. 2017, doi: 10.1007/s10518-016-9979-3.

[11] R. Frascadore *et al.*, "Local Strengthening of Reinforced Concrete Structures as a Strategy for Seismic Risk Mitigation at Regional Scale," *Earthquake Spectra*, vol. 31, no. 2, pp. 1083–1102, May 2015, doi: 10.1193/122912eqs361m.

[12] M. Di Ludovico, G. Manfredi, E. Mola, P. Negro, and A. Prota, "Seismic Behavior of a Full-Scale RC Structure Retrofitted Using GFRP Laminates," *J. Struct. Eng.*, vol. 134, no. 5, pp. 810–821, May 2008, doi: 10.1061/(ASCE)0733-9445(2008)134:5(810).

[13] C. Del Vecchio, M. Di Ludovico, A. Balsamo, A. Prota, G. Manfredi, and M. Dolce, "Experimental Investigation of Exterior RC Beam-Column Joints Retrofitted with FRP

Systems," *J. Compos. Constr.*, vol. 18, no. 4, p. 04014002, Aug. 2014, doi: 10.1061/(ASCE)CC.1943-5614.0000459.

[14] C. Del Vecchio, M. Di Ludovico, A. Prota, and G. Manfredi, "Analytical model and design approach for FRP strengthening of non-conforming RC corner beam–column joints," *Engineering Structures*, vol. 87, pp. 8–20, Mar. 2015, doi: 10.1016/j.engstruct.2015.01.013.

[15] C. Del Vecchio, M. Di Ludovico, S. Pampanin, and A. Prota, "Repair Costs of Existing RC Buildings Damaged by the L'Aquila Earthquake and Comparison with FEMA P-58 Predictions," *Earthquake Spectra*, vol. 34, no. 1, pp. 237–263, Feb. 2018, doi: 10.1193/122916EQS257M.

[16] G. J. O'Reilly and T. J. Sullivan, "Probabilistic seismic assessment and retrofit considerations for Italian RC frame buildings," *Bull Earthquake Eng*, vol. 16, no. 3, pp. 1447–1485, Mar. 2018, doi: 10.1007/s10518-017-0257-9.

[17] S. Taghavi, "Pacific Earthquake Engineering Research Center".

[18] A. S. Whittaker and T. T. Soong, "AN OVERVIEW OF NONSTRUCTURAL COMPONENTS RESEARCH AT THREE U.S. EARTHQUAKE ENGINEERING RESEARCH CENTERS".

[19] P. Ricci, F. D. Luca, and G. M. Verderame, "6TH APRIL 2009 L'AQUILA EARTHQUAKE, ITALY: REINFORCED CONCRETE BUILDING PERFORMANCE".

[20] G. De Martino, M. Di Ludovico, A. Prota, C. Moroni, G. Manfredi, and M. Dolce, "Estimation of repair costs for RC and masonry residential buildings based on damage data collected by post-earthquake visual inspection," *Bull Earthquake Eng*, vol. 15, no. 4, pp. 1681–1706, Apr. 2017, doi: 10.1007/s10518-016-0039-9.

[21] C. Del Gaudio *et al.*, "Empirical fragility curves from damage data on RC buildings after the 2009 L'Aquila earthquake," *Bull Earthquake Eng*, vol. 15, no. 4, pp. 1425–1450, Apr. 2017, doi: 10.1007/s10518-016-0026-1.

[22] T. Chrupalo *et al.*, "RISK MANAGEMENT PRODUCTS CONSULTANTS," vol. 1, 2012.

[23] D. Cardone and G. Perrone, "Developing fragility curves and loss functions for masonry infill walls," *Earthquakes and Structures*, vol. 9, no. 1, pp. 257–279, Jul. 2015, doi: 10.12989/EAS.2015.9.1.257.

[24] K. Sassun, T. J. Sullivan, P. Morandi, and D. Cardone, "Characterising the in-plane seismic performance of infill masonry," *BNZSEE*, vol. 49, no. 1, pp. 98–115, Mar. 2016, doi: 10.5459/bnzsee.49.1.98-115.

[25] D. Cardone and G. Perrone, "Damage and Loss Assessment of Pre-70 RC Frame Buildings with FEMA P-58," *Journal of Earthquake Engineering*, vol. 21, no. 1, pp. 23–61, Jan. 2017, doi: 10.1080/13632469.2016.1149893.

[26] D. Cardone, "Fragility curves and loss functions for RC structural components with smooth rebars," *Earthquakes and Structures*, vol. 10, no. 5, pp. 1181–1212, May 2016, doi: 10.12989/EAS.2016.10.5.1181.

[27] C. D. Vecchio, C. Molitierno, O. Yurdakul, L. Routil, and M. D. Ludovico, "ACTUAL REPAIR/RETROFIT COSTS IN DEVELOPING SEISMIC LOSS MITIGATION STRATEGIES".

[28] C. E. Bakis *et al.*, "Fiber-Reinforced Polymer Composites for Construction—State-of-the-Art Review," *J. Compos. Constr.*, vol. 6, no. 2, pp. 73–87, May 2002, doi: 10.1061/(ASCE)1090-0268(2002)6:2(73).

[29] D. Combescure and P. Pegon, "-Operator Splitting time integration technique for pseudodynamic testing Error propagation analysis".

[30] D. Cardone, M. Rossino, and G. Gesualdi, "Estimating fragility curves of pre-70 RC frame buildings considering different performance limit states," *Soil Dynamics and*

Earthquake Engineering, vol. 115, pp. 868–881, Dec. 2018, doi: 10.1016/j.soildyn.2017.11.015.

[31] M. T. De Risi *et al.*, "Modelling and Seismic Response Analysis of Italian Pre-Code and Low-Code Reinforced Concrete Buildings. Part I: Bare Frames," *Journal of Earthquake Engineering*, vol. 27, no. 6, pp. 1482–1513, Apr. 2023, doi: 10.1080/13632469.2022.2074919.

[32] A. Natale, "EFFECTIVENESS AND ECONOMIC FEASIBILITY OF BASE ISOLATED SEISMIC RETROFIT SOLUTIONS FOR BUILDINGS AND INFRASTRUCTURES".

[33] D. E. Biskinis, G. K. Roupakias, and M. N. Fardis, "Degradation of Shear Strength of Reinforced Concrete Members with Inelastic Cyclic Displacements," *ACI Structural Journal*, 2004.

[34] S. Matthys, T. Triantafillou, and International Federation for Structural Concrete, Eds., *Externally applied FRP reinforcement for concrete structures: technical report*. in Bulletin / International Federation for Structural Concrete, no. 90. Lausanne, Switzerland: Fédération internationale du béton (fib), 2019.

[35] Ordinance of the President of the Council of Ministers, OPCM no. 3779 (2009) Urgent interventions to deal with seismic events occurring in the Abruzzo region on April 6, 2009 and other urgent civil protection provisions, published in the Official Journal no. 132 of 10 June 2009. OPCM n. 3779 del 6 giugno 2009—''Ulteriori interventi urgenti diretti a fronteggiare gli eventi sismici verificatisi nella regione Abruzzo il giorno 6 aprile 2009 e altre disposizioni urgenti di protezione civile'', Pubblicata nella Gazzetta Ufficiale n. 132 del 10 giugno 2009'' (in Italian)

[36] Ordinance of the President of the Council of Ministers, OPCM no. 3790 (2009) Urgent interventions to deal with seismic events occurring in the Abruzzo region on April 6, 2009 and other urgent civil protection provisions, published in the Official Journal no. 166 of 20 July 2009. OPCM n. 3790 del 9 luglio—'' Ulteriori interventi urgenti diretti a fronteggiare gli eventi sismici verificatisi nella regione Abruzzo il giorno 6 aprile 2009 e altre disposizioni urgenti di protezione civile'', Pubblicata nella Gazzetta Ufficiale n. 166 del 20 luglio 2009 (in Italian)

[37] Ordinance of the President of the Council of Ministers, OPCM no. 3803 (2009) Urgent interventions to deal with seismic events occurring in the Abruzzo region on April 6, 2009 and other urgent civil protection provisions, published in the Official Journal no. 193 of 21 August 2009. OPCM no. 3803 of 15 August 2009—''Ulteriori interventi urgenti diretti a fronteggiare gli eventi sismici verificatisi nella regione Abruzzo il giorno 6 aprile 2009 e altre disposizioni urgenti di protezione civile'', Pubblicata nella Gazzetta Ufficiale n. 193 del 21 Agosto 2009 (in Italian)

[38] C. Del Vecchio, C. Molitierno, O. Yurkadul, L. Routil, and M. Di Ludovico, "Numerical modelling and FRP strengthening of reinforced concrete buildings for regional scale retrofitting," in *Proc. 10th ECCOMAS Thematic Conf. on Computational Methods in Structural Dynamics and Earthquake Engineering (COMPDYN 2025)*, Rhodes Island, Greece, Jun. 15–18, 2025.

[39] Computers & Structures Inc. (2023) Sap2000v.23

[40] Ordinance of the President of the Council of Ministers, OPCM no. 3881 (2010) Urgent interventions to deal with seismic events occurring in the Abruzzo region on April 6, 2009 and other urgent civil protection provisions, published in the Official Journal no. 142 of 24 June 2010. OPCM n. 3881 del 11 giugno 2010—''Ulteriori interventi urgenti diretti a fronteggiare gli eventi sismici verificatisi nella regione Abruzzo il giorno 6 aprile 2009 e altre disposizioni urgenti di protezione civile'', Pubblicata nella Gazzetta Ufficiale n. 142 del 24 Giugno 2010 (in Italian)